TECHNISCHE UNIVERSITÄT DRESDEN

Institut für Hydrologie und Meteorologie Lehrstuhl für Hydrologie

Sabine Seidel (née Walser)

OPTIMAL SIMULATION BASED DESIGN OF DEFICIT IRRIGATION EXPERIMENTS

Dresdner Schriften zur Hydrologie
Heft 12

Dresdner Schriften zur Hydrologie • Heft 12

TECHNISCHE UNIVERSITÄT DRESDEN

Institut für Hydrologie und Meteorologie Lehrstuhl für Hydrologie

Sabine Seidel (née Walser)

OPTIMAL SIMULATION BASED DESIGN OF DEFICIT IRRIGATION EXPERIMENTS

Dresden, März 2012

Dresdner Schriften zur Hydrologie

Heft 12

Dresdner Schriften zur Hydrologie
ISSN 1612-9024

Herausgeber: Gerd H. Schmitz, Franz Lennartz und Robert Schwarze
Institut für Hydrologie und Meteorologie
Lehrstuhl für Hydrologie
Bergstraße 66, D-01062 Dresden
E-mail: hydrologie@mailbox.tu-dresden.de

Eigenverlag der Technischen Universität Dresden
Umschlaggestaltung: TU Dresden, Universitätsmarketing
Titelfoto: Tobias Hansel
Druck: reprogress, Dresden

ISBN 978-3-86780-282-6
Autorin: Dipl.-Ing.agr Sabine Seidel (geb. Walser)
E-mail: Sabine.Seidel@tu-dresden.de

Optimal simulation based design of deficit irrigation experiments

Dissertation

in partial fulfilment of the requirements for the degree of
Doctor rerum naturalium (Dr. rer. nat.)

submitted to the Faculty of Forest, Geo and Hydro Sciences
Dresden University of Technology

by

Dipl.-Ing. agr. Sabine Seidel

(née Walser)

PhD commission:

Prof. Dr. Christian Bernhofer
Prof. Dr. Dr. Gerd H. Schmitz, TU Dresden
Prof. Dr. Urs Schmidhalter, TU München
Dr. Franz Lennartz, TU Dresden
Prof. Dr. Rudolf Liedl

Examination location and date: Dresden, 03/26/2012

Acknowledgments

First and foremost, I want to thank all members of the Institute of Hydrology and Meteorology, Technische Universität Dresden, for providing an excellent and inspiring working atmosphere. Special and sincere thanks go to my supervisor Professor emeritus Gerd H. Schmitz, head of the Department of Hydrology. I am deeply indebted to him whose useful suggestions, comments and encouragement helped me in all the time of research for and writing of this thesis. I would like to express my sincere gratitude to Professor Urs Schmidhalter of the Chair of Plant Nutrition, Technische Universität München, for his supervision and guidance since my studies of agriculture. His understanding, encouraging and important support throughout this work have provided a good basis for the present thesis. I greatly appreciate the guidance of Dr. Niels Schütze and would like to thank for his detailed and constructive comments and for his valuable advice and friendly help. Furthermore, I would like to express my thanks to all the people at the Chair of Hydrology who made my work at the Institute of Hydrology and Meteorology very pleasant. Especially I am obliged to my room-mate Sebastian Kloss for his help, support, interest, and valuable hints, and to Marcus Fahle, Marcus Guderle and Susanne Liske who supported my work. I wish to express my warm and sincere thanks to Pièrre Ruelle, Jean Claude Mailhol and all the staff members of Cemagref who gave me the opportunity to work with them for a few months in Montpellier, France. Moreover, I like to thank the staff members of the Experimental Station of Dürnast, Freising for kindly providing me advice and data for my research project. The financial support for 3.5 years with a scholarship (Sächsisches Landesstipendium) of the Sächsisches Staatsministerium für Wissenschaft und Kunst is gratefully acknowledged. Finally, I owe special gratitude to Niels Seidel whose patient love and support enabled me to complete this work. I would like to express my deepest gratitude to my parents Sonja and Max and my sister Eva who always encouraged and supported me. I would like to thank all my friends, especially to Rupi, Verena, Berna, Daniel, Martin and Stefan.

I dedicate this work to my family.

Summary

There is a growing societal concern about excessive water and fertilizer use in agricultural systems. High water productivities while maintaining high crop yields can be achieved with appropriate irrigation scheduling. Moreover, freshwater pollution through nitrogen (N) leaching due to the widespread use of N fertilizers demands for an efficient N fertilization management. However, sustainable crop management requires good knowledge of soil water and N dynamics as well as of crop water and N demand.

Crop growth models, which describe physical and physiological processes of crop growth as well as water and matter transport, are considered as powerful tools to assist in the optimization of irrigation and fertilization management. It is of a general nature that the reliability of simulation based predictions depends on the quality and quantity of the data used for model calibration and validation which can be obtained e.g. in field experiments. A lack of data or low data quality for model calibration and validation may cause low performance and large uncertainties in simulation results. The large number of model parameters to be calibrated requires appropriate calibration methods and a sequential calibration strategy. Moreover, a simulation based planning of the field design saves costs and expenditure while supporting maximal outcomes of experiments. An adjustment of crop growth modeling and experiments is required for model improvement and development to reliably predict crop growth and to generalize predicted results.

In this research study, a *new approach for simulation based optimal experimental design* was developed aiming to integrate simulation models, experiments, and optimization methods in one framework for optimal and sustainable irrigation and N fertilization management. The approach is composed of three steps:

1. The preprocessing consists of the *calibration and validation* of the crop growth model based on existing experimental data, the *generation of long time-series of climate data*, and the determination of the *optimal irrigation control*.

2. The implementation comprises the determination and experimental application of the simulation based *optimized deficit irrigation and N fertilization schedules* and an appropriate *experimental data collection*.

3. The postprocessing includes the *evaluation of the experimental results* namely observed yield, water productivity (WP), nitrogen use efficiency (NUE), and economic aspects, as well as a *model evaluation*.

Five main tools were applied within the new approach: an algorithm for inverse model parametrization, a crop growth model for simulating crop growth, water balance and N balance, an optimization algorithm for deficit irrigation and N fertilization scheduling, and a stochastic weather generator. Furthermore, a water flow model was used to determine the optimal irrigation control functions and for simulation based estimation of the optimal field design.

The new approach was implemented within three case studies presented in this work. Although each case study had a different focus, the new approach of simulation based optimal experimental design including the estimation of the optimal irrigation schedule was applied in all three case studies. In the first case study, a crop growth model was calibrated using field data and successfully validated against greenhouse data. The results showed that a transfer of calibrated models to different conditions is feasible when certain adaptations to the differing condition are accomplished. Moreover, potentials of yield (wheat) and WP (barley) – which exceeded the observed ones by 12 % and 41 % – were determined within a simulation-optimization study.

In the second case study, the impact of different drip line spacings in subsurface drip irrigated corn was estimated. Using a two-dimensional water flow model, optimal irrigation control functions for a uniform distribution of the irrigation water while minimizing deep percolation were determined for several initial soil moisture conditions. Moreover, an optimized real-time deficit irrigation schedule which was weekly adapted to precipitation was applied. The optimal design of the experiment enhanced WPs up to 30 % compared to other treatments at the same site. An appropriate field design (drip line spacings of 160 cm) increased profit by 27 % compared to one with a drip line spacing of 120 cm.

In the third case study, simultaneous scheduling of deficit irrigation and N fertilization in order to maximize WP and/or NUE was applied. The results demonstrate that the optimization framework can be successfully utilized since WP and NUE were increased by 22 % and 76 %, respectively. However, simultaneous scheduling of deficit irrigation and deficit N fertilization as well as crop growth modeling in greenhouses are still challenges.

It can be concluded that the new approach combines crop growth modeling and experiments with stochastic optimization. It contributes to a successful application of crop growth modeling based on an appropriate experimental data collection. The presented model calibration and validation procedure using the collected data facilitates reliable predictions. The stochastic optimization framework for deficit irrigation and N fertilization scheduling proved to be a powerful tool to enhance yield, WP, NUE and profit.

Zusammenfassung

In der heutigen Gesellschaft gibt es zunehmend Bedenken gegenüber übermäßigem Wasser- und Düngereinsatz in der Landwirtschaft. Eine hohe Wasserproduktivität kann jedoch durch geeignete Bewässerungspläne mit hohen landwirtschaftlichen Erträgen in Einklang gebracht werden. Die mit der weitverbreiteten Stickstoffdüngung einhergehende Gewässerbelastung aufgrund von Stickstoffauswaschung erfordert zudem ein effizientes Stickstoffmanagement. Eine entsprechende ressourceneffiziente Landbewirtschaftung bedarf präzise Kenntnisse der Bodenwasser- und Stickstoffdynamiken sowie des Pflanzenwasser- und Stickstoffbedarfs.

Als leistungsfähige Werkzeuge zur Unterstützung bei der Optimierung von Bewässerungs- und Düngungsplänen werden Pflanzenwachstumsmodelle eingesetzt, welche die physischen und physiologischen Prozesse des Pflanzenwachstums sowie die physikalischen Prozesse des Wasser- und Stofftransports abbilden. Hierbei hängt die Zuverlässigkeit dieser simulationsbasierten Vorhersagen von der Qualität und Quantität der bei der Modellkalibrierung und -validierung verwendeten Daten ab, welche beispielsweise in Feldversuchen erfasst werden. Fehlende Daten oder Daten mangelhafter Qualität bei der Modellkalibrierung und -validierung führen zu unzuverlässigen Simulationsergebnissen und großen Unsicherheiten bei der Vorhersage. Die große Anzahl an zu kalibrierenden Parametern erfordert zudem geeignete Kalibrierungsmethoden sowie eine sequenzielle Kalibrierungsstrategie. Darüber hinaus kann eine simulationsbasierte Planung des Versuchsdesigns Kosten und Aufwand reduzieren und zu weiteren experimentellen Erkenntnissen führen. Die Abstimmung von Pflanzenwachstumsmodellen und Versuchen ist zudem für die Modellentwicklung und -verbesserung sowie für eine Verallgemeinerung von Simulationsergebnissen unabdingbar.

Im Rahmen dieser Arbeit wurde ein *neuer Ansatz für ein simulationsbasiertes optimales Versuchsdesign* entwickelt. Ziel war es, Simulationsmodelle, Versuche und Optimierungsmethoden in einem Ansatz für optimales und nachhaltiges Bewässerungs- und Düngungsmanagement zu integrieren. Der Ansatz besteht aus drei Schritten:

1. Die Vorbereitungsphase beinhaltet die auf existierenden Versuchsdaten basierende *Kalibrierung und Validierung* des Pflanzenwachstumsmodells, die *Generierung von Klimazeitreihen* und die Bestimmung der *optimalen Bewässerungssteuerung.*
2. Die Durchführungsphase setzt sich aus der Erstellung und experimentellen Anwendung der simulationsbasierten *optimierten Defizitbewässerungs- und Stickstoffdüngungspläne* und der Erfassung der *relevanten Versuchsdaten* zusammen.
3. Die Auswertungsphase schließt eine *Evaluierung der Versuchsergebnisse* anhand ermittelter Erträge, Wasserproduktivitäten (WP), Stickstoffnutzungseffizienzen (NUE) und ökonomischer Aspekte, sowie eine *Modellevaluierung* ein.

In dem neuen Ansatz kamen im Wesentlichen folgende fünf Werkzeuge zur Anwendung: Ein Algorithmus zur inversen Modellparametrisierung, ein Pflanzenwachstumsmodell, welches

das Pflanzenwachstum sowie die Wasser- und Stickstoffbilanzen abbildet, ein evolutionärer Optimierungsalgorithmus für die Generierung von defizitären Bewässerungs- und Stickstoffplänen und ein stochastischer Wettergenerator. Zudem diente ein Bodenwasserströmungsmodell der Ermittlung der optimalen Bewässerungssteuerung und der simulationsbasierten Optimierung des Versuchsdesigns.

Der in dieser Arbeit vorgestellte Ansatz wurde in drei Fallbeispielen angewandt. Obwohl jede der drei Fallstudien einen anderen Bereich fokussierte, wurde in allen das optimale Versuchsdesign einschließlich der Optimierung der Bewässerungspläne implementiert. In der ersten Fallstudie konnte ein an Felddaten kalibriertes Pflanzenwachstumsmodell anhand von Gewächshausversuchen erfolgreich validiert werden. Die Ergebnisse legen nahe, dass eine Übertragung von Modellparametern auf andere Bedingungen möglich ist, sofern bestimmte Anpassungen durchgeführt werden. Zudem wurden potentielle Erträge (Weizen) und *WP*s (Gerste), welche die beobachteten jeweils um 12 % und um 41 % übertrafen, im Rahmen einer Simulations-Optimierungsstudie ermittelt.

In der zweiten Fallstudie wurde der Einfluss von unterschiedlichen Tropfschlauchabständen bei untergrundbewässertem Mais erörtert. Mit Hilfe eines zweidimensionalen Bodenwasserströmungsmodells konnte die Bewässerungssteuerung für unterschiedliche Anfangsbodenfeuchten so optimiert werden, dass die homogene Befeuchtung des Bodens durch die Bewässerung maximiert und zugleich die Tiefenperkolation minimiert wurde. Zudem wurde wöchentlich eine an den aktuellen Niederschlag angepasste Echtzeitdefizitbewässerungsplanung vorgenommen. Mit Hilfe dieser Versuchsdurchführung konnte *WP*, im Vergleich zu anderen Bewässerungsversuchen mit dieser Maissorte an dem Standort um bis zu 30 % erhöht werden. Durch ein optimales Felddesign mit einem Schlauchabstand von 160 cm wurde der Profit, im Vergleich zu einem Abstand von 120 cm, um 27 % erhöht.

In der dritten Fallstudie fand eine Optimierung der defizitären Bewässerungs- und Stickstoffdüngungspläne statt, um *WP* und *NUE* jeweils getrennt voneinander und kombiniert zu maximieren. Die Ergebnisse zeigen, dass sowohl *WP* bis zu 22 % als auch *NUE* um bis zu 76 % erhöht werden konnte. Dennoch stellen die kombinierte defizitäre Bewässerung und Stickstoffdüngung sowie die Pflanzenwachstumsmodellierung im Gewächshaus eine Herausforderung dar.

Der neue Ansatz kombiniert Pflanzenwachstumsmodellierung und Experimente mit stochastischer Optimierung. Er leistet einen Beitrag zu einer erfolgreichen Pflanzenwachstumsmodellierung basierend auf der Erfassung relevanter Versuchsdaten. Die vorgestellte Modellkalibrierung und -validierung unter Verwendung der erfassten Versuchsdaten trug wesentlich zu zuverlässigen Simulationsergebnissen bei. Darüber hinaus stellt die hier vorgestellte stochastische Optimierung von defizitären Bewässerungs- und Stickstoffplänen ein leistungsfähiges Werkzeug dar, um Erträge, *WP*, *NUE* und den Profit zu erhöhen.

Contents

Nomenclature

Abbreviations

CMA-ES Covariance-Matrix-Adaption Evolution Strategy

DAS days after sowing [d]

DS development stage

FAO Food and Agriculture Organization of the United Nations

FULL full irrigation

GET-OPTIS Global Evolutionary Technique for OPTimal Irrigation Scheduling

GPS Global Positioning System

ha hectare

LARS-WG Long Ashton Research Station Weather Generator

OCCASION Optimal Climate Change Adaption Strategies in IrrigatiON

pF common logarithm of the soil tension in hPa [-]

RF rain-fed

SDI subsurface drip irrigation

SVAT model Soil-Vegetation-Atmosphere Transfer model

TDR time-domain reflectometry

vGM van Genuchten/Mualem

Parameters

α vGM model parameter [m^{-1}]

distribution begin and end of fraction of macropores in the soil [cm]

DSLAI0.5 DS at crop area index 0.5 [-]

DSRate1 development rate in the vegetative stage in [d^{-1}]

DSRate2 development rate in the reproductive stage [d^{-1}]

EmrTSum daily sum of soil temperature from sowing to germination at a soil depth of -10 cm [°C]

Fm maximum assimilation rate [(g $C0_2$)/(m^2 h^{-1})]

HvsDS crop height as function of DS [cm]

K_s saturated hydraulic conductivity [$m\,s^{-1}$]

m vGM model parameter [-]

n vGM model parameter [-]

PARext PAR extinction coefficient [-]

pressure end soil tension when flow in macropore ends [cm]

pressure ini soil tension when flow in macropore starts [cm]

Q_{eff} quantum efficiency at low light [(g $C0_2$ m^{-2} h^{-1})/(W m^{-2})]

SpLAI specific leaf weight [(m^2 m^{-2})/(g DM m^{-2})]

θ_r residual water content [cm^3 cm^{-3}]

θ_s saturated water content [cm^3 cm^{-3}]

y_{half} effect on assimilate production of water stress [-]

Symbols

AE water application efficiency [%]

b model bias

c water price [€ ha^{-1}]

C_F labor and energy costs for irrigation [€ ha^{-1}]

C_{FT} fixed production costs [€ ha^{-1}]

CO_2 carbon dioxide

d recommended dose of nitrogen [kg ha^{-1}]

$\triangle D$ daily increments of the development stage

DM dry matter [t ha^{-1}]

d_o observed harvesting dates [days]

d_p predicted harvesting dates [days]

dr development rate at reference temperature and reference day length

EF modeling efficiency

ET_c potential crop evapotranspiration [mm]

ET_{ref} reference crop evapotranspiration [mm]

$fd(D_l)$ modifier accounting for day length D_l

$f_t(T_a)$ modifier accounting for air temperature T_a

GYP grain yield per plant [g per plant]

HI harvest index [%]

h_o observed plant heights [cm]

h_p predicted plant heights [cm]

i situation

I irrigation water amount [mm]

j calibration period

$\triangle l$ drip line spacing [cm]

L amount of mineral N lost to deep percolation [kg ha^{-1}]

LAI leaf area index [-]

M_n total mineralization of soil during the growth period [kg ha^{-1}]

MSE mean squared error

n total number of situations

N nitrogen

NH_4 ammonium

NO_3 nitrate

$\triangle N_{soil}$ nitrogen depletion from the root zone

$\overline{O}$ observed mean value

O_i observed values

P effective precipitation [mm]

PAR photosynthetically active radiation [$\mathrm{W\,m^{-2}}$]

P_c crop price per unit weight [€ $\mathrm{t^{-1}}$]

PD plant density [plants per $\mathrm{m^2}$]

$P_f - P_i$ difference between the total N requirement of the crop and the amount of N absorbed up to time of fertilization [$\mathrm{kg\,ha^{-1}}$]

$\prod$ profit [€ $\mathrm{ha^{-1}}$]

P_i predicted values

P_o observed values

P_{out} output price [€ $\mathrm{t^{-1}}$]

ψ_o observed soil tension [hPa]

ψ_p predicted soil tension [hPa]

PWP permanent wilting point (pF 4.2)

Q^{I-II} fraction of applied water volume flowing from section I to section II

Q_{Mi} predicted value for a percentaged decrease of the parameter

Q_0 predicted result with the predefined parameter

Q_{Pi} predicted value for a percentaged increase of the parameter

q_t optimal irrigation control function

r correlation coefficient

R model error

R radiation [$\mathrm{W\,m^2}$]

$R\,(I)$ revenue per hectare [€ $\mathrm{ha^{-1}}$]

$R_i - R_f$ difference between initial and final soil mineral N [$\mathrm{kg\,ha^{-1}}$]

$RMSE$ root mean square error

RUE radiation use efficiency [%]

SI_{Pi} sensitivity index for percentaged variation of the parameter

Sp seepage [mm]

SW soil water depletion from the root zone [mm]

$\hat{\sigma}_{O_i P_i}$ covariance of O_i and P_i

$\hat{\sigma}^2_{O_i}$ sample estimates of the variance of O_i

$\hat{\sigma}^2_{P_i}$ sample estimates of the variance of P_i

t time per calibration period

T treatment

θ_o observed volumetric soil water content [$\mathrm{cm^3\,cm^{-3}}$]

θ_p predicted volumetric soil water content [$\mathrm{cm^3\,cm^{-3}}$]

$\theta_{t=0}$ initial relative soil water content

TAW total applied water [mm]

TDM_o observed total dry matter [$\mathrm{t\,ha^{-1}}$]

TDM_p predicted total dry matter [$\mathrm{t\,ha^{-1}}$]

TSW 1000-seed weight [g]

V water volume [mm]

V_P percolation [mm]

w weighting factor

W watt

W_{el} deficit level at which the net income equasl the income at full irrigation when land is limited [mm]

W_{ew} deficit level at which the net income equasl the income at full irrigation when water is limited [mm]

W_l amount of water applied where the profit per unit of land will be maximized [mm]

W_m yield maximizing amount of water applied [mm]

WP water productivity [$\mathrm{kg\,m^{-3}}$]

WUE water use efficiency [$\mathrm{kg\,m^{-3}}$]

W_w amount of water applied where the total farm profit increases with the irrigation of additional land [mm]

Y yield [$\mathrm{t\,ha^{-1}}$]

Y_o observed yield [$\mathrm{t\,ha^{-1}}$]

Y_p predicted yield [$\mathrm{t\,ha^{-1}}$]

z position of instrumentation

Z_P objective function for plant parameter derivation

Z_S objective function for soil parameter derivation

1. Introduction

A doubling in global food demand commonly projected for the next 50 years poses huge challenges for the crop production and its sustainability. Agriculturalists are the main managers of the arable lands. However, society is becoming increasingly concerned with agricultural use of water and nitrogen which are two critical resources for crop growth.

Irrigation of crops is crucial to the world's food production and the role of irrigation is expected to increase still further. Today, agriculture accounts for about 70 % of all water withdrawals. Over the next 30 years, 70 % of gains in cereal production are expected to come from irrigated areas (FAO, 2002). Due to the organization, the developing countries are assumed to expand their irrigated land from 202 million ha in 1997 – 99 to 242 million ha by 2030. Most of this expansion will occur in land-scarce areas where irrigation is already important, which makes an increase of water productivity (WP) essential. However, irrigated agriculture faces several challenges like decreasing groundwater tables, lower soil moisture levels due to temperature rise projected for climate change, and salinization.

Nitrogen (N) plays a key role in plant nutrition, it is the mineral element required in the greatest quantity by cereal crops and the nutrient most often deficient. However, today's recovery of N in crop plants is usually less than 30 – 50 % worldwide (Tilman et al., 2002; Fageria and Baligar, 2005), leading to environmental pollution and high crop production costs. Consequently, an efficient management of N resources is an extremely important aspect of sustainable crop production management (Sepaskhah et al., 2006).

Consequently, increasing WP by avoiding excessive deep percolation and unnecessary high root water uptake and enhancing nitrogen use efficiency (NUE) by matching N application to crop N demand while maintaining high crop yields play a key role for sustainable crop production. Considering the complexity of processes like crop growth, soil water and N dynamics, and crop water and N demand, attention should be focused on crop growth simulation modeling. Physiological crop growth simulation models which describe the mentioned processes are powerful tools for sustainable crop production management.

The reliability of the crop growth model predictions depends on an appropriate model calibration and validation based on collected data. Wallach (2006) reported of observed

data as a major source of uncertainty in crop growth modeling. Consequently, well performed field or greenhouse experiments with the decisive data collected in an appropriate resolution are required. Moreover, the relevant experimental data for model calibration and validation to provide robust simulation based recommendations on irrigation and N fertilization management have to be identified.

The adjustment of crop growth models and experiments is not only required to allow reliable generalization of predictions (e.g. when scaling up from field to region) and model transfer (e.g. from greenhouse to field conditions), but also for model improvement and development.

Field and greenhouse experiments are costly, time-consuming and laborious. The overall aim of experiments should be the maximization of the outcomes while saving costs and labor. Simulation models assist the optimal planning of the experimental design. On the one hand, simulation models can determine the optimal position of instruments (e.g. to measure soil moisture). On the other hand, crop growth modeling allows a reduction of the number of treatments due to generalization. However, in practice quite often important data is missing or was not monitored continuously. Moreover, the instrumentation is placed quite often at an inappropriate location leading to a lack of information (e.g. about the horizontal water distribution).

When the relevant experimental data is available, a sequential calibration strategy for soil and plant parametrization with the aim to prevent compensation effects, and an appropriate calibration method to cope with a large number of parameters are required. In addition, for model evaluation further experimental data not used within the calibration procedure are needed.

Adequately calibrated and validated physiological crop growth simulation models assist the optimization of the irrigation and N fertilization management. Stochastic optimization methods allow to estimate potential yields, WP and NUE, and to determine optimal irrigation and N fertilization schedules to maximize them. However, an integrating approach which combines crop growth modeling, experiments for model calibration and validation, and the optimization of irrigation and N fertilization management is missing.

The present research study addresses the mentioned challenges. It presents a *new approach for simulation based optimal experimental design* with the following main objectives:

- better understanding and prediction of crop growth under deficit irrigation and/or deficit N fertilization,
- identification of the relevant experimental data to provide robust simulation based recommendations on irrigation and N fertilization management,

- enhancement of the informative value of experimental data and reduction of expenditure via an optimal experimental design,
- determining of a sequential calibration strategy and an appropriate calibration method for soil and plant parametrization,
- development of a combined framework which integrates crop growth modeling, experiments, and stochastic optimization,
- determination of optimal deficit irrigation and deficit N fertilization schedules to achieve maximal WP, NUE and/or profits.

The main challenge of this research study was to develop the new approach and to apply it within three case studies. The present work is divided into four parts. The first part provides fundamentals regarding the increase of WP and NUE in crop production and the contribution of physiological crop growth models therein. The corresponding literature review mainly focuses on contributions to improved experimental designs and to simulation based deficit irrigation and/or N fertilization scheduling. In the second part, the new approach of simulation based optimal experimental design is presented.

Three case studies where the new approach was implemented are presented in the third part. Case study I focused on model parameter transfer from field to greenhouse conditions. Case study II dealt with real-time deficit irrigation scheduling and the appropriate field design to maximize profit. In case study III, the simultaneous simulation based optimization of deficit irrigation and N fertilization was observed. The discussion, conclusions and outlook in Part IV complete the present research study.

Part I.

Fundamentals and literature review

2. Water productivity in crop production

To increase yields and/or to produce more revenue from less water poses a great challenge for the agricultural sector. Over the past three decades, an increase of *WP* has been achieved largely through higher crop yields per hectare. However, with declining crop yield growth, attention has turned to the potential offered by improved management of water resources (Kijne et al., 2003).

According to the authors, increasing *WP* is a challenge at various levels: The first level is to continue to increase crop yields without increasing transpiration. This can be reached through breeding and certain agronomic practices. The second level is to reduce losses on field, farm and system level, which can be achieved by appropriate irrigation methods, irrigation control and irrigation strategies like controlled deficit irrigation. The third level is to increase economic productivity of water and profit. The latter depend on the relationship between crop yields and applied water and, especially in the case of drip irrigation, on the field design.

2.1. Water productivity

In general, *WP* is defined as the yield over the amount of total water applied. However, there is no common agreement on the use of the term and definitions are based on the background of the researcher or stakeholder; it may convey a physical ratio between yields and (productive or unproductive) water use or between the value of the product and water use (Rodrigues and Pereira, 2009; Zwart and Bastiaanssen, 2004). Moreover, *WP* may be expressed in terms of money (Vazifedousta et al., 2008).

Several definitions of *WP* that are important across scales (from crop to basin) and domains of analysis (from breeder to engineer) can be found in Molden et al. (2003) and (Vazifedousta et al., 2008). Moreover, the regarded period may differ, considering the total water applied from sowing to harvesting, of one year, and may or may not include water applications for salt leaching. In the following, six common definitions of *WP* in $\mathrm{kg\,m^{-3}}$ ($WP_{€}$ in $€\,\mathrm{m^{-3}}$) are introduced.

$$WP = \frac{\mathrm{Y}}{P + I} \tag{2.1}$$

$$WP_{SW} = \frac{\mathrm{Y}}{P + I + SW} \tag{2.2}$$

$$WP_{IRR} = \frac{\mathrm{Y}}{I} \tag{2.3}$$

$$WP_{ET} = \frac{\mathrm{Y}}{ET_c} \tag{2.4}$$

$$WP_{RF} = \frac{Y - Y_{RF}}{P + I} \tag{2.5}$$

$$WP_{€} = \frac{P_c}{ET_c} \tag{2.6}$$

where Y is the actual yield (at 15 % humidity) in $\mathrm{t\,ha^{-1}}$, Y_{RF} is actual yield (humidity of 15 %) in $\mathrm{t\,ha^{-1}}$ of a non-irrigated (rainfed) treatment with similar plant density and row spacing. I is the amount of irrigation water applied, P is effective precipitation, ET_c is the crop evapotranspiration and SW is soil water depletion from the root zone during the growing season due to soil moisture measurements, all in mm. P_c is the price of the marketable yield in € per ha.

A very common definition of WP considers irrigation and precipitation (Eq. 2.1), whereas WP_{SW} additionally considers the soil water depletion from the root zone during the growing period. WP_{IRR} only considers irrigation and ignores precipitation. WP_{ET} relates yield to the actual seasonal crop water consumption. WP_{RF} may be applied if the yield achieved by a non irrigated (rainfed) treatment (Y_{RF}) is subtracted from the yield achieved by an irrigated treatment (Y). To observe economic aspects, $WP_{€}$ may be appropriate.

In general, WP depends on several factors including crop type, climatic demand, soil characteristics, irrigation system, water management, agronomic practices and economic and policy incentives to produce. An increase of WP can be achieved by obtaining more yield per unit of water and by converting non-beneficial depletion to beneficial depletion (water savings), or by reallocating to higher-valued uses (Molden et al., 2003). On-farm strategies like full or controlled deficit irrigation can be evaluated using WP indicators.

The term water use efficiency (WUE) most commonly refers to what is defined above as WP and is mainly used by plant physiologists, molecular biologists and plant breeders (Barker et al., 2003). Figure 2.1 shows a typical curve of WP over grain yield for several field studies conducted in Syria.

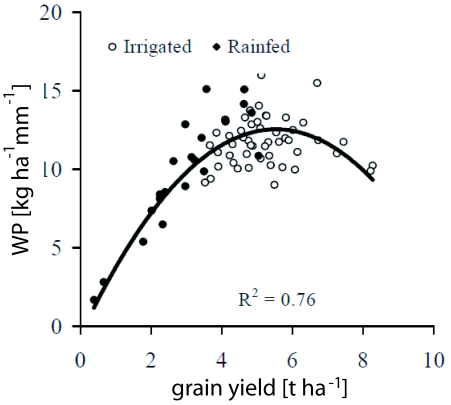

Figure 2.1.: Relationship between crop water productivity and grain yield for durum wheat under supplemental irrigation and rainfed conditions in northern Syria. Adapted from Oweist and Hachum (2004) and revised.

2.2. Increase of crop yield

Regarding the numerator of the *WP* equation, an increase of crop yield can be achieved through breeding and adequate agronomic practices. According to Barker et al. (2003), varietal improvement through plant breeding has been the major source of increase in *WP* over the past three decades. Although breeding in not a task of this study, a brief summary of the current improvements will be given due to its importance in enhancing *WP*.

Most of the yield increases have not been due to increases in biomass but almost entirely due to improved ratio of grain to biomass (harvest index, *HI*) which may now be approaching its theoretical limit in many of the major crops (Kijne et al., 2003). Further challenges are the improvement of the photosynthesis (e.g. by adopting C_4 metabolism into C_3 crops), improving spike fertility, the increase of *RUE*, the minimization of floret abortion, and a prevention of yield losses e.g by biotic stress resistance (Reynolds et al., 2009).

Moreover, breeding focused on the improvement of the resistance to diseases of cultivars, and their adaptation to abiotic stresses like droughts, water-logging, soil acidity, salinity and extreme temperatures (Reynolds et al., 2009). Many promising properties for coping with drought stress have been introduced through conventional breeding. These include changing the length of the growing season and the timing of the sensitive stages, selecting for small leaves and early stomata closure to reduce transpiration, for high root activity and deep rooting systems, and selecting for tolerance to salinity. A commonly feature of the breeding programs is the use of wild relatives of crop plants as sources for drought tolerance. Moreover, biotechnology is considered to have a great potential for the development of

drought tolerant crops, but this potential has not been fully realized yet. Slow progresses in breeding for drought tolerance is often attributed to the genetic complexity of the trait and its interaction with the environment. One way of genetically increasing *WP* is to modify canopy development in order to reduce evaporation from the soil surface (Kijne et al., 2003).

There are several agronomic practices for increasing *WP*. According to the review article of Hatfield et al. (2001) it is possible to increase *WP* by 25 to 40 % through soil management practices mainly due to enhanced precipitation use efficiency in rainfed agriculture. Farmer may apply water-conservation practices like alternate-row irrigation, reduced or zero tillage, raised beds mulching, residue management, appropriate fertilization and direct seeding to enhance *WP*. Further strategies include controlled deficit irrigation, supplemental irrigation and water harvesting for productive purposes. In practice, many of these strategies and practices are combined since they are complementary. However, some measures are location-specific or only applicable for a limited set of soils and crop conditions, and some do have tradeoffs in terms of higher labor and management demands (Kijne, 2003).

2.3. Irrigation

Crop irrigation – which can be conducted through various methods – is defined by irrigation control parameters, namely the timing of the irrigation, the duration of the irrigation event, the discharge rate (or intensity) and thus the amount of irrigation water applied. For a sustainable and profitable irrigated crop production, the irrigation method, the irrigation control parameters, and the field design (drip line and row spacings) have to be considered.

2.3.1. Irrigation methods

The irrigation method determines to what extent it is possible to reduce evaporation from the soil surface while maintaining adequate soil moisture levels in the root zone to avoid drought stress (Kijne, 2003). There are three commonly used methods to supply irrigation water to the plants: surface irrigation, sprinkler irrigation and (sub)surface drip irrigation (Brouwer et al., 1988).

Surface irrigation is the application of water by gravity flow to the surface of the field. Either the entire field is flooded (basin irrigation, e.g. to grow rice) or the water is fed into small channels (furrows, e.g. to grow corn or vegetables) or strips of land (borders, e.g. for growing pasture or alfalfa). Regarding natural conditions, evenly and not sloped lands and clay soils with low infiltration rates are ideally suited to surface irrigation. Soil evaporation is supposed to be high at surface irrigation.

At **sprinkler irrigation**, water is pumped through a pipe system and then sprayed over or under the crop canopy. Different types of sprinkler irrigation are center pivot, under or over tree orchard sprinkler systems and hand or lateral move portable systems, amongst others. Sprinkler irrigation is suited for most row, field and tree crops. It is adaptable to any farm-able slope and best suited to sandy soils with high infiltration rates and irrigation water free of suspended sediments. However, it is not suitable for soils which easily form a crust, and under very windy conditions.

With **drip irrigation**, water is conveyed under pressure through a pipe system to the fields, where it drips slowly onto the soil through emitters or drippers which are located close to the plants. Only the immediate root zone of each plant is moistened. Drip irrigation is suited to irrigating individual plants, trees or row crops such as vegetables and sugarcane.

Subsurface drip irrigation (SDI) enables the application of small amounts of water to the soil through drip lines placed below the soil surface and hence increases the water application efficiency. Many study results indicate that crop yield for SDI was greater than or equal to other irrigation methods, and less water was required in most cases (Camp, 1998; Camp et al., 2000; Lamm and Trooien, 2003). Moreover, soil evaporation is supposed to be lowest for SDI. However, SDI systems show higher investment costs than other pressurized irrigation systems.

Management skills, economic factors, crop types and site conditions (soil type, slope, climate, water quality and availability) mainly influence the choice of an irrigation method (Burt, 2000). However, there is a huge potential for saving water while maintaining or increasing yields if farmers change from surface irrigation to localized irrigation. Investment in water efficient technologies is best facilitated when water is valuated and priced appropriately (Tilman et al., 2002).

The water application efficiency (AE) – which is the average amount of irrigation water that contributes to a stated target (e.g. soil moisture deficit) divided by the average depth of irrigation water applied (Burt, 2000) – is generally highest within drip irrigation, followed by sprinkler and surface irrigation. O'Neill et al. (2008) compared furrow, SDI and sprinkler irrigation systems and reported of 30 % saved total amount of water for SDI and 8 % for sprinkler compared to furrow irrigation, respectively.

2.3.2. Irrigation scheduling and irrigation control

For an optimal management of deficit irrigated crop production systems, the problem of intra-seasonal **irrigation scheduling** under limited seasonal water supply is of main importance. An optimal distribution of the limited irrigation water during the growing season adapted to the actual weather conditions, the soil properties and the drought susceptibility of the crop reduces the applied irrigation water amount while achieving high yields

(Schmitz et al., 2007; Schütze and Schmitz, 2010). Hence, allocation and distribution of irrigation water are of primarily importance for irrigation farmers. The irrigation schedule defines the timing of the irrigation depending on the actual soil water content and the crop water demand.

Irrigation schedules may be determined based on evapotranspiration or pan evaporation (observed or calculated), based on direct measurements of soil and plant properties, simulation based or sensor based. For the latter, irrigation water will be applied when a certain threshold (e.g. soil tension) is reached, which is measured by instrumentation (e.g. tensiometers installed in the root zone). Different irrigation scheduling strategies are possible, for instance full irrigation where the crop water demand is matched while drought stress is avoided, partial root drying where alternate wetting and drying of parts of the root zone takes place (Kirda et al., 2005), and controlled deficit irrigation (English, 1990), see Section 2.4.

Irrigation control is a part of irrigation scheduling. It affects the soil moisture distribution which is influenced by the control parameters discharge rate (or intensity), duration of the irrigation and thus the amount of irrigation water applied. An optimal irrigation control aims to reach a homogenous distribution of the soil water in the root zone with minimal losses due to deep percolation or surface runoff.

In drip irrigation, the discharge rate mainly influences the water bulb. In general, high discharge rates result in an increased lateral component of the wetting front. The water flow under drip irrigation is a three dimensional problem but becomes two-dimensional when considered as a line source (e.g. parallel drip lines). The discharge rates are often predefined due to the installed irrigation system whereas irrigation timing, duration and water amounts are variable.

For an optimal irrigation control (low percolation and homogenous distribution of the soil moisture), the field design (row spacing and the location of source e.g. drip line or furrow) plays an important role, especially for drip irrigation systems. It affects yields, *WP* and the profit of an irrigation system.

2.3.3. The influence of the field design on profitability

In some cases, increased profits by investment and material savings may be more meaningful to farmers compared to water savings. The economic profitability of capital intensive SDI systems is dominated by the installation and material costs of the irrigation system. Hereby, the costs mainly depend on the field design, whereas the gains mainly depend on the marketable yields. Thus, the aim is to determine a field design and an adequate irrigation control and schedule which maximize yields while minimizing costs due to installation and material of the irrigation system.

For that, understanding of the pattern of the moistened soil volume around the source of water is essential. Irrigation control, heavily dependent on the soil hydraulic properties, has a high impact on the pattern of the moistened soil volume around the source. The latter can be obtained by either direct measurements of the soil wetting front in the field or by simulation modeling (Elmaloglou and Diamantopoulos, 2009). According to Lamm and Trooien (2003), increasing the spacing between drip lines is one of the most important factors in reducing high investment costs of SDI systems. The optimal drip line spacing is related to the crop and its rooting pattern, the soil characteristics, soil water redistribution, in-season precipitation, the comparative costs of drip lines, yields and possible off-site hazards caused by deep percolation (Lamm and Trooien, 2003). Stone et al. (2008) found that the distance between corn rows and SDI drip lines greatly influenced the crop growth and grain yield, both decreasing significantly with growing distance.

Camp (1998) published a comprehensive review of several publications for over 30 crops and various soil types with drip line spacings of SDI systems ranging from 0.25 to 5 m for different soils where most results indicated that alternate row spacing of about 1.5 m would be appropriate for most uniformly spaced row crops like corn. This provides one drip line for every two rows, usually located between the rows. Darusman et al. (1997) and Camp et al. (1998) reported that subsurface placement of drip lines at wider spacings has significant potential for profitable irrigation. In their review article, Lubana and Narda (2001) represent results of modeling soil water dynamics under drip irrigation. The authors propose that multidimensional analysis of soil moisture dynamics under drip irrigated fields should be converted into computer algorithms. Singh et al. (2006) developed a simulation model using a semi-empirical approach and a dimensional analysis method for determining the geometry of the moistened soil zone under SDI line sources.

Many studies have been made to analyze economic profitability of irrigated crop production (Lu et al., 2004, 2005; Stone et al., 2006; Clop et al., 2009). Worth mentioning is the study of Bontemps and Couture (2002) dealing with the problem of estimating irrigation water demand. An economic model including farmer behavior description and an optimization algorithm was used to compute a database serving for the estimation of profit functions via a nonparametric derivation procedure. The authors defined the farmers profit per hectare as a function of output price, yield, fixed production costs and costs due to labor and energy for each watering.

Rodrigues and Pereira (2009) analyzed the feasibility of deficit irrigation of sprinkler irrigated corn, wheat and sunflower through an analysis of the economic water productivity. The authors predicted several scenarios for deficit irrigation to determine the net irrigation requirements using a simulation model which computed ET_c and performed a soil water balance simulation based on the dual crop coefficient approach. Soil hydraulic properties were obtained through Pedro-transfer functions relative to a soils database and the scenar-

ios were predicted for the observed weather conditions. The *WP*s were then determined for various combinations of yield and irrigation amounts.

According to Provenzano (2007), surprisingly little attention has been paid to estimate the optimal soil water distribution under SDI to avoid poor management and low *WP*s. Furthermore, studies on simulation based optimization of both, irrigation control and irrigation scheduling, and a combination with an evaluation of field designs aiming to maximize profit and *WP* are not available.

2.4. The concept of controlled deficit irrigation

A promising irrigation scheduling strategy to maximize *WP* is controlled deficit irrigation where water is applied mainly during drought sensitive growth stages of a crop. Outside these periods, irrigation is limited or even unnecessary if precipitation provides a minimum supply of water (English, 1990). This practice may be preferable to full irrigation when water supplies are limited or irrigation costs are high. Exemplary, Kirda et al. (2005) report of water savings of 50 % due to the applied deficit irrigation strategy by only reducing corn grain yield by 10 – 25 % compared to full irrigation.

The management of controlled deficit irrigation is very different from conventional irrigation management. The irrigation manager must decide what level of deficit to allow and must recognize when that level has been reached. The choice may be made to allow deficits to occur at some times and not others, and/or to apply water at a lower level than full irrigation in order to achieve the higher efficiencies and lower costs that are possible under deficit irrigation. The potential benefits of deficit irrigation derive from three factors: reduced costs of production, greater irrigation *WP* and the opportunity costs of water (English and Raja, 1996).

Crop water production functions (CWPFs) are a compact presentation of the relationship between irrigation practices and yield (Schütze et al., 2011b). CWPFs show the relationships between crop yield and the water supplied for one specific site and one year (see Fig. 10.12). English and Raja (1996) used collected data of three field experiments to derive CWPFs to estimate the degree to which the crops could be under-irrigated without reducing income. After an initial sharp increase, the productivity reaches its maximum at a given amount of supplied water to the plant and then decreases or remains at a relatively high level with further increasing water supply (Zhang, 2003). The curving of the function at higher levels of applied water reflects various losses (deep percolation, greater evapotranspiration) as water use approaches full irrigation (English, 1990). The decline of the curve occurs due to lodging, reduced aeration in the root zone, leaching of nutrients and diseases associated with wet soils (English, 1990).

Revenue functions relate applied water to gross income (Fig. 2.2). Since crop yield multiplied by a constant (crop price) is equal to gross income (Eq. 2.7), the relation between irrigation water use and gross income will have the same general shape as the CWPF. The revenue function is the product of the CWPF and the crop price, defined by the equation:

$$R(I) = P_c \cdot Y(I) \tag{2.7}$$

where $R(I)$ is revenue per hectare [€ ha^{-1}], $Y(I)$ is the crop yield per unit land (expressed as a function of applied irrigation water I) in t ha^{-1}, I is the depth of irrigation water applied per unit land [mm] and P_c is the price per unit weight paid for the crop [€ t^{-1}] (English and Raja, 1996). The cost function represents fixed and operating costs. The profit, which is calculated by subtracting costs from revenues, is indicated by the vertical difference between these two functions.

Figure 2.2 which is based on English and Raja (1996) illustrates the approach of controlled deficit irrigation. It shows a curved revenue and a straight cost function. W_m is the yield maximizing amount of water applied where the marginal WP is zero (an additional application of water will not produce more yield). At the level of W_1, the profit per unit of land will be maximized (land limited case). At this point, the slope of the cost curve equals the slope of the gross income curve.

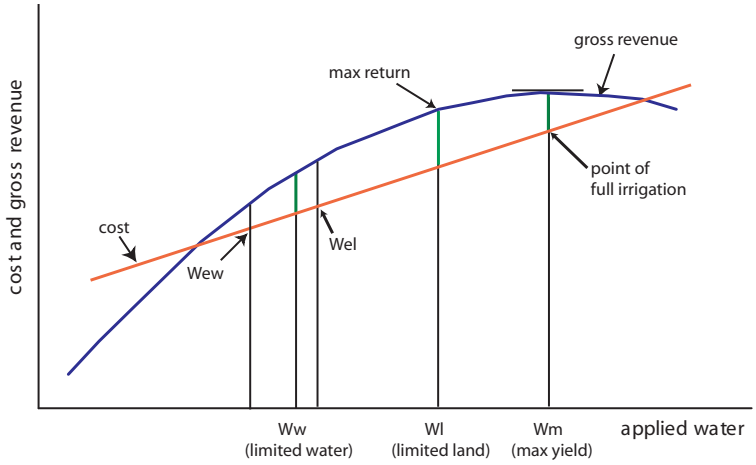

Figure 2.2.: Revenue and cost functions adapted from English and Raja (1996). The curved line (blue) shows the revenue function which relates gross income to applied water, and the straight line (red) shows the cost function which represents fixed and operating costs.

According to the authors, efficiency and profit both increase with reduced levels of applied water, thus the net income per unit of applied water is increased. If water is reduced below W_l, a point will be reached (W_{el}) where the net income per unit land equals the net income from full irrigation. The same is true for the case of W_{ew}, the amount of water applied where net income equals the income at full irrigation when water is limited.

Within the range between W_m and either W_{el} or W_{ew}, deficit irrigation will be more profitable than full irrigation. If saved water could bring additional land (with the same increased profit per unit of land) under irrigation, the total farm profit increases (water limited case). In this case, irrigation would take place at level W_{w}. The net income from the additional land represents the opportunity costs of water. Obviously, the marginal *WP* is of high importance.

According to English (1990), the essential problem of controlled deficit irrigation are the highly variable and unpredictable CWPFs. Due to the variability of weather, soils, initial soil moisture and distribution uniformity, the soil water stored in the root zone is difficult to predict. Combining these uncertainties with the variability of crop responses to weather and diseases, yield water relations become quite unpredictable. These uncertainties imply economic risks. The risk associated with deficit irrigation can be minimized through proper irrigation scheduling and by avoiding water stress during growth stages when crops are especially sensitive to drought stress. For most crops, the critical crop growth stages are the seedling and flowering stages (Barker et al., 2003). The risk with deficit irrigation may be low in cases when the response curve of crop yield to water supply has a wide plateau, hence a considerable amount of water can be saved without a significant yield reduction compared with full irrigation (Zhang, 2003).

However, there are circumstances where deficit irrigation is not appropriate, e.g. for potato where soil moisture deficits may cause changes in tuber shape. Otherwise, drought stress may enhance quality in other crops. It improves protein percentage of wheat and other grains, increase fiber length and strength of cotton, and increases the sugar percentages in grapes, sugar beets and other crops (English and Raja, 1996).

3. Nitrogen use efficiency in crop production

Most plants need nitrogen – a component of protein and nucleic acid and important for crop growth – in relatively large amounts as compared to other plant nutrients (this is not true for legumes which are able to fix atmospheric nitrogen). N is the most widely used fertilizer nutrient and the demand for it is likely to grow in future (Sepaskhah et al., 2006).

Agriculture is a major source of greenhouse gas emissions, for instance 14 % of annual N emissions is released by agricultural soils. More than 20 % of the European Union countries ground waters are facing excessive N concentrations, with a continuous increasing trend in the most intensive areas of livestock breeding and fertilizer consumption (Casa et al., 2011). Recovery of N in crop plants is usually less than 30−50 % worldwide – due to its loss by volatilization, leaching, surface runoff, and denitrification – and not only responsible for higher cost of crop production, but also for environmental pollution (Tilman et al., 2002; Fageria and Baligar, 2005).

Leaching is expected to be the dominant way in which N is lost in soil-plant systems. According to Mmolawa and Or (2000), mass flow (or convective transport) is the dominant process by which nutrients are transported to plant roots. Nitrate$-N$ (NO_3-N) is relatively nonreactive and therefore susceptible to movement through diffusion and mass transport in the soil water. Nitrate components are readily soluble in water and they are usually not adsorbed on the negatively charged soil clay particles (Mmolawa and Or, 2000). Thus, NO_3-N is likely to be lost through surface water runoff and deep percolation of water.

A significant amount of the applied N is lost from agricultural fields harming ecosystems by causing eutrophication and low-oxygen conditions in lakes and rivers. Gaseous N losses mostly involve denitrification and volatilization of NH_4. To cope with these problems, an increase of nitrogen use efficiency and a reduction of N leaching in agricultural production are required.

3.1. Nitrogen use efficiency

Nitrogen use efficiency (NUE) in kg grain kg N^{-1} is defined as

$$NUE = \frac{Y}{N + \triangle N_{soil}} \tag{3.1}$$

where Y is the actual grain yield, N the amount of N fertilizer applied, and $\triangle N_{soil}$ the N depletion from the root zone during the growing season. Low NUE values are a result of excessive N present in the soil-plant system (Johnson and Raun, 2003).

A similar behavior of applied N and applied water regarding yield can be observed. According to Tilman et al. (2002) and Hatfield and Prueger (2001), NUE decreased with increasing N application rates due to diminishing returns. Noteworthy, high yielding varieties also express their genetic potential to achieve high yields at low N levels (Reynolds et al., 2009). However, there is still little understanding of the interactions between crop water use and N application rates (Hatfield and Prueger, 2001). This is especially true for crop growth under limited water and N supply.

3.2. N fertilization management

There are several methods to determine the required amount of N fertilizer for a growing period. A widely used method to determine the amount of N fertilizer is the **N balance method** where the recommended dose d of N is

$$d = (P_f - P_i) - (M_n + R_i - L - R_f)$$

where $P_f - P_i$ is the difference between the total N requirement of the crop and the amount of N absorbed up to time of fertilization, M_n is total mineralization of soil during the growth period, $R_i - R_f$ is the difference between initial and final soil mineral N, and L is the amount of mineral N lost to deep percolation (Wallach, 2006).

A key component of sustainable agriculture is **precision agriculture** (also called precision farming or site-specific management) which offers great potential to increase control over N losses (Van Alphen and Stoorvogel, 2000). Precision agriculture aims to optimize field-level management and to reduce environmental loading by applying fertilizers and pesticides during the greatest crop demand at or near the plant roots, and in smaller or more frequent applications, and thus reduces losses from excessive applications and from reduction of losses due to nutrient imbalances and reduced chemical loading (Bongiovanni and Lowenberg-Deboer, 2004). Environmental impacts are reduced due to the consideration of the field's spatial variability, while farmers obtain a return of their investment by saving on fertilizer and phytosanitary costs.

The adoption of precision agriculture techniques for N fertilization management has the potential for improving agronomic, economic and environmental efficiency (Casa et al., 2011). Different approaches have been proposed for the N fertilization management like "on-the-go" methods, in which the fertilizer amount to be applied is determined instantaneously, by taking into account crop status as detected for example by tractor-mounted sensors, or methods based on the definition of N prescription maps built on spatial information layers (Casa et al., 2011).

Moreover, a better matching of nutrient inputs to crop demand in time and space can be supported by simulation modeling (Van Alphen and Stoorvogel, 2000; Ravikumar et al., 2011).

3.3. Combination of controlled deficit irrigation and deficit N fertilization

To optimize *WP*, cultivar, water use and nutrient management decisions have to be appropriately combined. According to Hatfield et al. (2001), increases in *WP* may come from improved plant growth and yield that are a result of a proper soil nutrient status. *WP* can be improved through N management, which in turn, influences yield components like grain number per unit of land area.

Sepaskhah et al. (2006) determined the three-dimensional relationship between yield as a function of total water amount (irrigation water and seasonal precipitation) and applied N plus residual N by multiple regression analysis (Fig. 3.1). The resulting function can be called **crop water nitrogen production function** (**CWNPF**, Walser and Schütze (2010)). Figure 3.1 clearly shows that the highest yield was not achieved at full irrigation and full N fertilization, and that high yields can be reached with limited water and N applications.

However, there is a large divergence of results shown in the literature on *WP* related to soil nutrient management (Hatfield et al., 2001). An evaluation of the impact of N management strategies on crop yield should be more closely linked to *WP* to develop better management practices. According to Hatfield et al. (2001), challenges for research are to understand the water nutrient interactions and to incorporate this information into tools that can assist producers in making management decisions that will lead to increased *WP* and *NUE*.

Obviously, there is still research required regarding the combination of controlled deficit irrigation and deficit N fertilization and the optimal distribution of both during one crop growth period to maximize *WP* and *NUE*.

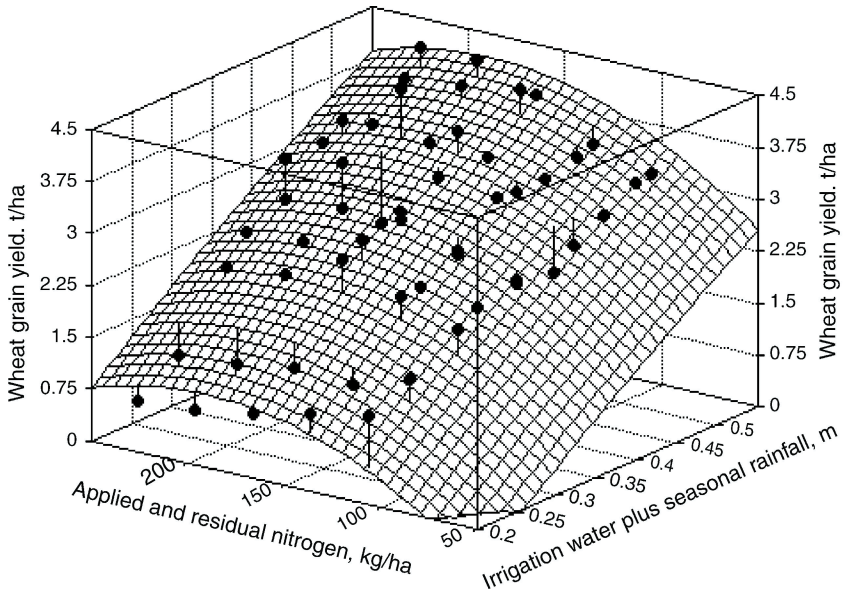

Figure 3.1.: Three-dimensional relationship between grain yield of wheat as function of applied water plus seasonal precipitation and applied N plus residual N based on three years of field experiments adapted from Sepaskhah et al. (2006).

4. Crop growth modeling

The fact that laboratory and field measurements necessary for assessment of deep percolation and N leaching from agricultural fields are expensive and possible crop growth predictions have prompted the development of models capable of simulating crop growth and water and N dynamics.

4.1. Physiological crop growth models

In the past 30 years, physically based agrohydrological models have been developed to simulate crop growth and soil water processes (Vazifedousta et al., 2008). They are based on equations that describe the processes involved in crop growth and development, amongst others (Wallach, 2006). Crop models support the evaluation of different irrigation and fertilization management or climate scenarios and hence allow to generalize predictions of crop production. Moreover, they are powerful tools to test hypotheses and to describe and understand complex systems and processes. For instance, they help to understand the relationship between applied water, applied N and yield. Moreover, crop growth models are used in decision support systems for prognostic planning of crop production e.g. for irrigation and fertilization scheduling or to predict possible impacts of climate change on agriculture (Semenov, 2007, 2009).

Crop growth models models differ widely in complexity and original purpose. The way the processes are modeled can be based on empirical relationships (empirical models), or on fundamental scientific principles explaining the growth course from the underlying physiological processes in relation to the environment (mechanistic models). Dynamic system models include state variables which are described over time by equations (e.g. soil mineral N), explanatory variables which are measured or observed (e.g. field capacity), and parameters which are by definition constant across all situations of interest (e.g. efficiency of photosynthesis of a certain variety) (Wallach, 2006). In the following, the mechanistic model Daisy and the empirical model Pilote are introduced and applied in various field and greenhouse experiments.

4.1.1. Model description of SVAT model Daisy

Daisy (Hansen, 2002) is a well-tested physically based 1D and 2D Soil-Vegetation-Atmosphere Transfer (SVAT) model for simulating water balance, heat balance, solute balance, organic matter turnover, and crop development. The mechanistic model consists of the three main components bioclimate, vegetation and soil, and demands for site specific driving variables (weather and management data) and vegetation and soil parameters (Fig. 4.1).

Daisy allows several different process descriptions of water flow, evapotranspiration, crop growth and solute transport. In total it is able to simulate about 100 different processes with about 200 process models, implying that different process models are available for some of the processes (Styczen et al., 2010). The model can make use of either hourly or daily climate data. The minimum data required in order to estimate potential evapotranspiration are global radiation and air temperature.

The water balance model comprises a surface and a soil water balance and includes water uptake by plants. Precipitation, irrigation and evapotranspiration represent driving variables or boundary conditions. Simulation of the matrix flow is based on the finite difference solution to solve Richards equation for water flow which combines Darcy´s law with conservation of mass. The second order partial differential Richards equation requires knowledge of two boundary conditions. The upper boundary is determined by the infiltration rate, soil evaporation rate or, in the case of ponding, a known potential at the surface. The lower boundary is defined by a known potential if the position of the groundwater table has been externally defined. In this case, capillary rise can occur. Another possible lower boundary condition is free drainage. Then, percolation is determined by the conditions within the soil itself. Water flow in the unsaturated zone can take place as Darcy flow within the soil matrix or as gravity flow in distinct macropores.

According to Styczen et al. (2010), Daisy can be applied in a one-dimensional version for ordinary sprinkler or drip irrigation but not for partial root drying, which requires two dimensions and simulation of abscisic acid production in roots. Under the SAFIR project (Ragab, 2010), Daisy was extended with the possibility of two-dimensional simulations based on finite volume solutions to the same equations used in Daisy 1D. The implemented 2D model named rectangle supports a simple, rectangular grid of vertical and horizontal lines. The 1D functionality of Daisy is available if the user chooses the vertical movement model.

Transpiration is determined by the root water uptake which depends on the rooting depth and the rooting density distribution in connection with the soil water status within the rooting depth. The water uptake is modeled by the single root approach which assumes that water moves radially towards the root surface where it is taken up at the same rate it arrives at the surface. Water stress occurs when the water uptake by the roots is less

than the potential transpiration. The water stress model is based on the assumption that transpiration and CO_2 assimilation are governed by stomata responses, and that stomata are open when intercepted water is evaporated from the leaf surfaces.

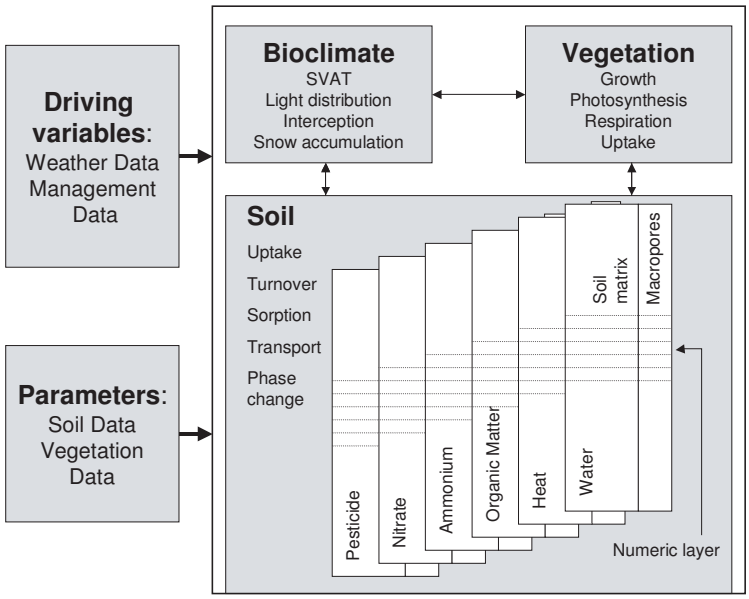

Figure 4.1.: Main components of SVAT model Daisy (Hansen, 2002).

The crop model implemented in Daisy, by far the most complex model in Daisy, is able to simulate photosynthesis, plant respiration, temporal variation in leaf area index (LAI), rooting depth, root density, dry matter production, and crop N demand and content, amongst others. The crop model simulates the canopy photosynthesis as a function of LAI, global radiation, air temperature and water and/or N stress. The photosynthesis model is based on the calculation of light distribution (calculated on the basis of Beer´s law) within the canopy and single light response curves. In the calculation of the light distribution, the canopy is divided into distinct layers each containing a fraction of the total LAI. When a canopy consists of more than one crop, the absorbed light allocated to each of the crops in a given canopy layer is proportional to the considered crop´s contribution to the total LAI within the layer. The gross photosynthesis is calculated by accumulating the contribution from the individual layers. Stomata opening is a function of various parameters, including abscisic acid in xylem sap, which is generated in the root system as a function of the water uptake and pressure potential in the soil (Styczen et al., 2010). This process is particularly important when describing partial root drying. Moreover, the exchanges of sensible heat, water vapor, and CO_2 between the canopy, soil, and atmosphere are predicted.

The growth period in the plant growth model is divided into three temperature and day length based development stages (DS), namely emergence (DS 0), flowering (DS 1) and maturation (DS 2). A database in Daisy provides parameters for several crops like wheat, barley, corn, rye and, potato, each with more than 60 parameters. The daily increments of the development stage, $\triangle$D, are calculated from equation

$$\triangle D = dr\, f_t\,(T_a)\ \cdot\ f_d(D_l) \tag{4.1}$$

where dr is the development rate at reference temperature and reference day length, $f_t\,(T_a)$ and $fd\,(D_l)$ are modifiers accounting for air temperature, T_a, and day length, D_l, respectively. The modifier functions are obtained by linear interpolations between tabulated values of response versus environmental factor (Hansen, 2002).

Plant uptake of mineral N is determined either by the N demand of the plant or the availability of mineral N in the soil. The former is predicted on the basis of a potential N content in the plant, which is determined on the basis of the accumulated dry matter production and the development stages of the plant, and the actual N content of the plant. The latter is determined on the basis of the actual content of mineral N in the soil and the transport (mass flow and diffusion) from the bulk soil to the roots. The plant may take up N in the form of either ammonium or nitrate. The nitrogen uptake model is based on the approach of potential nitrogen demand, which is predicted by the crop model. The actual nitrogen uptake is either determined by this potential demand or by the availability of nitrogen in the rooting zone, i.e. the rate at which nitrogen can be transported to the root surfaces and subsequently taken up by the root system. It is assumed that uptake in the form of ammonium has priority over uptake in the form of nitrate. However, as ammonium generally is strongly sorbed in most soils most of the uptake normally takes place as nitrate.

N stress occurs when the N concentration in the plant gets below a certain threshold. The leaching of ammonium and nitrate is predicted by the solute transport model hence transport in macropores may be included or excluded. A no-transport option for ammonium can be selected in order to save computer time. Leaching is a result of numeric solutions to the convection-dispersion equation for ammonium and nitrate, respectively. The upper boundary condition of this second order partial differential equation is always a flux condition, the lower boundary condition is a zero-gradient condition.

4.1.2. Model description of crop growth model Pilote

Pilote (Mailhol et al., 1997) is an empirical crop growth model for simulating soil water balance at a daily time step and for predicting yield. According to Mailhol et al. (2011), the soil water balance module consists of a three-reservoir system. The upper reservoir

(0 – 10 cm soil depth) determines the water balance at the soil surface. Evaporation at the soil surface is governed by the LAI. The second reservoir accounts for the root section and its capacity increases with root growth. The third reservoir represents the remaining part until the maximum rooting depth. Water is first taken from the shallow reservoir until total depletion by evaporation and crop water uptake, then from the second one by the crop only. The soil water balance among reservoirs is calculated on the basis of field capacity and permanent wilting point (PWP). Maximal evapotranspiration and actual evapotranspiration are involved in the water stress index calculation. Under water stress conditions, actual evapotranspiration linearly decreases from maximal evapotranspiration with the depletion level of the second reservoir. The water stress index is obtained accordingly to this crop water uptake approach, and is exported to the crop module as environment coefficient.

The crop module is based on the simulation of the LAI and its response to the water stress index. Grain yield is evaluated by multiplying the total dry matter calculated based on Beer's law with the harvest index. The climatic data required are precipitation, global radiation, average temperature and reference evapotranspiration.

Pilote was developed and applied to the experimental site of the research institute Cemagref (Montpellier, France). Model validation has been carried out for different crops under different environmental contexts (Mailhol et al., 1997, 2004; Khaledian et al., 2008; Taky et al., 2009). The results of Khaledian et al. (2008) indicate that Pilote satisfactorily simulates LAI, soil water reserve, grain yield and dry matter yield at that site. For example in 2008, Pilote predicted the grain yield well for two SDI treatments (predicted vs. observed grain yields): 14.7 vs. 15.0 t ha^{-1} and 15.2 vs. 15.1 t ha^{-1}, respectively.

4.2. Optimal experimental design for model parametrization

For model calibration, validation and further crop growth predictions, sufficiently large and representative data sets are crucial. An adequate parametrization of the soil and the plant parameters based on field or greenhouse data is required to improve the fit between predicted and observed data. However, literature dealing with an adequate experimental design in order to generate data for model parameter estimation is very scarce.

4.2.1. Experimental design

Plant growth and plant performance can continuously be analyzed with a so-called precision phenotyping platform, which comprises non-destructive sensing of plant and soil properties combined with large containers which exclude rooting depth constraints for shallow

rooting plants (Schmidhalter, 2005a; Thoren and Schmidhalter, 2009; Winterhalter et al., 2011). Such a platform facilitates the screening of crops under highly managed conditions (Schmidhalter, 2005b). Winterhalter et al. (2011) report of monitoring canopy water mass and canopy temperature of well-watered and drought stressed corn using non-destructive high throughput sensing carried out on GPS based vehicles. Although these platforms are developed primary for breeding and management decision purposes, the application of such promising platforms for crop modeling is still rare.

In the study presented by Vazifedousta et al. (2008), the collected field data for calibration and validation of a physically based agrohydrological model are listed in a table, including the collection method, frequency and purpose of the data. Furthermore, the authors describe the calibration procedure using a non-linear parameter estimation program for an inverse estimation of the soil parameters and irrigation depth. Part of the crop parameters were determined on the basis of field observations and/or literature. For an analysis of three different on-farm strategies namely deficit irrigation scheduling, optimal irrigation intervals and extend of cultivated area, the calibrated model was applied. For that, all parameters but the irrigation time (fixed intervals of 5, 10, 15 and 20 days) and irrigation depths (fixed from 1 to 20 cm) were held constant. A program for multiple running of the model using different parameter values each time was linked to the agrohydrological model. Under water scarcity conditions, reducing the cultivated area resulted in the highest *WP* and economic gains. Although data input, soil parameter calibration and model validation are described extensively, detailed information about the experimental design and the location of instrumentation are not provided. Moreover, continuous measurements in high resolution are missing (e.g. soil moisture was only observed weekly via a gravimetric method).

4.2.2. Model parameter estimation

According to Wallach (2006) – a comprehensive book which deals with the evaluation, analysis, parametrization and application of dynamic crop models – a major problem is to obtain the values of the model parameters using both field data and the information about crop growth and development. The author claimed that parameter estimation is a rather open field with only few proposed solutions. He reported that the complexity of crop models mostly leads to many parameters, often more than the number of data. Heidmann et al. (2008) reported that the processes related to crop growth are complex and difficult to parametrize. According to the authors, systematic or automatic calibration and validation procedures for crop models are rare.

Wallach (2006) emphasizes methods and defines some rules for crop model parameter estimation. The first step is to determine the different types of information available which

is provided by literature or expert knowledge, and experimental data. The second step is to select the parameters to be estimated from data via methods like sensitivity analysis, statistical choice or based on literature. The third step is to choose a method for parameter estimation, for example least squares, maximum likelihood or Bayesian methods (Wallach, 2006).

To deal with the problem of local modeling where the parametrization for a given variety may become too site-specific regarding climate, soil and management, Heidmann et al. (2008) firstly created a common parametrization and secondly a variety-specific parametrization. The authors presented the results of a calibration of the model Daisy on potato experiments where three years of field experiments with drip irrigation and fertigation were carried out at six different sites across Europe, cultivating seven varieties of potato. Heidmann et al. (2008) assumed that this variety-specific parametrization reflect the variety properties better and are less site-specific, more representative and more suitable for use across Europe.

4.2.3. Model parameter estimation based on greenhouse data

Crop cultivation in greenhouses or vegetation halls shows several advantages over field experiments including favorable micro climate for year round cultivation, controllable conditions and simplified data collection. Greenhouse experiments can be used e.g. for testing management strategies at a small scale to transfer findings to open fields and/or to a regional scale. Despite the demand of physically based process description within mechanistic crop growth models, simplifications of the equations and different morphological behavior of plants grown in greenhouses result in model limitations. Still a great challenge is the transfer of model parameters from open field to greenhouse conditions or vice versa which will be carried out in case study I.

The most important factor affecting crop growth and development in greenhouses is solar radiation since, apart from its indirect effect on greenhouse air temperature, it governs transpiration and photosynthesis (Baxevanou et al., 2010). Especially intercepted total solar radiation per crop is hardly measurable and comparable to field conditions due to exposed plant positions (e.g. in border rows or free-standing pots) which may complicate crop growth modeling tremendously. Many studies refer to the relationship between yield and radiation. In general, plants neighboring gaps yield higher because they intercept a larger amount of light (Pommel et al., 2001). Drouet and Kiniry (2008) investigated the effect of planting pattern of corn on the proportion of light intercepted associating a three dimensional model of shoot geometry with a three dimensional light model. Simulations showed that crop development stage and row spacing had a strong effect on daily transmitted photosynthetically active radiation (PAR) fraction.

Kumar et al. (2010) developed a simple dynamic greenhouse climate model and gave a brief overview about simulation models to predict the micro climate of a greenhouse. However, they are primary used as a design tool for greenhouses. To cope with the greenhouse conditions, the model HORTISIM (Gijzen et al., 1998) used climate conditions inside the greenhouse which were calculated from outdoor weather for the calculation of crop production and climate in greenhouses.

According to Wang and Boulard (2000), radiative heterogeneity in greenhouses significantly influences crop activity, particularly transpiration and photosynthesis. Quanqia et al. (2008) report that crop yield was positively related to radiation use efficiency (RUE) for many conducted experiments. The authors observed significant differences between different planting patterns with respect to the amount of PAR intercepted by plants. The factor limiting the increase in yield was not the deficiency of light radiation but the low RUE. Jongschaap et al. (2006) analyzed the conversion of direct solar PAR into diffuse radiation and its effects on greenhouse crop production with simulation models. The authors reported that the diffuse radiation penetrated more deeply into the canopy than direct solar PAR increasing photosynthesis rates at deeper layers.

There is still research required regarding the optimal field design and data collection for reliable model calibration and validation, but also regarding appropriate model parameter estimation. Moreover, transfer of model parameters from open field to greenhouse conditions or vice versa is still a challenge.

5. Irrigation and N fertilization scheduling

Irrigation and N fertilization schedules can be determined empirically (e.g. by evapotranspiration measurements or the N balance method), sensor based, or simulation based using crop growth models. In the following, several meaningful studies dealing with irrigation and N fertilization scheduling will be presented.

5.1. Irrigation scheduling

Many studies deal with irrigation scheduling (Evett et al., 2000; Sepaskhah et al., 2006; Nalliah et al., 2009; Payero et al., 2009). Camp (1998) represented a comprehensive review of several empirical studies analyzing over 30 crops cultivated under subsurface drip irrigation (SDI) systems. The author reported that irrigation frequencies ranging from one to seven days had no effect on corn yield when soil water storage was managed within acceptable stress levels. According to Lamm and Trooien (2003), higher water use efficiencies were obtained with a 7 day frequency compared to 1, 3 and 5 day frequencies due to better storage of in-season precipitation and reduction in deep percolation below the root zone. Ayars et al. (1999) refer to reduced deep percolation using high frequency irrigation.

Schütze and Schmitz (2010) reported of automated soil and plant-based sensing irrigation scheduling methods to increase WP. The authors solved the multidimensional and nonlinear optimization problem of deficit irrigation scheduling (finding the ideal schedule for maximum crop yield with a given water volume) with a tailor made stochastic framework called OCCASION (Optimal Climate Change Adaption Strategies in IrrigatiON) which offers straightforward application facilities. The framework consists of a weather generator, the evolutionary optimization algorithm GET-OPTIS and a mechanistic crop growth model. The optimization technique allows for risk assessment in yield reduction considering different sources of uncertainty like climate, soil conditions and management. The resulting stochastic crop water production functions (SCWPF) allow to assess the impact of climate variability on potential yield. The framework was successfully applied to an experimental site in southern France, where the impacts of predicted climate variability on irrigated corn

were analyzed via SCWPFs. However, the authors argue that more sophisticated methods are required within deficit irrigation. Garcia y Garcia et al. (2009) propose that further work should focus on the impact of the intra-seasonal weather variability and soil water conditions during different crop stages.

5.2. N fertilization scheduling

Regarding N fertilization, many studies indicate that *NUE* could be increased by better matching nutrient inputs to crop demand in time and space (Cassman et al., 2002; Tilman et al., 2002). Several studies have been published dealing with the determination of either more empirically or simulation based estimated irrigation and/or N fertilization schedules.

According to the noteworthy study of Van Alphen and Stoorvogel (2000), research regarding simulation of the N dynamics in agricultural soils and in particular simulating N leaching has focused mainly on the site-specific variation of single fertilizer dosages applied to the start of the growing season with varying rates based on soil sampling, yield measurements or both. Thus, the authors combined real-time mechanistic simulations with the approach of management units to optimize N fertilization in both temporal and spatial dimensions. The method used a mechanistic simulation model to quantify soil mineral N levels and N uptake rates on a real-time basis. N fertilization took place once a critical threshold level of N was reached within the simulation results. The thresholds were defined in relation to actual uptake rates. Spatial variation was considered through the approach of management units with relatively homogeneous characteristics regarding water regime and nutrient dynamics based on intensive soil sampling. Real-time simulations were conducted on a weekly basis to optimize the fertilizer application. Fertilizer rates were determined using historical weather data from an average year. In field experiments conducted with wheat, precision N fertilization proved efficient in reducing fertilizer inputs by 23 %, while slightly improving grain yields (+3 %) compared to traditional fertilization. In this study, timing proved a more influential factor than spatial precision due to low spatial variability.

5.3. Combination of irrigation and N fertilization scheduling

An interesting empirically based study for irrigation and N fertilization scheduling was provided by Sepaskhah et al. (2006). The authors determined equations for the determination of water and N levels at variable seasonal precipitation leading to maximum crop yield or profit in a semi-arid region. The optimum water use of deficit irrigated winter wheat was obtained by an economic analysis using water production and cost functions

as described by English (1990). An empirical yield model (yield versus applied water and N, see Fig. 3.1) approximately showed the true response of yields based on three years of experiments. In order to include the seasonal precipitation in the analysis for optimum irrigation water and applied N, the production function including irrigation water plus seasonal precipitation and applied N plus soil residual mineral N was obtained by multiple regression analysis. The greatest income per unit applied water was achieved under water limiting condition (and it increased with increasing seasonal precipitation), whereas increase for land limiting condition was negligible. Optimum N application was influenced mainly by the residual N but not by the water or land limiting conditions. Further, the possibility of using determined functions to serve for irrigation planning scenarios for crops was investigated. For deficit irrigation planning, the authors determined the relationship between seasonal precipitation and the sum of precipitation in the autumn and winter seasons. To predict the seasonal precipitation, they applied the determined equation and the observed sum of precipitation in the autumn and winter season.

There are several simulation models that calculate both, irrigation water and N requirements, from a number of simple water balance models like CROPWAT (Smith, 1992), over single-field models such as Daisy Hansen (2002) or SALTMED (Ragab, 2010) to decision support models (Styczen et al., 2010; Gayler et al., 2002).

In the EU project SAFIR[1], a management model for decision support was developed that combines irrigation and N fertilization management according to modeled soil water conditions and plant N status combined with risk assessment related to pathogens and heavy metals (Styczen et al., 2010). It may be used for pre-investment analysis or to evaluate a growing strategy for the next season. The model system uses the SVAT model Daisy (Hansen, 2002) which calculates crop growth, water and N dynamics and heavy metals and pathogen fate in the soil. Crop profits are calculated and multiple scenario runs (e.g. different irrigation and fertilization strategies) are possible. The model system integrates analysis of when to irrigate and fertigate, based on soil water content criteria, assessment of crop N requirements, and analyzes of health and environmental aspects of the applied water. The model includes an irrigation and N fertilization strategy module linked to Daisy for its water and N demands. The irrigation start and stop threshold values for initiating and ending irrigation depend on the irrigation strategy, the irrigation method and the crop and were determined partly through discussions with SAFIR participants and partly from a study of the measurements of soil water in the experimental plots in combination with the soil retention properties. N fertilization is initiated when the predicted actual N content in the plant is lower than the critical N content of the plant plus the daily N requirement multiplied by the typical time space between two fertigations.

[1] www.safir4eu.org

Although many studies deal with empirically or simulation based estimation of irrigation and/or N fertilization scheduling, in none of the studies known by the author, a simulation based stochastic optimization of irrigation and N fertilization under water and/or N limited conditions was implemented. Moreover, the simultaneous optimization of the irrigation schedule and the irrigation control was not accomplished yet for drip irrigation (it has only been studied noteworthy for furrow irrigation systems by Schmitz et al. (2007)). Furthermore, real-time simulation based irrigation scheduling considering weather variability was not accomplished yet.

Part II.

New approach for simulation based optimal experimental design

For successful simulation based crop production management, the quality and quantity of the experimental data used for model calibration and validation is crucial. Within the present research study, a *new approach for simulation based optimal experimental design* was developed aiming to integrate simulation modeling, experiments and stochastic optimization methods for sustainable irrigation and N fertilization planning and management. The approach consists of three steps:

1. The preprocessing consists of the *calibration and validation* of the crop growth model based on existing experimental data, the *generation of long time-series of climate data*, and the determination of the *optimal irrigation control*.

2. The implementation comprises the determination and experimental application of the simulation based *optimized deficit irrigation and N fertilization schedules* and an appropriate *experimental data collection*.

3. The postprocessing includes the *evaluation of the experimental results* namely observed yield, water productivity (WP), nitrogen use efficiency (NUE), and economic aspects, as well as a *model evaluation*.

Five main tools were applied within the approach: (i) the stochastic population-based algorithm CMA-ES (Hansen, 2008) for inverse model parametrization, (ii) the crop growth models Daisy (Hansen, 2002) or Pilote (Mailhol et al., 1997) for simulating crop growth, water and N balance, (iii) the tailor-made evolutionary optimization algorithm GET-OPTIS (Global Evolutionary Technique for OPTimal Irrigation Scheduling, (Schütze et al., 2012)), and (iv) the stochastic weather generator LARS-WG (Semenov and Barrow, 2002) to generate long time-series of climate data. Moreover, (v) water flow model Hydrus 2D (Šimůnek et al., 1999) was applied to determine the optimal irrigation control functions and for simulation based planning of the experimental design.

The new approach was applied within three case studies presented in Part III. Beyond the implementation of the approach, case study I focused on model parameter transfer from field to greenhouse conditions. Case study II dealt with real-time deficit irrigation scheduling and the optimal field design to maximize profit. In case study III, the simultaneous simulation based optimization of deficit irrigation and N fertilization was observed. Figure 5.1 shows the concept of the new approach.

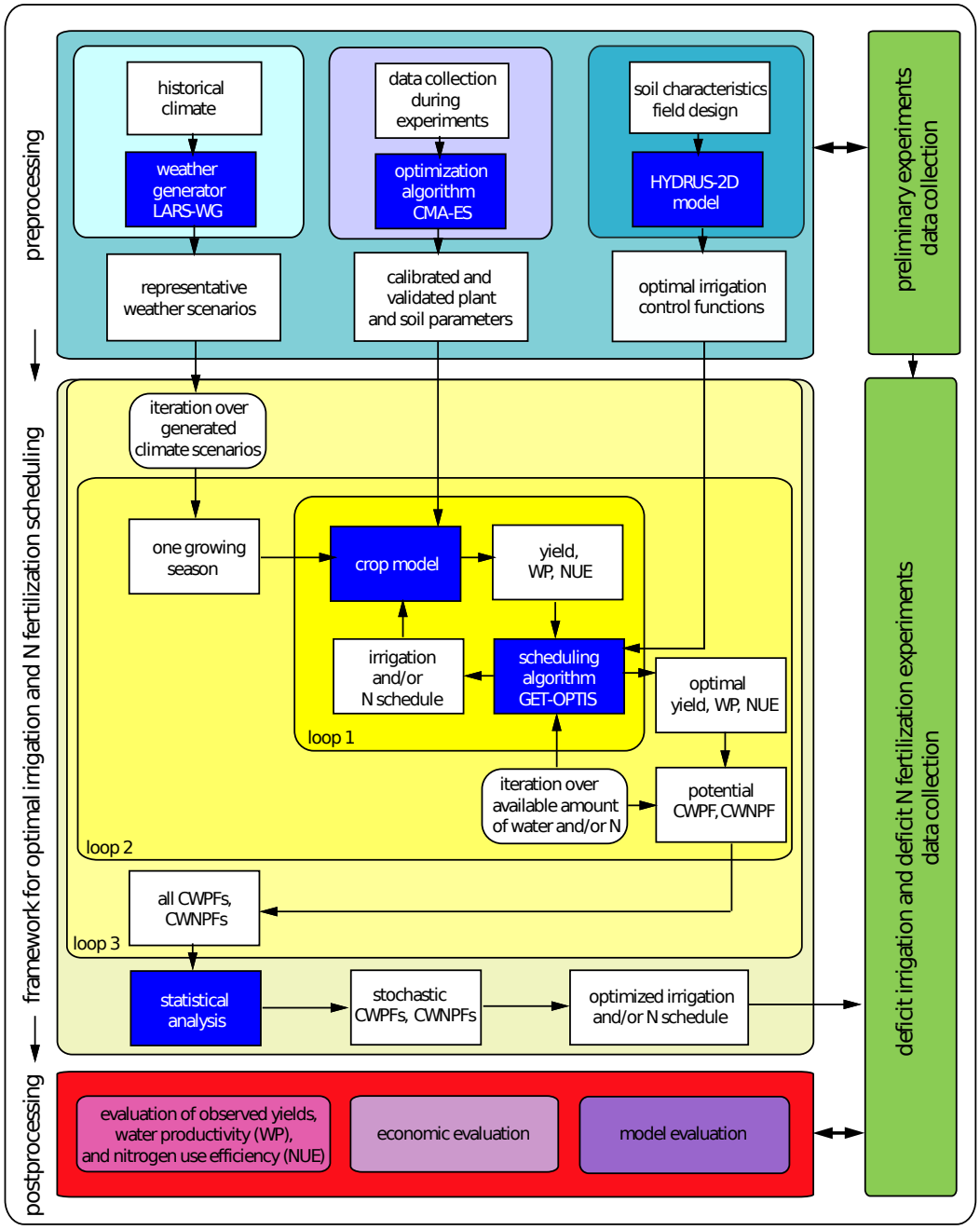

Figure 5.1.: The new approach of simulation based optimal experimental design consisting of (i) the preprocessing, (ii) the determination and experimental application of the optimized deficit irrigation schedules and (iii) the postprocessing.

6. Preprocessing steps

In the following, the preprocessing steps namely model parametrization and assessment, the generation of long time-series of climate data and the determination of the optimal irrigation control function are presented.

6.1. Model parametrization and assessment

According to Wallach (2006), **explanatory variables** which are measured or observed have to be distinguished from **parameters** which are by definition numerical values and constant across all situations of interest. Parameter values, which often have a biological or physical meaning, result from estimation procedures or sometimes from bibliographic reviews or expert opinions and their precision is necessarily limited by the variability and possible lack of adequacy of the available data.

Wallach (2006) reported that different approaches for parametrization are feasible: i) to decide a prior on a small number of parameters to be adjusted, ii) to do a sensitivity analysis of the model and adjust the most sensitive parameters, iii) to start with a small number of parameters and then add additional parameters, one at a time, if they reduce residual variance and iv) to adjust as many parameters as necessary to fit the model within a fixed margin. Within frequenist approaches of parameter estimation (e.g. least squares, maximum likelihood), the parameter value is approximated by using a sample of data and the parameters are fixed (contrary to random variables) which leads to a point estimate of the model parameters. By contrast, the Bayesian approach is more popular for estimation parameters of complex mathematical models (Wallach, 2006). Within the Monte Carlo method, a random set of parameter values is generated from which one derives an approximate of the posterior distribution. According to the author, Monte Carlo methods are probably the most promising methods for estimating parameters of complex nonlinear models.

Within the present study, inverse modeling was applied to estimate soil and plant parameters. Hereby, the differences of observed and predicted values are minimized iteratively to enable accurate and fast adaption of model parameters to observed data (Vrugt and Dane,

2005). The stochastic population-based method for optimal parameter estimation of non-linear and non-convex functions **Covariance-Matrix-Adaption Evolution Strategy** (**CMA-ES,** Hansen (2008)) belonging to the class of evolutionary algorithms was applied.

The objective functions for soil and plant parameter estimations were the weighted sums of the root mean square errors (*RMSE*) between observed and predicted values. The *RMSE* is defined as

$$RMSE = \sqrt{\frac{\sum_{i=1}^{n}(O_i - P_i)^2}{n}} \tag{6.1}$$

where O_i and P_i are the observed and predicted values that are compared for situation i and the total number n for $1 \leq i \leq n$ (Wallach, 2006). A low *RMSE* value indicates that the estimated value tend to be close to the observed value. An advantage of *RMSE* is that is has the same units as P_i and O_i. However, large differences are heavily weighted. Within the calibration procedure, the objective function has to be minimized.

The sequence of the calibration procedure is crucial. In general, soil and plant parameters have to be calibrated separately to prevent mutual compensation. That is confirmed by Heidmann et al. (2008) who recommend to start calibrating the water dynamics and then continue with the crop growth and N dynamics. Soil parameters have to be calibrated with plausible soil water data at the best not influenced by vegetation (e.g. prior to sowing or after harvesting).

6.1.1. Calibration of the soil parameters

The soil parameters are crucial for simulation based irrigation scheduling. For accurate soil parameter determination, it is important that plausible soil water content and/or soil tension data are available for a long period (including precipitation or irrigation events) and for a high range of values. The calibration of the van Genuchten/Mualem (vGM) parameters namely saturated and residual water contents θ_s and θ_r [$\mathrm{cm^3\,cm^{-3}}$], α and n [-][1], and the saturated hydraulic conductivity K_s [$\mathrm{m\,s^{-1}}$] makes a sensitivity analysis unnecessary. However, a sensitivity analysis may be required for further model parameters (e.g. macropore parameters). In this study, soil parameters were calibrated prior to plant parameters.

[1] Parameter m of the van Genuchten/Mualem model is taken as $m = 1 - 1/n$. The vGM model parameter n is not equal to the symbol n (total number) in the objective functions.

6.1.1.1. Objective function for soil parametrization

The objective function for the estimation of the soil parameters consists of the weighted sum of the *RMSE* of the measured and predicted soil water contents and/or soil tension data for all positions and for all calibration periods. The following Equation 6.2 shows the objective function based on soil water content and soil tension data:

$$Z_S = \sum w_j \cdot \sqrt{\frac{\sum_{i=1}^{n}(\theta_{o,i}(z,\, t_j) - \theta_{p,i}(z,\, t_j))^2}{n}} + \sum w_j \cdot \sqrt{\frac{\sum_{i=1}^{n}(\psi_{o,i}(z,\, t_j) - \psi_{p,i}(z,\, t_j))^2}{n}} \tag{6.2}$$

where Z_S is the objective function for the derivation of the vGM parameters and parameter K_s, w_j the weighting factor (may vary for every term) for every calibration period j, $\theta_{o,i}$ and $\theta_{p,i}$ [$\mathrm{cm}^3\,\mathrm{cm}^{-3}$] are the observed and predicted soil water contents, $\psi_{o,i}$ and $\psi_{p,i}$ are the observed and predicted soil tensions [hPa] for situation i and the total number n for $1 \leq i \leq n$, and z, t_j are the position of the instrumentation and time per calibration period j.

The plausibility of the observed data is of high importance. Implausible data e.g due to ground frost needs to be removed. Moreover, a representative position of instrumentation in various soil depths for extensive observations (irrigation events, root water uptake, deep percolation) is crucial. Long time-series of collected data contribute to good calibration results.

6.1.2. Calibration of the plant parameters

Several crop modules and default values for plant parameters are included in crop growth models, but due to large differences between varieties, there may be a need for parametrization. To identify the most sensitive plant parameters of the applied crop growth model, a sensitivity analysis has to be carried out. Depending on the requirements of the applied crop growth model, observed data of yields, total biomass, *LAI*, length of growth period, plant heights and development stages amongst others enhance the quality of the calibration results. However, as the yield is of major importance it should be weighted heavily in the objective function of the calibration.

In this study, calibration mainly took place on the basis of grain yield and total biomass, whereas simulation results were validated using all available explanatory variables (e.g. grain yield, total biomass, *LAI*, length of growth period and plant heights). In the three

case studies, plant parameters were calibrated using observed plant data from the same cultivar grown in past growing periods or at different sites. The plant parameters were validated against field or greenhouse data.

6.1.2.1. Sensitivity analysis

According to Wallach (2006), a sensitivity analysis identifies the parameters which have a small or a large influence on the output. It has various objectives: i) to check that the model output behaves as expected when the input varies, ii) to identify which parameters need to be estimated more accurately, and iii) to identify input variables which need to be observed with maximum accuracy (Wallach, 2006). A sensitivity analysis is helpful to understand the model behavior when it is used for prediction or for decision support. The most intuitive method is to vary one factor at a time while the other factors are fixed. The principle of a sensitivity analysis is to calculate a sensitivity index for each parameter and to select parameters with high sensitivity index values. The sensitivity index for percentaged variation of the parameter SI_{Pi} is defined as

$$SI_{Pi} = \frac{\mid Q_{Pi} - Q_{Mi} \mid}{Q_0} \tag{6.3}$$

where Q_{Pi} is the predicted value for a percentaged increase of the parameter, Q_{Mi} is the predicted value for a percentaged decrease of the parameter and Q_0 is the simulation result with the predefined parameter.

The higher the sensitivity index, the higher the sensitivity of the parameter respective the parameter variation. The sensitivity of a model with respect to the model component of interest is likely to depend on additional components. For instance, the sensitivity of a crop model is often highly dependent on the values of climate or soil variables (Wallach, 2006).

6.1.2.2. Objective function for plant parametrization

The objective function for the plant parameter estimation consists of the weighted sum of the *RMSE* of the available observed and predicted plant variables:

$$\begin{aligned} Z_P = \quad & w_j \cdot \sqrt{\frac{\sum_{i=1}^{n} (TDM_{o,i}\text{-}TDM_{p,i})^2}{n}} + w_j \cdot \sqrt{\frac{\sum_{i=1}^{n} (h_{o,i} - h_{p,i})^2}{n}} \\ & + w_j \cdot \mid Y_{o,i} - Y_{p,i} \mid + w_j \cdot \mid d_{o,i} - d_{p,i} \mid \end{aligned} \tag{6.4}$$

where Z_P is the objective function for plant parameter derivation, w_j is a weighting factor (may vary for every term) for every calibration period j, $TDM_{o,i}$ and $TDM_{p,i}$ are the observed and predicted values of total dry matter [t ha^{-1}], $h_{o,i}$ and $h_{p,i}$ are the observed and predicted plant heights [cm], $Y_{o,i}$ and $Y_{p,i}$ are the observed and predicted grain yields [t ha^{-1}], and $d_{o,i}$ and $d_{p,i}$ are the observed and predicted harvesting dates [days] for situation i for $1 \leq i \leq n$.

The weighting varied depending on the plant variable (e.g. higher importance of yield compared to plant height) and how representative and plausible the collected data was (e.g. according to sample size).

6.1.3. Model assessment

To determine the value of the applied crop model, a model validation (or evaluation) is required. The term validation concerns determining whether a model is adequate for its intended purpose or not whereas the term evaluation refers to how well a model represents crop responses (Wallach, 2006). For better understanding, in this study the term validation is used within soil and plant parametrization (preprocessing), whereas the term evaluation is used within the deficit irrigation experiments where the calibrated and validated model is applied (postprocessing). The numerical and graphical measures for model validation and evaluation are identical.

A first approach for model assessment is to compare model predictions with observed data. Model assessment can include graphs comparing observed and predicted values, numerical measures of quality or qualitative conclusions about the quality of a model. The following model assessment measures are based on the comprehensive book on model evaluation of Wallach (2006) if not indicated otherwise.

6.1.3.1. Graphical comparisons between observed and predicted values

The agreement between model results and observations can be evaluated visually from plots of observed and predicted data. Graphs of model predictions can be plotted against observed values, including the calculation of the regression. Moreover, observed and calculated values can be plotted against time or another variable, for instance days after sowing. To examine model errors and their variability, residue graphs (model error plotted against observed value) may be used (see Fig. 13.1). They are useful to show trends in residues if model errors are plotted against observed value or explanatory variables (e.g. total water applied). If the model is correctly specified, there should be no trends in the residues.

6.1.3.2. Numerical comparisons between observed and predicted values

In general, a limited number of model results are of primary interest, e.g. yield or water demand. An evaluation of the agreement between observed and modeled variables include qualitative as well as quantitative techniques (Heidmann et al., 2008). Wallach (2006) divides four groups of measures: i) simple measures of the difference between observed and predicted values (e.g. model bias, root mean square error), ii) measures which are normalized (e.g. modeling efficiency, correlation coefficient), iii) measures that can be decomposed into separate contributions and thus give additional information about the sources of error (e.g. concordance correlation coefficient) and iv) measures based on a threshold of model quality (e.g. total deviation index). According to the author, the idea of using more than one measure in order to bring out different aspects of model agreement is favorable.

The residue R (or model error) is defined as the difference between observed and predicted values:

$$R = O_i - P_i \tag{6.5}$$

where O_i and P_i are the observed and predicted values that are compared for situation i. The model bias (b) measures the average difference between several observed and calculated values:

$$b = \frac{1}{n}\sum_{i=1}^{n}(O_i - P_i) \tag{6.6}$$

where n is the total number of situations for $1 \leq i \leq n$. A positive b attests an underestimation by the model, a negative b conversely attests a model over prediction. However, under- and over predictions may compensate and mislead to a model bias near zero.

The above mentioned *RMSE* (Eq. 6.1) and the mean square error (*MSE*) defined as

$$MSE = \frac{\sum_{i=1}^{n}(O_i - P_i)^2}{n} \tag{6.7}$$

eliminate the problem of compensation. Low *RMSE* and *MSE* values indicate that the predicted values tend to be close to the observed values.

A widely used normalized measure, the modeling efficiency (*EF*), is given by

$$EF = 1 - \frac{\sum_{i=1}^{n}(O_i - P_i)^2}{\sum_{i=1}^{n}(O_i - \overline{O})^2} \tag{6.8}$$

where $\overline{O}$ denotes the observed mean values. *EF* ranges from $-\infty$ to 1. An *EF* between 0.8 and 1 is generally viewed as an acceptable level of performance, whereas an $EF \leq 0$ is viewed as unacceptable. For a perfect model, *EF* is 1.

Another often used normalized measure is the correlation coefficient (r) between observed and predicted values defined by

$$r = \frac{\hat{\sigma}_{O_i P_i}}{\hat{\sigma}^2_{O_i}\, \hat{\sigma}^2_{P_i}} \tag{6.9}$$

where $\hat{\sigma}^2_{O_i}$, $\hat{\sigma}^2{}_{P_i}$ and $\hat{\sigma}_{O_i P_i}$ are the sample estimates of the variance of O_i , the variance of P_i and the covariance of P_i and O_i, respectively. The range of r is $-1 \leq r \leq 1$, whereas r=1 indicates that there is a perfect linear relationship between P_i and O_i. For further measures, please refer to Wallach (2006).

6.1.4. Preliminary simulations for an optimal experimental layout

For an adequate data collection, the position of the instrumentation is important. The optimal position of the instrumentation depends on the crop and its rooting characteristics, the characteristics of the soil, the irrigation method and the irrigation scheduling.

If a sensor based irrigation strategy is applied (irrigation takes place if a certain threshold e.g. soil tension is reached), an optimal position for this sensor has to be determined. This sensor should be located where the highest root density and water uptake scan be found during the growth period. A switch to a sensor installed at a lower soil depth with growing rooting depths may be favorable. Some sensors should be shifted from the main axis of irrigation to reflect lateral distribution.

An infiltration experiment assists the finding of an optimal position or choice of the instrumentation for sensor based irrigation scheduling. The high water applications of the infiltration experiment lead to an intense vertical and lateral distribution of the soil water.

The optimal realization of the infiltration experiment can be supported by preliminary simulation runs using model Hydrus 2D (Šimůnek et al., 1999). These simulations assist to determine the optimal position for or choice of sensors and an optimal implementation of the infiltration experiment (duration of irrigation, total water amount and pulsed irrigation). Provisional soil parameters estimated using laboratory analysis results (Schaap et al., 2001) can be used for first simulation runs.

Moreover, the infiltration event prior to sowing supports the determination of the soil parameters. Due to the infiltration experiment, a high range of observed values (at best from dry initial conditions to saturation) occurs which assists the soil parametrization results.

The measured soil moisture and/or soil tension data of the infiltration event are used for soil parameter calibration runs. If the accomplishment of an infiltration event is impractical, further available soil moisture and/or soil tension data are required.

6.2. Generation of long time-series of climate data

LARS-WG (Semenov and Barrow, 2002) is a stochastic weather generator which can be used to generate representative weather scenarios for long term climate characteristics based on historical climate data of a specific site, under both current and future climate conditions (Racsko et al., 1991; Semenov and Barrow, 2002). It can be used to generate long time-series suitable for e.g. the assessment of agricultural risk and impacts of climate change (Semenov and Barrow, 1977; Lawless and Semenov, 2005; Semenov, 2009).

For that, observed daily weather for a specific site is analyzed to compute site parameters. These site parameters are used to generate synthetic daily weather for that specific site which statistically resemble observed weather. All synthetic climate data undergo a variety of statistical test (t-test, F-test) for means and variances of weather variables. In the present case studies, observed daily weather data recorded over 15 (case studies I and III) and 17 years (case study II) were used to set up the weather generator to generate up to 500 realizations of daily weather (solar radiation, minimum and maximum temperature and precipitation).

6.3. Determination of the optimal irrigation control functions

The optimal irrigation control functions for different drip line spacings were determined using **water flow model Hydrus 2D** (Šimůnek et al., 1999). The latter is a widely used numerical model for simulating the transient two-dimensional movement of water and nutrients in soil and has been tested under various experiments including subsurface drip irrigation. Hydrus 2D uses the Galerkin finite-element method to solve Richards equation (Šimůnek et al., 1999).

In case study II, the optimal irrigation control functions for two different field designs with drip line spacings of 120 cm (corn row spacing of 75 cm) and 160 cm (corn row spacing of 60 cm) were estimated. Three dimensional Hydrus 3D simulation runs were conducted to show the formation of an axially symmetric water bulb along the drip line, in the same manner representable by Hydrus 2D. Hydrus 2D was then utilized to derive characteristic irrigation control functions for the determination of optimal irrigation times and water

amounts. The objective was to provide an almost uniform distribution of the irrigation water supplying irrigation water to all crop rows with a high adequacy. Meanwhile, deep percolation provoked by heavy water application amounts and/or elevated initial soil moisture contents had to be minimized. For details refer to case study II (Section 11.5).

Within the other case studies, the adaptation of the irrigation control to the field design played a minor role since drip lines where placed at the crop rows (case study I, III) or sprinkler irrigation lead to uniform irrigation water applications (case study I).

7. Stochastic optimization framework

For an optimal management of crop production, the problem of intra-seasonal irrigation scheduling under limited water supply plays a key role. To cope with that, a stochastic framework for optimal irrigation scheduling was applied aiming to optimally distribute irrigation water one growing period to achieve maximum yield or *WP*. In case study III, the optimization framework was applied to simultaneously and optimally distribute irrigation water and *N* over one growing period to reach maximum *WP* and *NUE*.

7.1. Stochastic optimization framework

For optimal irrigation and *N* fertilization scheduling, the planning tool **OCCASION** (Optimal Climate Change Adaption Strategies in IrrigatiON) of Schütze and Schmitz (2010) was adapted.

7.1.1. Optimization algorithm

To solve the optimization problem of optimal irrigation and *N* fertilization scheduling, the tailor-made global optimization technique **GET-OPTIS** (Global Evolutionary Technique for OPTimal Irrigation Scheduling) developed for the planning tool OCCASION (Schütze et al., 2012) coupled with model Daisy or Pilote and the stochastic weather generator LARS-WG was applied.

The problem specific evolutionary optimization algorithm GET-OPTIS starts with a set of solutions – called population – which is in this case a random set of schedules. Every member of the set has a fitness value assigned to it which is directly related to the objective function, its crop yield, *WP* and/or *NUE*. The fitness, i.e. the grain yield, *WP* and/or *NUE* is calculated by running Daisy or Pilote with the specified irrigation and fertilization schedule of the member. In sequential steps, the population of schedules is modified by applying four steps, aiming to imitate biological evolution: selection, crossover, mutation, and reconstruction. The procedure is then repeated until a convergence criterion is reached, or the maximum value of steps is exceeded.

In contrast to the common evolutionary algorithms, the presented GET-OPTIS reduces the computational effort by restricting the selection of the individuals – which would have to be evaluated by simulations – to feasible solutions (Schütze and Schmitz, 2010).

7.1.2. Generation of the crop water (nitrogen) production functions

The stochastic optimization framework consists of three loops (see Fig. 5.1). The objective of the *inner loop* is to maximize yield, *WP* and/or *NUE* for a specific climate scenario, a specific crop and a given amount of irrigation water and N during one growth period. The optimal schedules are determined by the evolutionary optimization algorithm GET-OPTIS. Within the *second loop* where an iteration over the irrigation and/or the N fertilization amount takes place, one potential CWPF or CWNPF can be constructed. A sufficient amount of CWPFs or CWNPFs is generated within the *third loop* (where an iteration over the weather scenarios occurred) in order to accurately compute the characteristics of the random sample of CWPFs or CWNPFs in a non-parametric way (Schütze and Schmitz, 2010). Hence, a Monte Carlo procedure using the generated synthetic climate data is applied to determine the CWPFs or CWNPFs.

In the case of an optimization of the irrigation schedule, the resulting crop water production functions (CWPF) represent the relation between yield and irrigation water applied. The CWPFs are analyzed statistically (calculation of quantiles), now called stochastic crop water production functions (SCWPF). In the case studies, the 90 % or the 95 % quantiles of cumulative irrigation amount of the generated set of schedules were used as the tool for irrigation decision. At real-time scheduling, occurring precipitation was subtracted from the one week's estimated irrigation depth. In the case of a simultaneous optimization of the irrigation and N fertilization schedule, crop water nitrogen production functions (CWNPFs) and stochastic crop water nitrogen production functions (SCWNPFs) are generated, respectively. For further information, refer to Schmitz et al. (2007) and Schütze and Schmitz (2010).

7.1.3. Application of the stochastic optimization framework

The framework for optimal irrigation and/or N fertilization scheduling can be applied in three different ways: the schedules may be determined (i) once at the beginning of the experiment, or (ii) once after harvesting, or (iii) the schedule may be adapted to the observed climate data (real-time irrigation scheduling).

In case study I, optimization runs were conducted after harvesting for determination of potential yield and *WP*. In case study II, the irrigation schedule was adapted weekly to external events (mainly precipitation and irrigation events) considering observed weather

data and weather forecasts. The so-called real-time irrigation scheduling may be applied in field experiments with a high variability of precipitation. The variability of precipitation is trivial in greenhouses, vegetation halls or under rain-out shelters where precipitation is excluded. Thus, a derivation of the optimal irrigation schedule at the beginning of the experiment is adequate (case study III).

Within the presented case studies, the optimization algorithm was adapted according to the required objective function, which was the maximization of yield or *WP* and, in case study III, the simultaneous maximization of *WP* and *NUE*. According to the experimental setups, a constant flow rate was given for the irrigation events. The latter were possible every few days, daily or only after an irrigation break of a few hours considering the specifications of the irrigation control and the irrigation system.

7.1.4. Crop growth model requirements

According to Kloss et al. (2011), the crop growth models chosen for simulation based optimization within the stochastic framework have to meet certain criteria:

- good representation of plant physiology within the crop growth model, including realistic and plausible response of crop to water stress,
- model parameters have to be transferable in space and time for a robust model application,
- ability to account for spatial distribution of water in soil when dealing with modern irrigation systems such as micro irrigation,
- ability to consider climate variability to take full benefit from the generated climate series when evaluating impacts of climate change,
- a time resolution of days instead of weeks for better consideration of plant response to water stress,
- ability for batch processing since several hundred simulations have to be evaluated in order to obtain the SCWPF.

In general, computational effort and therefore run time for a simulation might be an issue but can be mitigated by high-performance computing (Kloss et al., 2011). Due to the increased simulation time of model Daisy 2D (version 4.57), only Daisy 1D (version 4.01) was used within the optimization framework (run time for Daisy 1D was about 30 s and for Daisy 2D about 30 min, respectively). However, the experimental setup did not demand for a two-dimensional consideration either. Model Pilote was supported by Hydrus 2D/3D simulations to represent the more complex SDI field design (case study II).

8. Data collection during the experimentation

In order to generate a sufficiently large and representative data set, the experimental design is crucial. During the experimentation, the relevant data have to be collected to provide adequate explanatory variables for simulation modeling. The data can be used for calibration and validation purposes or may be needed as input variables (driving variables). Unknown parameters (e.g. soil parameters) can be determined indirectly by an inverse modeling technique based on observed data.

The following data is required for irrigation and N fertilization management:

- **Meteorological data** in a high resolution. Most crop growth models run on daily basis and require average daily weather data.
- The **applied fertilization** and **irrigation water amounts** and **drainage** have to be monitored accurately.
- **Soil properties** (bulk density, soil texture and K_s). Soil texture may be determined for the derivation of provisional van Genuchten/Mualem parameters which may be applied in preliminary simulation runs.
- For **soil water content** measurements, time domain reflectometry (TDR) probes (Campbell Scientific, USA) are suitable. Water content may be determined gravimetrically to verify the observed values. For **soil tension** measurements, tensiometers (measuring range of about pF 0 – 2.9, USM-GmbH, Germany) or pF-Meters (measuring range of pF 0 – 7, ecoTech, Germany) may be installed. The measuring interval should be at least 30 min to 1 h. Measurements have to begin before sowing and end after harvesting.
- Meaningful **plant variables** for use in crop growth modeling include biomass, LAI, plant heights and crop development stages. Biomass may be determined several times by cutting small cultivated areas if an adequate number of plants or planted area is available. LAI, plant heights and crop development stages should be estimated weekly with special attend to phenologically important stages like flowering.

- Harvested **grain yield** and **total dry matter** (including dry matter partitioning) have to be determined. Grain yield and total dry matter may be oven dried to a humidity content of 0 %. Furthermore, plant density and maximum rooting depth are of interest.
- **Soil N content** can be determined via soil sampling. These samples should be taken at least before sowing and after harvest to estimate the depletion of soil N.
- To estimate **plant N condition** and possible N stress, Chlorophyll Meters (Spectrum Technologies Inc., UK) are suitable.
- Data regarding **yield quality** (e.g. 1000 − seed weight or N content of the grains) may be helpful.

Table 8.1 lists the required data, suggestions for collection methods, collection frequencies and purposes of the data.

Table 8.1.: Overview of the data to be collected for crop growth model calibration and validation. The listed collection methods are only suggestions. The collected data can be used for calibration/validation purposes (cal/val) or as a input variable (iv).

data	collection method	frequency	purpose
meteorological data	meteorological station	1 minute – hourly	iv
irrigation amount	irrigation system	at each irrigation	iv
fertilization amount	fertilization system	at each fertilization	iv
soil texture	international pipette method	once before soil parameter calibration	iv
bulk density	core method	once	iv
hydraulic conductivity	falling-head method	once	iv
soil water content	TDR probes	15 min – hourly	cal/val
soil tension	tensiometer, pF-Meter	15 min – hourly	cal/val
leaf area index	Leaf area meter	weekly	cal/val
biomass	field observation and drying in oven	several times	cal/val
plant height	field observation	weekly	cal/val
crop development stage	field observation	weekly	cal/val
plant density	field observation	once after harvesting	iv
rooting depth	field observation or literature	once after harvesting	iv
total dry matter (including dry matter partitioning)	field observation and drying in oven	once after harvesting	cal/val
grain yield	field observation and drying in oven	once after harvesting	cal/val
yield quality	various	once after harvesting	iv
soil N content	Kjeldahl procedure	before sowing and after harvesting	iv
plant N condition	Chlorophyll Meter	weekly	iv

9. Postprocessing steps

In the following, the postprocessing steps for an adequate evaluation of the experimental results and model prediction are described.

9.1. Evaluation of the experimental results

To evaluate management strategies, observed data like yield and total dry matter and the determination of *WP*, *NUE* and profit are required.

9.1.1. Yield and total dry matter

After harvest, yield (for a certain humidity) and total dry matter (mostly for a humidity of about 0 %) in $\mathrm{t\,ha^{-1}}$ have to be determined. For that, the harvested fresh matter has to be oven dried until constant weight in a box-type furnace and then weighted.

9.1.2. Water productivity and nitrogen use efficiency

Experimental results can be evaluated by comparing *WP* values of conducted treatments among themselves and to literature values. The review article of Zwart and Bastiaanssen (2004) lists ranges of WP_{ET} for irrigated wheat ($0.6-1.7\,\mathrm{kg\,m^{-3}}$) and corn ($1.1-2.7\,\mathrm{kg\,m^{-3}}$). According to Dehghanisanij et al. (2009); O'Neill et al. (2008) and Rodrigues and Pereira (2009), typical *WP*s for corn under drip irrigated systems vary from 0.3 to $2.4\,\mathrm{kg\,m^{-3}}$. In the case study of Cantero-Martinez et al. (2003), WP_{SW} for barley was rather low ranging from 0.24 to $0.65\,\mathrm{kg\,m^{-3}}$. A survey of scientific literature reveals that *NUE* for corn ranges from 26 to $55\,\mathrm{kg\,grain\,kg}\,N^{-1}$ (Barbieri et al., 2008; Varga et al., 2008).

9.1.3. Economic aspects

The field design may play an important role regarding the material and installation costs of an irrigation system and thus regarding profitability. A suitable approach to calculate the profitability of an irrigation system was done by Bontemps and Couture (2002) who

defined the farmers profit per hectare as a function of output price, yield, fixed production costs and costs due to labor and energy for each watering. According to the authors, profit per hectare of the farmer can be defined as

$$\prod = P_{out} \cdot Y - C_{FT} - \sum_{t=0}^{T-1} (c \cdot I + C_F) \tag{9.1}$$

where $\prod$ is the profit [€ ha^{-1}], P_{out} the output price [€ t^{-1}], Y the grain yield [t ha^{-1}], C_{FT} the fixed production costs [€ ha^{-1}], c the water price [€ ha^{-1}], I the quantity of irrigation water applied [mm] and C_F the costs of irrigation due to labor and energy [€ ha^{-1}].

The experienced prices of material and installation of an irrigation system, further fixed costs and crop prices can be considered to evaluate the profitability of crop production for different field designs and management strategies.

9.1.4. Evaluation of the model results

The model performance can be evaluated using graphical and numerical comparisons between observed and predicted values. Several appropriate measures are described in Section 6.1.3.

Part III.

Application of the new approach to three case studies

10. Case study I: Evaluation of the transferability of a SVAT model

10.1. Objectives and summary

SVAT models are commonly used to describe crop seasonal dynamics including the prediction of crop yield and water balance. In the case of absent detailed information, a straight forward application of the model using given parameter sets may take place against rather different soil and/or climate conditions. The objective of this study was to (i) calibrate and validate the SVAT model Daisy 1D utilizing data of two sites (field, greenhouse) and two crops (wheat, barley), (ii) to evaluate the model's ability to employ plant parameters determined on basis of field data against greenhouse data, and (iii) to estimate potential *WP* (barley) and potential yield (wheat), see Figure 10.1.

This case study reports results of field and greenhouse experiments where wheat and barley were cultivated under a field rain-out shelter (wheat and barley) and in a greenhouse (only barley). In the greenhouse, barley was cultivated and drip irrigated in container filled with a soil taken from the field. The Daisy was inversely calibrated using the optimization algorithm CMA-ES and validated against experimental site data in two steps. Firstly, soil parameters were calibrated and validated using soil water content data of the field. Afterward, plant parameter of wheat were calibrated and validated on field data. In the case of barley which was only grown in 2009, calibration of plant data was carried out using field data whereas Daisy was validated against independent greenhouse data. For validation, the specific condition in a container greenhouse experiment was taken into account.

The study shows that Daisy performed well with simulating lightly drought stressed crop growth and water balance. For both crops and sites, optimal irrigation schedules were determined in a simulation-optimization study. For wheat, a potential grain yield of $9.05\,\mathrm{t\,ha^{-1}}$ can be achieved with 210 mm at that site when applying an optimal irrigation schedule. Potential *WP*s for barley were $4.1\,\mathrm{kg\,m^{-3}}$ (field) and $2.3\,\mathrm{kg\,m^{-3}}$ (greenhouse). Mean barley yields of 5.78 and $2.55\,\mathrm{t\,ha^{-1}}$ with optimal irrigation water amounts of 140 and 110 mm can be reached for field and greenhouse, respectively. The study was published by Walser et al. (2011a).

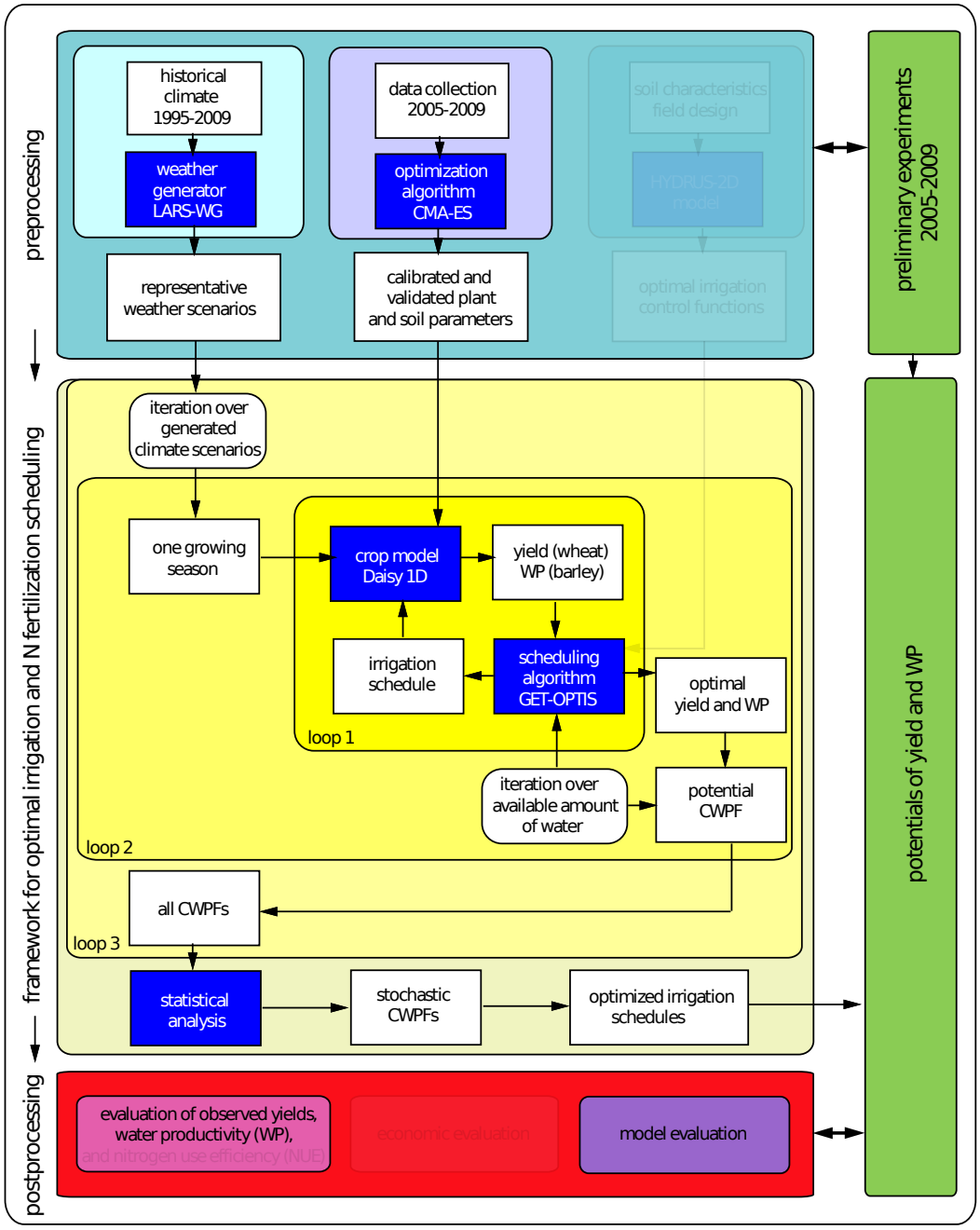

Figure 10.1.: The new approach of simulation based optimal experimental design consisting of (i) the preprocessing, (ii) the determination and experimental application of the optimized deficit irrigation schedules and (iii) the postprocessing for case study I. Not implemented steps of the approach are transparent.

10.2. Experimental site and experimental setup

The rain-out shelter and glass greenhouse experiments were conducted at the Dürnast Experiment Station of the Technische Universität München, Germany (48°24'11" N, 11°41'23" E, 473 m altitude). The average temperature and precipitation at that site are about 8 °C and 800 mm, respectively. Average temperature in summer is about 20 to 25 °C. precipitation occurs mainly from Mai to August. The 5 layered soil is sandy loam to loam with a high field capacity of about 235 mm.

An exceptional rain-out shelter construction is used in the experimental fields of the Experimental Station. The shelter roof closes automatically when precipitation occurs to enable a control of applied water. The construction features a bar with sprinkler for irrigation and further sensors. The experimental site was divided into four main rows (each 30 x 2 m); every main row was divided into 7 plots (each 4 x 2 m), see Figure 10.3. That field area exists twice side by side to enable crop rotation (referred to as east and west). In each main row, one crop or cultivar was sown into 15 seeding rows. For soil parameter determination, two sites were selected due to data availability, referred to site S1 (row 4, plot 4) and S2 (row 1, plot 7).

Figure 10.2.: Rain-out shelter field experiment with wheat and barley in 2009 (left picture), and greenhouse experiments with barley in 2009 (right picture) at the Dürnast Experiment Station of the Technische Universität München, Germany.

Different wheat (*Triticum* L.) and barley (*Hordeum vulgare* L.) cultivars were tested for drought stress sensibility from 2005 to 2009. The present study focused on winter wheat variety Cubus and summer barley variety Barke due to data availability. Four irrigation strategies were applied: early drought stress (before flowering), late drought stress (after flowering), full irrigation (each with two replicates) and rainfed (no replicate). The experiments with variety Cubus were conducted from 2005 to 2009 (four growth periods) at the

rain-out shelter. Sowing and harvesting dates of winter wheat cultivar Cubus ranged from mid October to around end of July.

The experiments conducted with summer barley cultivar Barke only took place in 2009. In the field, barley was grown in two rows, whereas wheat was cultivated in the other two rows (Fig. 10.3). Barley was sown at the field site on 06/04/2009 and harvested on 22/07/2009.

The greenhouse experiments with barley cultivar Barke were conducted in containers (0.95 x 0.55 x 0.73 m) without drainage (see Fig. 10.2). Sowing and harvesting dates were 26/03/2009 and 07/08/2009, respectively. Barley was sown in four rows per container. A tension controlled drip irrigation system was installed. Three tensiometers per container were installed at soil depths of 20, 40 and 60 cm. When a threshold ranging from −200 to −300 hPa at −20 cm soil depth was reached, an irrigation of 10 mm was applied, followed by an irrigation break of 3 h. Three irrigation strategies were applied: early drought stress (before flowering), late drought stress (after flowering) and full irrigation, each with three replicates. In field and greenhouse experiments, nutrients were not limited.

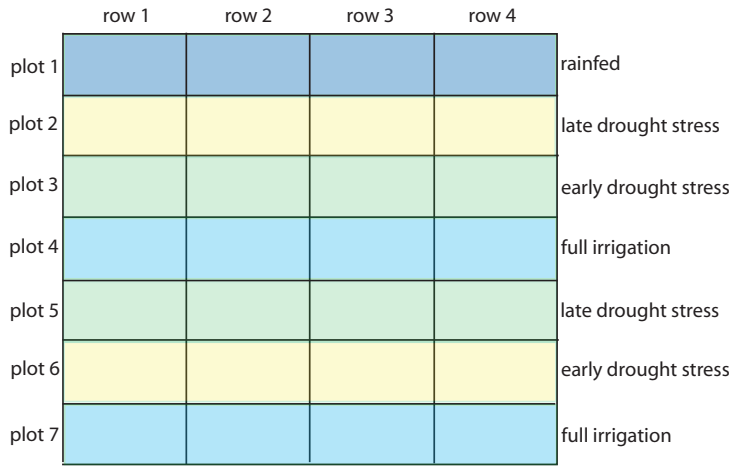

Figure 10.3.: Experimental setup of the rain-out shelter (west) for wheat and barley in 2009.

10.3. Data collection during the experimentation

Plant heights, development stages, biomass, grain yield and total dry matter were determined for both crops. Within the field experimentation, biomass was observed 1 to 4 times before harvest by cutting small areas from 0.1 to 0.6 m^2. Harvesting dates for wheat were 03/08/2005, 16/08/2006, 19/07/2007, 31/07/2008 and 30/07/2009. Barley grown on the field was harvested on 30/07/2009. Plant height and development stages of barley were determined on 21/05, 28/05, 01/06 and 08/06/2009 with four repetitions per plot (see Table 10.2). Soil water content was observed hourly using EnviroSCAN (Sentec, Australia) from 06/05/ to 29/07/2005, from 22/12/2006 to 20/07/2007, from 30/11/2007 to 05/05/2008 and from 26/05 to 05/08/2009 with probes at 10, 20, 40, 60, 80, and 100 cm soil depth. For winter wheat, the EnviroSCAN probes were installed a few weeks or months after sowing. For summer barley, the soil water content was observed hourly from 22/05 to 05/08/2009. Soil tension was not observed continuously (in most years from end of April until mid of July) and with a resolution of only three to four days. Meteorological data was provided by station number 8 of the Bayerische Landesanstalt für Landwirtschaft [1] at a distance of about 2.5 km from the experimental site.

Within the greenhouse experimentation, soil water content was determined gravimetrically on 30/04/2009 at 20, 40 and 60 cm soil depth for every container. Soil tension was observed hourly in 3 soil depths (20, 40 and 60 cm), but measuring started not until May and showed partly implausible data. Technical problems occurred at the monitoring of the irrigation amounts in the greenhouse. Plant heights, development stages and biomass were estimated several times, additionally grain yield and total dry matter were determined after harvesting (see Table 10.2). A meteorological station was installed in the greenhouse to provide 10 min data. Data was collected from 10/04 to 30/07/2009. The roof and side windows of the greenhouse closed automatically at night and whenever it was rainy. LAI was not observed successfully neither in the field nor the greenhouse experiment.

10.4. Calibration and validation of the model parameters

Soil and plant parameters were calibrated separately to avoid compensation effects. For soil and plant parameter calibration, the optimization algorithm CMA-ES was applied. The periods used for plant and soil parameter calibration and validation for both crops are illustrated in Figure 10.4. The soil parametrization was only conducted for the field since the soil for the greenhouse experiment was taken from the field and observed soil water data of the greenhouse experiment was insufficient. The plant parameters were determined for wheat and barley.

[1] www.lfl.bayern.de/agm/daten.php?statnr=8

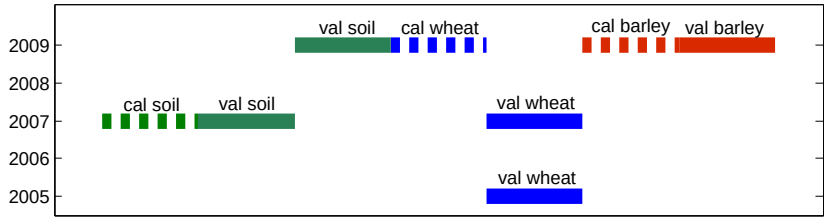

Figure 10.4.: Calibration (cal) and validation (val) periods for soil parameters and plant parameters (wheat and barley) from 2005 to 2009.

10.4.1. Model setup and soil parametrization

SVAT model Daisy was set up for wheat (2005 – 2009) and barley (2009 for greenhouse and field). Exemplary setup and weather files can be found in Appendix B. The set up of wheat was used for soil parameter estimation.

10.4.1.1. Model setup

The management (plowing, seeding date, fertilization, irrigation events, harvesting) was selected according to the applied management measures for each year. Within the soil module of model Daisy, five soil layers were defined (15, 30,79, 92, 190 cm soil depth). The maximal rooting depth was set to 150 cm soil depth. Since the initial water content was not known, an initial warm up phase of one year was simulated using observed weather data and the preceding crop rape.

In model Daisy, the spatial resolution of the Richards equation is defined by the soil layers and the geometry. For the setup file for wheat, the spatial dimension of the 5 soil layers (horizons) was set to 15, 30, 79, 92 and 190 cm soil depth. The geometry was defined by 37 points from 0.5 to 190 cm soil depth. Between these supporting points, the soil water contents and soil tensions was predicted. At first, upper and lower boundary conditions were set to atmosphere and free percolation.

10.4.1.2. Soil parameter calibration and validation

For a first estimation, soil parameters determined by ROSETTA (Schaap et al., 2001) utilizing laboratory analysis results (soil texture, bulk density and K_s) were applied (see Table A.1) and simulations were compared to the measured soil water content data. The latter were roughly reproduced, but especially when irrigation began in April (175 days

after sowing, DAS), water flow was described unsatisfactorily. Therefore, an optimization of the soil parameters for both full irrigated rain-out shelter sites S1 and S2 using CMA-ES took place. A determination of the van Genuchten/Mualem parameters θ_s, θ_r, α, n and the soil parameter K_s for 5 soil layers led to 25 coupled parameters to be calibrated. The following objective function with a definition of the parameters and specific bounds for parameter variations was applied:

$$Z_S = \sum \sqrt{\frac{\sum_{i=1}^{n} (\theta_{o,i}(z,t_j) - \theta_{p,i}(z,t_j))^2}{n}} \tag{10.1}$$

where Z_S is the objective function for soil parameter estimation, $\theta_{o,i}$ and $\theta_{p,i}$ [$\mathrm{cm}^3\,\mathrm{cm}^{-3}$] are the observed and predicted soil water contents and z, t_j are the position and time per calibration period j for situation i ($1 \leq i \leq n$).

The soil parameters were determined using data from two full irrigated rain-out shelter sites S1 and S2. In 2007, wheat cultivar Cubus was sown at site S1, in 2009 in site S2, respectively. The soil parameters of both sites were calibrated separately. Due to data availability, soil water content data from January to July 2007 was selected for calibration (07/01 – 22/01, 07/02 – 05/03 and 09/05 – 20/07/2007). For validation, daily water content values for each soil depth from 31/12/2006 to 06/01/2007, from 24/01 to 06/02 and from 06/03 to 08/05/2007 and from 22/05 to 05/08/2009 were used. For the simulation runs, hourly observed soil water content data were aggregated via arithmetic averaging to daily soil water content data.

After first optimization results, two adaptations of the model setup took place. The observed water contents showed high dynamics in the upper layer (10 and 20 cm soil depth) when irrigation occurred. At a soil depth of 40 cm, these dynamics were much smoother and sharply decrease with deeper layers. Therefore, macropores due to preceding crop rape were assumed in the top soil. Consequently, an approach to implement macropores (macro) in model Daisy was applied leading to four additional parameters to be calibrated: begin and end of fraction of macropores in the soil (*distribution* in cm) and soil tension when flow in macropore starts and ends (*pressure ini* and *pressure end* in cm). Macropores were limited to soil depths of 20 to 50 cm. After calibration, the optimized parameters substituted the ones determined by ROSETTA (Schaap et al., 2001).

Moreover, simulation results showed high dynamics in deeper layers. Due to almost constant water contents near saturation observed from 80 to 100 cm soil depth, the lower boundary condition was changed into lysimeter hence percolation started at a water content near saturation. Figures 10.5 and 10.6 compare measured and predicted soil water contents of sites S1 and S2 after calibration of the soil parameters and the adaptations described above (but before the calibration of the plant parameters). For validation, additionally data of 2009 was used.

In general, adaption was better for site S2 (*RMSE* of 2.6 cm^3 cm^{-3}) than for site S1 (*RMSE* of 2.8 $cm^3\,cm^{-3}$), especially in layers 10, 20 and 40 cm (see Table 10.1). Higher differences of measured and predicted values due to field heterogeneity at a soil depth of 10 cm are acceptable. Higher dynamics after irrigation can be found in site S1 layer -20 cm compared to site S2. Macropore ends were estimated to be at 38 cm (S1) and 49 cm (S2). Accurate simulations of the upper soil layers which mainly contribute to the root water uptake are of higher importance than accurate prediction of the lower layers. In general, the soil parameters were highly variable between both plots S1 and S2 leading to the assumption that the soil heterogeneity is high at that site. For instance K_s ranged from 3.03 to 14.56 $cm\,d^{-1}$ (see Table A.1 in the Appendix).

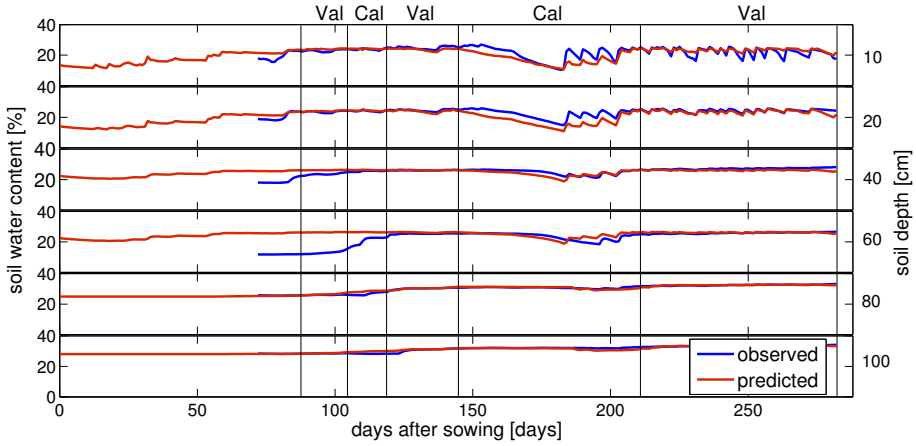

Figure 10.5.: Observed and predicted water contents of site S1 in 2007 after calibration of the soil parameters. The validation and calibration periods of 2007 are marked with Val and Cal, respectively.

Due to data availability, validation in 2009 was only possible for S2 in the period of irrigation. Adaption was less accurate than in 2007. The model underestimated the soil water content but predicted well the dynamics.

In the case of barley, the calibrated soil parameters of site S1 were applied since barley was sown at that site in 2009 (see Table A.1 in Appendix). The same soil parameters were used for the greenhouse simulations since the soil was taken nearby that site and soil water content and soil tension measurements of the greenhouse experiment were insufficient for calibration.

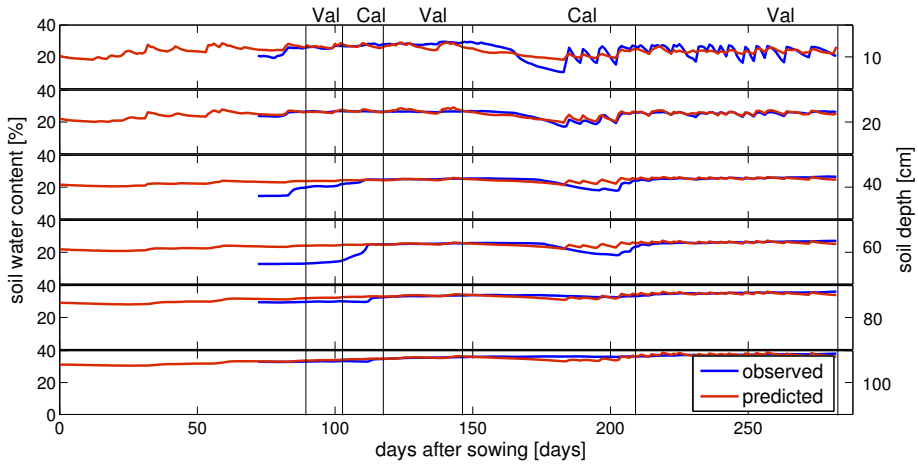

Figure 10.6.: Observed and predicted water contents of site S2 in 2007 after calibration of the soil parameters. The validation and calibration periods of 2007 are marked with Val and Cal, respectively.

Table 10.1.: *RMSE* of the van Genuchten/Mualem parameters θ_s, θ_r, α, n , parameter K_s, and three macropore parameters. The *RMSE* was determined for the calibration and the validation period and for both periods (cal/val) for the soil water contents of sites S1 and S2 (all soil depths) in cm^3 cm^{-3}.

RMSE	S1	S2
calibration	2.3	2.1
validation	3.3	3.0
cal/val	2.8	2.6

10.4.2. Plant parameter calibration and validation

To identify the most sensitive plant parameters, a sensitive analysis was carried out for both crops. For first estimations, predefined parameter sets from the database of Daisy were applied. After calibration, the optimized parameters substituted the ones from the database (see Table 10.5).

10.4.2.1. Calibration of the wheat plant parameters

For calibration of the wheat plant parameters, the observed values of plant height and biomass (both determined 4 times), grain yield, total dry matter and harvesting date of the fully irrigated treatment of site S2 in 2009 were used within the following objective function:

$$Z_P = \quad 10 \cdot \sqrt{\frac{\sum_{i=1}^{4}(DM_{o,i} - DM_{p,i})^2}{4}} + 10 \cdot \sqrt{\frac{\sum_{i=1}^{4}(h_{o,i} - h_{p,i})^2}{4}} \tag{10.2}$$

$$+ \mid Y_{o,i} - Y_{p,i} \mid + \frac{|d_{o,i} - d_{p,i}|}{1000}$$

where Z_P is the objective function for plant parameter derivation, $TDM_{o,j}$ and $TDM_{p,j}$ are the observed and predicted values of dry matter (or biomass) [t ha^{-1}], $h_{o,j}$ and $h_{p,j}$ are the observed and predicted plant heights [cm], $Y_{o,j}$ and $Y_{p,j}$ are the observed and predicted grain yields [t ha^{-1}], and $d_{o,j}$ and $d_{p,j}$ are the observed and predicted harvesting dates [days] for situation i for $1 \leq i \leq n$. Total dry matter and plant heights were weighted higher compared to grain yield and harvesting date.

Eleven parameters selected based on Abrahamsen (2006) were tested within a sensitivity analysis (see Eq. 6.3). The parameters were increased and decreased by 5, 10, 25, 50 and 100 %. Fig. A.1 in the Appendix exemplary shows the variation of the parameter *DSRate1* and its influence on the *LAI*. The most significant parameters regarding yield were selected (see Table 10.5) and calibrated using the CMA-ES algorithm.

The other plant parameters proposed by Abrahamsen (2006) showed sensitivity indexes below 0.1. Additionally, parameter *EmrTSum* (daily sum of soil temperature from sowing to germination at a soil depth of 10 cm) was estimated and set to 234 °C. Table 10.2 shows the observed plant variables used for calibration.

Table 10.2.: Observed plant heights [cm], biomass [t ha^{-1}] and grain yields [t ha^{-1}] for wheat and barley used for plant parameter calibration in 2009.

	date	wheat	barley
plant height	21/05	73.3	49.8
	28/05	80.7	71.4
	01/06	83.2	76.6
	08/06	88.1	87.3
biomass	19/05	5.9	1.3
	02/06	11.9	4.6
	13/06	14.2	8.2
	02/07	17.1	13.2
grain yield	30/07	8.1	5.8

10.4.2.2. Crop model validation for wheat

For validation, plant data of 2005 and 2007 was used (Table 10.3). In general, the yield predictions showed good results (Table 10.3). Grain yield in the period of calibration (2009) was predicted very well with a difference of 0.02 t ha^{-1}. In 2005 and 2007, predicted and observed yields differed 0.92 and 1.37 t ha^{-1}, respectively. Simulations of biomass were based on three biomass cuts in 2005 and 2007 (validation) and showed lower fittings. However, in 2005 and 2007, cultivar Cubus was sown in site S1 whereas calibration took place with the data of S2 from 2009, thus the results may also reflect soil heterogeneity. The simulation of the harvesting date was adequate. For model Daisy, the harvesting date is equal to ripening, whereas in agricultural practice, harvest as well depends on machine and human availability. Thus, weighting in the objective function was lowest for that parameter.

Table 10.3.: Observed and predicted grain yield (Y), total dry matter (TDM), biomass, all in [t ha^{-1}] and harvesting dates and model error for wheat in 2009 (calibration) and 2005 and 2007 (validation).

	observed	predicted	model error
2009 (calibration)			
Y	8.11	8.13	−0.02
TDM	16.99	15.93	1.06
harvesting date	30/07	27/07	3 days
2005 (validation)			
Y	7.87	8.79	−0.92
TDM	17.04	16.38	−0.66
harvesting date	03/08	27/07	6 days
biomass cut on 08/06	9.98	10.89	−0.91
biomass cut on 22/06	13.25	15.22	−1.97
2007 (validation)			
Y	8.31	9.68	−1.37
TDM	15.90	17.25	−1.35
harvesting date	19/07	15/07	4 days
biomass cut on 30/05	13.06	13.43	−0.37

Figures 10.7 and 10.8 compare the observed and predicted total dry matter and plant heights of 2009. Adaptation of the predicted values to the observed ones performed well, $RMSE$ of the objective function was 0.0514, of the normalized plant height of 0.0053 cm and of the normalized total dry matter 0.0001 t ha^{-1}, respectively. Further water content predictions using the calibrated plant parameter improved the adaption of the model, especially at 20 cm soil depth (not shown). The $RMSE$ in that soil depth decreased from 1.45 to 1.11 after the application of the calibrated plant parameters.

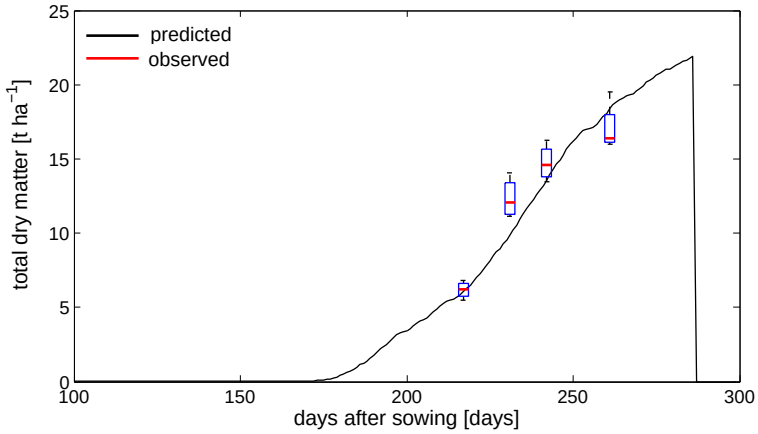

Figure 10.7.: Comparison of predicted and observed total dry matter [t ha^{-1}] of wheat in 2009.

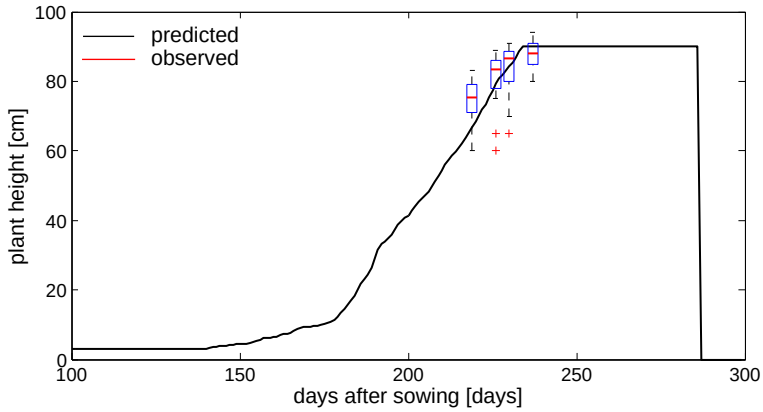

Figure 10.8.: Comparison of predicted and observed plant heights [cm] of wheat in 2009.

Moreover, all four irrigation treatments were simulated using the calibrated model and compared to the observed grain yields (Table 10.4). The modeling efficiency *EF* for all irrigation amounts was only −7.6. However, for all treatments with an irrigation amount higher than 100 mm, *EF* increased to −1.6. The bad performance of model Daisy when severe drought stress occurred is shown by the residue graph where high residues can be found for irrigation water amounts lower than 100 mm (Fig. 10.9b), whereas no clear trend can be found for the predicted yields (Fig. 10.9a).

In general, model Daisy was able to simulate crop growth under light drought stress but performed only moderate under severe drought stress. That was confirmed by Schütze and Schmitz (2010). Especially when the applied irrigation water amount was lower than 100 mm, crop model performance was poor. This leads to the assumption that model Daisy is weak in predicting crop growth under severe drought stress.

However, in this case study, further calculations were done including precipitation and supplemental irrigation, hence severe drought stress was not object of investigation. The differing sites of cultivation of wheat in 2009 (S2) and 2005/07 (S1) and thus the high soil heterogeneity between both sites may be another reason for differences in prediction.

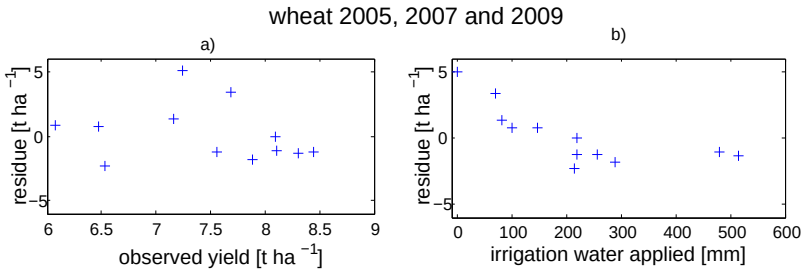

Figure 10.9.: Residue graphs for winter wheat in 2005, 2007 and 2009 using model Daisy 1D. The residue is plotted against the observed grain yield [t ha^{-1}] and the applied irrigated water [mm].

10.4.2.3. Calibration of the barley plant parameters

Model Daisy 1D was set up for barley grown in the field and in the greenhouse. The model setups were adapted according to the management and site conditions. For both conditions, the soil parameters of wheat (site S1) were applied. To simulate the closed bottom of the container in the greenhouse (no drainage), an additional imaginary clay layer of 5 cm with a very low hydraulic conductivity (K_s=0.048 cm d^{-1}) was implemented. Exemplary setup files for the field and the greenhouse experiments can be found in Appendix B.

For calibration of the barley plant parameters, grain yield, total dry matter, biomass and plant height of the fully irrigated treatment in 2009 were used (Fig. 10.2) whereas grain yield and total dry matter were weighted higher compared to plant height and biomass (Eq. 10.3).

Table 10.4.: Observed and predicted grain yields, model errors [t ha^{-1}] and applied irrigation water amount I [mm] for wheat for four irrigation scheduling strategies.

grain yield	early drought stress	late drought stress	full irrigation	rainfed
2005 observed	7.69	6.08	7.56	6.53
2005 predicted	4.29	5.27	8.79	8.83
model error	3.40	0.81	1.23	−2.5
I	70	100	220	214
2007 observed	6.47	8.45	8.31	7.88
2007 predicted	5.73	9.69	9.68	9.73
model error	0.74	−1.24	−1.37	−1.85
I	146	256	516	289
2009 observed	7.24	7.16	8.10	7.01
2009 predicted	2.20	5.86	8.12	8.11
model error	5.04	1.3	−0.02	−1.1
I	0	83	219	479

It is assumed that the exposed positions of the containers in the greenhouse lead to higher total radiation for crops sown on the border of the container. This is confirmed by the harvested grain yield where the yield of the two border rows increased the one of the inner rows by about 100 %.

However, meteorological stations can not consider this effect. Actually, they measured reduced radiation values (by about 60 %) due to shading by the roof and side walls compared to outside the greenhouse. Hence, climate input data for crop models may underestimate the total radiation of crops. To reduce the explained effect caused by the exposed crops, validation took place only against both shaded inner crop rows.

Eleven parameter recommended by Abrahamsen (2006) were analyzed by a sensitivity analysis, see Equation 6.3. The same parameters as for wheat and additionally parameter $DSRate2$ showed adequate sensitivity. Moreover, parameter $HvsDS$ which influences plant height was adapted due to higher observed plant heights of about 100 cm compared to the default value of 75 cm. The applied objective function for plant parametrization was:

$$Z_P = 0.1 \cdot \sqrt{\frac{\sum_{i=1}^{4}(TDM_{o,i} - TDM_{p,i})^2}{4}} + 10 \cdot \sqrt{\frac{\sum_{i=1}^{4}(h_{o,i} - h_{p,i})^2}{4}} \tag{10.3}$$

$$+100 \cdot \mid Y_{o,i} - Y_{p,i} \mid +100 \cdot \mid d_{o,i} - d_{p,i} \mid$$

where Z_P is the objective function for plant parameter derivation, $DM_{o,i}$ and $DM_{p,i}$ are the observed and predicted values of dry matter [t ha^{-1}], $h_{o,i}$ and $h_{p,i}$ are the observed and predicted plant heights [cm], $Y_{o,i}$ and $Y_{p,i}$ are the observed and predicted grain yields

[t ha^{-1}], and $d_{o,i}$ and $d_{p,i}$ are the observed and predicted harvesting dates [days] for situation i for $1 \leq i \leq n$, respectively. Total dry matter was weighted much lower compared to the wheat parametrization. The reason was the low sample size in the case of the greenhouse experiments (3 containers per treatment) which made representative sample taking difficult.

The plant parameter optimization took place based on four plant height and biomass observations and on the grain yield data (see Table 10.2). For the resulting best parameter combination (see Table 10.5), *RMSE* was 1.34 t ha^{-1} for total dry matter and 10.7 cm for plant heights. The absolute differences were 0.0013 t ha^{-1} for grain yield. The calibrated parameters replaced the default values of the Daisy crop file.

Table 10.5.: The most sensitive plant parameters of winter wheat and summer barley referred to yield. Default values (dv) due to Daisy database and calibrated values (cal) for field conditions using the optimization algorithm CMA-ES.

plant parameter	unit	dv wheat	cal wheat	dv barley	cal barley
DSRate1	d^{-1}	0.024	0.0228	0.032	0.032
DSRate2	d^{-1}	–	–	0.021	0.021
Fm	(g $C0_2$)/(m^2 h^{-1})	5.0	4.5633	3.5	3.7933
Q_{eff}	(g $C0_2$ m^{-2} h^{-1})/(W m^{-2})	0.05	0.0473	0.04	0.0453
DSLAI0.5	–	0.15	0.1002	0.15	0.1698
SpLAI	(m^2 m^{-2})/(g DM m$^{-2)}$	0.022	0.0289	0.031	0.0239

10.4.2.4. Crop model validation for barley

Simulation results for the fully irrigated treatment (I =196 mm) in the field were very good, observed and predicted grain yield and total dry matter both were 5.8 and 12.9 t ha^{-1}, respectively. Observed grain yield and total dry matter of barley (inner rows) in the greenhouse were predicted well, too. However, the harvesting date was highly underestimated. The observed harvesting occurred at 07/08/2009, the predicted harvesting at 05/07/2009, respectively. The total radiation sum for ripening was reached 30 days later than estimated by Daisy. Both *DSRate* parameters depend on temperature and day length. The latter is determined based on the geographic position, which does not represent the climatic condition in a greenhouse. Therefore, *DSRate*1 and *DSRate*2 were manually adapted and changed to 0.03525 and 0.01766 for greenhouse conditions, respectively. This adaptation led to longer growth durations until 25/07/2009 and even better results for yield (observed vs. predicted grain yield: 2.48 vs. 2.38 t ha^{-1} and observed vs. predicted total dry matter: 5.71 vs. 5.77 t ha^{-1}), see Table 10.6.

Table 10.6.: Observed and predicted grain yields (Y), total dry matter (TDM), both in $t\,ha^{-1}$, and harvesting dates for barley. Observed grain yields of the greenhouse experiments were estimated separately for inner rows ($rows_{inner}$) and for border rows ($rows_{border}$) of each container. R means no increase of radiation, 70 % R, 75 % R, 80 % R and 85 % R mean an increase of global radiation input data by 70 %, 75 %, 80 % and 85 %, respectively.

	observed			predicted				
	$rows_{inner}$	$rows_{border}$	field	R	70 % R	75 % R	80 % R	85 % R
Y	2.48	5.54	5.77	2.38	5.37	5.66	5.95	5.98
TDM	5.71	10.87	12.85	5.77	11.88	12.47	13.07	12.66
harvest	07/08	07/08	22/07	25/07	20/07	20/07	20/07	19/07

Due to the assumed underestimation of the total radiation sum for crops by model Daisy, observed radiation in the field and in the greenhouse were compared. The average global radiation observed inside the greenhouse was about 60 % lower than the radiation observed in the field.

An increase of radiation input data estimates the amount of received radiation of the field crops and the free-standing crops of the border rows. It has to be paid attention on the fact that the model predictions were validated only against the inner rows of the containers. The increase of radiation of about 75 – 80 % led to predicted grain yields of 5.66 – 5.95 $t\,ha^{-1}$, which are in the range of the observed grain yield in the field (5.77 $t\,ha^{-1}$).

Thus, the reduction of radiation received by crops grown at the inner rows due to the greenhouse conditions is assumed to be 75 – 80 %. Moreover, an increase of radiation of 75 % led to grain yields of 5.66 $t\,ha^{-1}$ similar to the observed one of the border rows (5.54 $t\,ha^{-1}$). Hence, the received radiation of the border rows compared to the inner rows is assumed to be about 75 % higher.

Due to technical restrictions, irrigation water amount in the greenhouse for full irrigation was observed to be 974 mm, but is assumed to be lower. The unknown irrigation amounts impede a simulation of further irrigation strategies. An extensive validation of the water flow was difficult due to implausible data. In general, the predicted soil water tension was moderately confirmed by the observed ones with good results for soil depths of 40 and 60 cm.

10.5. Application of the stochastic optimization framework

For determining the yield (wheat) and the *WP* (barley) potential, the optimization technique GET-OPTIS for optimal irrigation scheduling with limited water supply coupled with the calibrated model Daisy 1D were applied under "no-rain conditions" using a Monte Carlo simulation-optimization (Schütze and Schmitz, 2010). For that, long time-series of climate data were generated. The 0.5 %, 1 %, 10 %, 50 %, 90 % and 99 % quantiles of the CWPFs, the SCWPFs were calculated. For barley, only the potential CWPF for 2009 was estimated.

10.5.1. Generation of the climate data

LARS-WG was used to generate long time-series for field and greenhouse which statistically resemble observed weather for each specific site. For wheat, precipitation, minimal and maximal temperature and radiation data for a sample of 500 years was generated on the basis of 15 years (1995 – 2009) of observed data (daily averages of precipitation, temperature and radiation) of the Bayerische Landesanstalt für Landwirtschaft (weather station number 8).

In general, temperature and radiation showed accurate adaptation to historical weather data. Only monthly precipitation based on climate data of the Dürnast Experimental Station showed moderate adaptation leading to the assumption that convective summer precipitations are not represented accurately. However, precipitation was not considered during the growth period, since wheat and barley were grown under the rain-out shelter. For barley, only the potential CWPFs for 2009 (field and greenhouse) were determined.

10.5.2. Estimation of the yield potential of wheat

Prior to the "no-rain condition" Monte Carlo simulation-optimization to estimate the potential wheat grain yield, 500 years including precipitation were simulated to evaluate the influence of irrigation, radiation and temperature.

10.5.2.1. Simulation runs including precipitation

Simulations with the 500 generated years using the management data and the observed irrigation schedule of the fully irrigated treatment of 2009 (constant I of 219 mm for all years) including precipitation were performed. For that, parameter $EmrTSum$ was set to 100 °C to allow ripening within simulation time even if autumn was cold. Simulation results showed that yield was almost normally distributed with an average grain yield of

8.62 t ha^{-1} (median: 8.60 t ha^{-1}, skewness coefficient: 0.0158). The symmetry shows the strong influence of the normally distributed radiation and temperature on yield at full irrigation (precipitation is not normally distributed), see Figure 10.10.

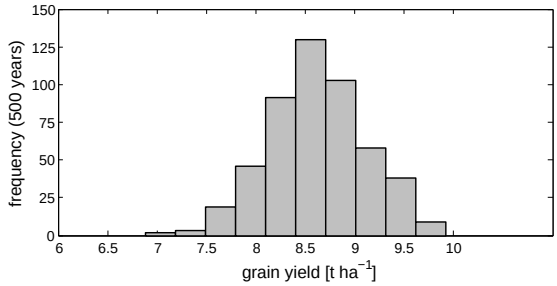

Figure 10.10.: Predicted wheat grain yield [t ha^{-1}] for a irrigation water amount of 219 mm including precipitation for a sample of 500 years. Precipitation was included.

10.5.2.2. Simulation-optimization under "no-rain conditions"

An optimized irrigation schedule with the objective to maximize grain yield was determined using a sample of about 200 generated years. Precipitation was excluded during the utilization of the rain-out shelter. The same setup file of the fully irrigated treatment of 2009 was applied, but the irrigation amounts ranged from 50 to 510 mm. A conditional distribution for a given water amount of 210 mm (similar to the observed precipitation of 219 mm in 2009) can be seen in Figure 10.11.

In general, the predicted yield variability was low. When the irrigation amount was low, soil moisture had a great influence on yield. Fig. 10.12a) and 10.12b) show that the variability of yield is about 2.7 t ha^{-1}. Variance was high for low irrigation amounts due to varying initial water contents at the operation of the rain-out shelter in March. Within irrigation amounts higher than 260 mm, variance of the median (about 8.89 t ha^{-1}) of the SCWPFs was almost constant (about 0.23) showing the influence of temperature and radiation at full irrigation.

The generated SCWPFs for wheat indicate that irrigation amounts higher than 260 mm do no longer increase yield (for a reliability of 50 %), see Figure 10.12. That was confirmed by observations e.g. in year 2006 where an irrigation amount of 213 mm (6.5 t ha^{-1}) and 418 mm (6.2 t ha^{-1}) even led to a decrease in yield. Thus, irrigation amount was unnecessarily high in many experimental treatments at that site (see Table 10.4).

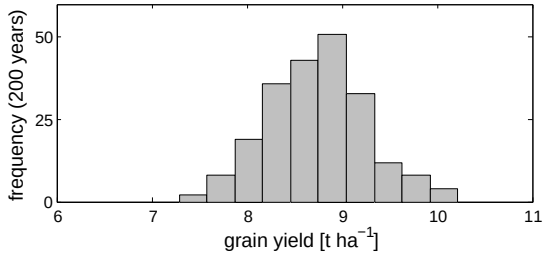

Figure 10.11.: Conditional probability function of wheat grain yield [t ha^{-1}] for a total water amount of 210 mm. The sample size was 200 years.

Variance for yield was highest (about 0.45) for irrigation amounts of 60 – 160 mm when the influence of irrigation, temperature and radiation overlap.

The predicted potential grain yield for 210 mm using the simulation-optimization approach was 9.05 t ha^{-1} (Fig. 10.11 and Table 10.12). The potential grain yield at a *WP* of 4.3 kg m^{-3} was increased compared to the observed grain yield of 8.1 t ha^{-1} at a *WP* of 3.7 kg m^{-3} of 2009 (see Table 10.7), respectively. This implies an increase of 12 % for grain yield and 16 % for *WP*. However, due to the high soil water storage capacity of the soil and precipitation in winter and spring, the potential yield increase due to optimized irrigation schedules was only moderate.

10.5.3. Estimation of the water productivity potential of barley

In the case of barley grown in the field, optimal irrigation schedules for 2009 (field and greenhouse) were estimated. Temperature and radiation inside the greenhouse were determined from outdoor weather and a few weeks lasting measurements inside the greenhouse (10/04 – 30/07/2009) via regression analysis. Hereby, a differentiation of daily radiation data for days when the greenhouse roof was closed and when it was open occurred. The correlation coefficient (r) for temperature was 0.99, for radiation (open roof) 0.96 and radiation (closed roof) 0.97. Precipitation was set to zero.

For both conditions, an optimal irrigation schedule for 2009 using GET-OPTIS optimization algorithm which maximized *WP* for a certain grain yield was determined. Minimal and maximal applicable irrigation water amounts were 5 and 200 mm for the field, and 10 mm and 400 mm for the greenhouse, respectively. Minimum breaks between two irrigation events were 7 days and 1 day for the field and for the greenhouse, respectively. The observed irrigation water amounts applied were 196 mm for the field and 974 mm (questionable due to technical restrictions of the irrigation system) for the greenhouse, respectively.

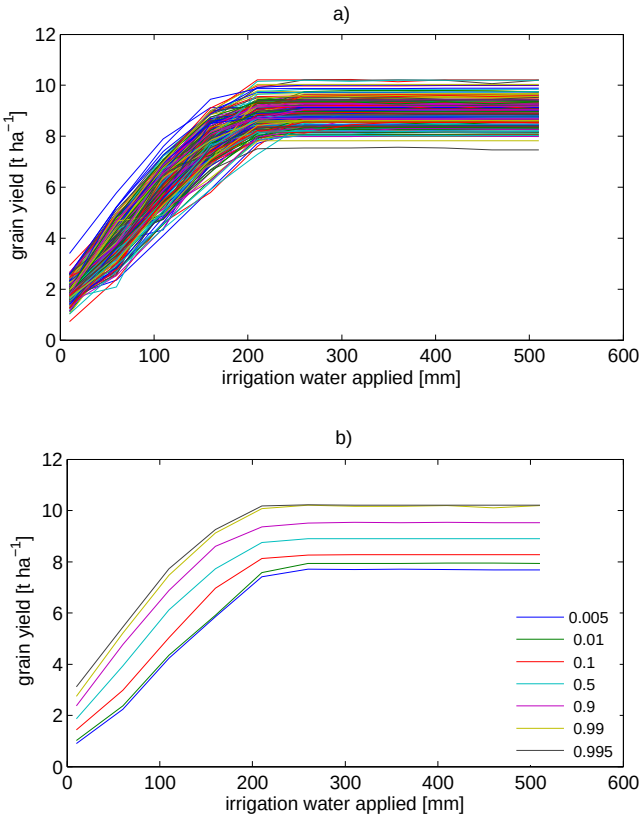

Figure 10.12.: Figures a) and b) show the determined wheat CWPFs and SCWPFs for a sample size of 200 years, respectively.

For barley cultivated in the field, a grain yield of 5.78 t ha^{-1} with applying 140 mm of irrigation water can be achieved (Fig. 10.14). That means a saving of 56 mm of irrigation water compared to the fully irrigated treatment. The yields were only lightly increased. The resulting potential *WP* of 4.1 kg m^{-3} is about 41 % higher than the observed one (2.9 kg m^3).

For barley grown in the greenhouse, the optimized irrigation schedule with an irrigation amount of 110 mm (including the predetermined 30 mm for germination) led to a grain yield of 2.55 t ha^{-1} (Fig. 10.15). In the greenhouse experiment, the questionable application of 974 mm of irrigation water only reached a grain yield of 2.48 t ha^{-1}.

The *WP*s were 2.3 (predicted) and 0.3 kg m^{-3} (observed), see Table 10.7. Thus, the potential *WP*s estimated using the simulation-optimization approach were 2.3 (greenhouse) and 4.1 kg m^{-3} (field).

Table 10.7.: Observed and optimized grain yields Y [t ha^{-1}], applied irrigation water amounts I [mm] (without 30 mm for germination) and determined water productivities WP [kg m^{-3}] for wheat and barley of 2009.

	observed			optimized		
	Y	I	WP	Y	I	WP
wheat field	8.1	219	3.7	9.05	210	4.3
barley field	5.77	196	2.9	5.78	140	4.1
barley greenhouse	2.48	*974**	*0.3*	2.55	110	2.3

The I marked with * is questionable due to technical restrictions of the irrigation system.

Figure 10.13 shows the characteristics of grain yield and WP with increasing applied water for barley grown in the greenhouse. In general, WP decreases with increasing irrigation water applied. This is not the case under greenhouse conditions from 0 to 75 mm applied water because of the initial soil moisture in the containers. Thus, even small irrigation amounts lead to yield increases. In the field, WP of barley decreases due to the high initial soil water content (not shown). Obviously, irrigation amounts and frequencies were much lower for both optimized irrigation schedules compared to the applied irrigation schedules (Fig. 10.14 and 10.15).

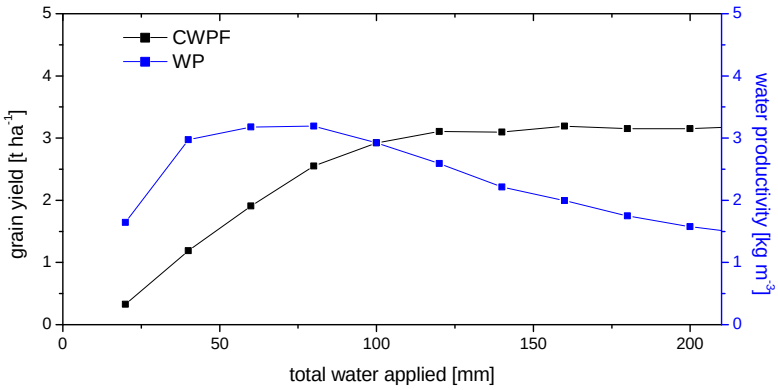

Figure 10.13.: Predicted barley grain yields [t ha^{-1}] and WPs [kg m^{-3}] for greenhouse conditions. The predetermined irrigation water applied for germination (30 mm) are not considered.

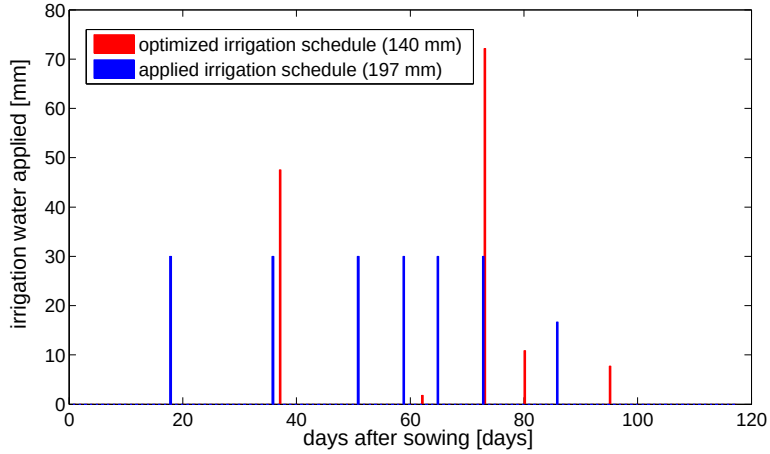

Figure 10.14.: Observed and optimized irrigation schedules for barley grown under field conditions.

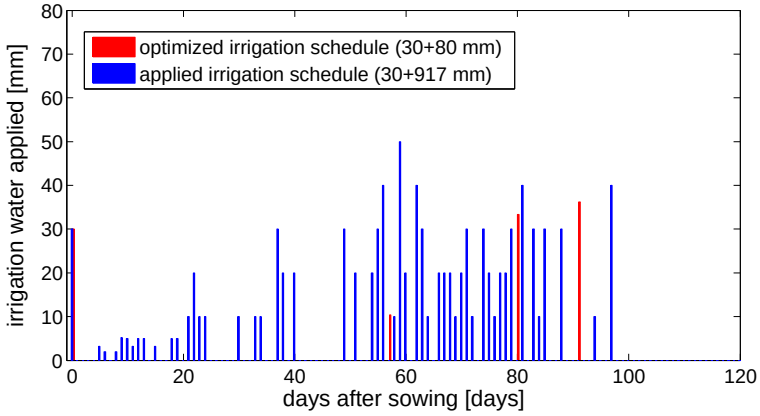

Figure 10.15.: Observed and optimized irrigation schedules for barley grown under greenhouse conditions (including the predetermined 30 mm for germination).

10.6. Discussion and conclusions

Regarding the optimal design of the experiments, some limitations occurred. Most of the data was provided during or after the experimentation in 2009 which made preliminary infiltration experiments for soil parametrization impossible and impeded appropriate data collection. Moreover, real-time irrigation scheduling or determination of the irrigation schedules at the beginning of the growth period was prevented. Data quantity and quality for calibration and validation was partly inadequate (e.g. soil tension measurements). However, due to data availability for several years (wheat) and the parameter transfer (barley), model parametrization was successful. Optimal irrigation schedules to determine the *WP* and yield potentials were determined after harvesting. Calculations of *WP* were conducted whereas *N* and economic aspects were not considered.

In general, SVAT model Daisy predicted well crop growth and water contents. In spite of the different conditions between the rain-out shelter and the greenhouse, the plant parameters could be calibrated using field data and validated successfully against greenhouse data. For that, a differentiation in two inner and two border crop rows within each container was required. The soil parameters were determined using field data of site S2 in 2009, but were applied onto different plots in 2005 and 2007. More accurate water content data and soil tension data in high resolutions may have improved predictions. Concerning the water content simulation in the field, also soil heterogeneity may be responsible for differing simulation results.

Regarding crop model performance at drought stress, the model performed only moderate when irrigation amounts were very low (see Fig. 10.9b). Reason for that may be limitations within model Daisy.

Due to the shading by the greenhouse roof and side walls, lower yields were observed in the greenhouse compared to the field. The calibrated model using field data could not reflect the longer growth durations and the early growth in length in the greenhouse, hence further adaption of two model parameters to greenhouse conditions was required. In this case study, the experimental setup allowed to only consider inner crop rows of the containers for model validation. These crop rows are assumed to grow under similar conditions to field conditions due to the shading by neighboring rows. With an increase of radiation by 75 – 80 %, predicted yields in the greenhouse were similar to the ones in the field. However, the required radiation increase is variable as it depends on the frequency of the roof opening: the more often the roof is open, the higher is the incoming radiation and the lower is the radiation increase needed for the simulation runs.

The application of the optimization framework aimed to determine the potentials of *WP* (barley) and yield (wheat) in 2009. With the optimized schedule and an irrigation water amount of 210 mm, a potential wheat grain yield of 9.05 t ha^{-1} instead of the observed

$8.1\,\mathrm{t\,ha^{-1}}$ is achievable. However, this yield increase of 12 % is only moderate due to the high soil water storage capacity and winter and spring precipitation which hinter drought stress.

For barley, mean grain yields of 5.78 and $2.55\,\mathrm{t\,ha^{-1}}$ with optimal irrigation water amounts of 140 and 110 mm could be reached for field and greenhouse, respectively. The potential *WP*s using the simulation-optimization approach were 2.3 for barley grown in the greenhouse and $4.1\,\mathrm{kg\,m^{-3}}$ for barley grown in the field, respectively. The optimized irrigation schedule highly increased *WP* for barley (field) by about 41 % compared to the observed *WP*.

11. Case study II: Real-time deficit irrigation scheduling

11.1. Objectives and summary

In this case study, real-time irrigation scheduling for estimating a deficit irrigation schedule – which maximizes *WP* and achieves a given yield of about $14\,\mathrm{t\,ha^{-1}}$ with a reliability of 95 % – was applied. The irrigation schedule was provided by the optimization algorithm GET-OPTIS and the crop growth model Pilote. It was completed by scenario series generated by the parametrized weather generator LARS-WG for simulating long term climate characteristics, actual weather data and weather forecasts. During the growing season the irrigation schedule was adapted weekly according to actual weather data using the optimization framework. Preprocessing steps included the determination of optimal irrigation control functions using model Hydrus 2D. The aim was to provide sufficient water to all crop rows while diminishing percolation. Observations of *WP* and an economic analysis evaluated the implemented approach, see Figures 11.1 and 11.7.

In 2009, the optimization framework was applied to two subsurface drip irrigated (SDI) plots at an experimental site in Montpellier, France. Observed corn yields were satisfactory for the fully irrigated treatment (FULL) and both deficit irrigated SDI treatments. Grain yields of about $11.8\,\mathrm{t\,ha^{-1}}$ with total water amounts of 339 mm for treatment SDI160 (row distance 75 cm, drip line distance 160 cm) and 312 mm for treatment SDI120 (row distance 60 cm, drip line distance 120 cm) were reached, respectively. The control treatment yielded $16\,\mathrm{t\,ha^{-1}}$ with 478 mm total water applied to the surface drip irrigated treatment (FULL). The observed *WP*s were 3.8 ± 0.4 (SDI120), 3.5 ± 0.6 (SDI160) and 3.3 ± 0.3 kg $\mathrm{m^{-3}}$ (FULL). The study confirmed that using the optimization framework increased *WP* more than 13 % compared to FULL and up to 30 % compared to other treatments from 2007/08 at the same site. Regarding the profitability, the field design with a drip line distance of 160 cm was most profitable because of adequate yields and low initial installation and material costs of the irrigation system compared to field designs with drip line distances of 60, 120 and 200 cm. Further information regarding the study can be found in Walser et al. (2010).

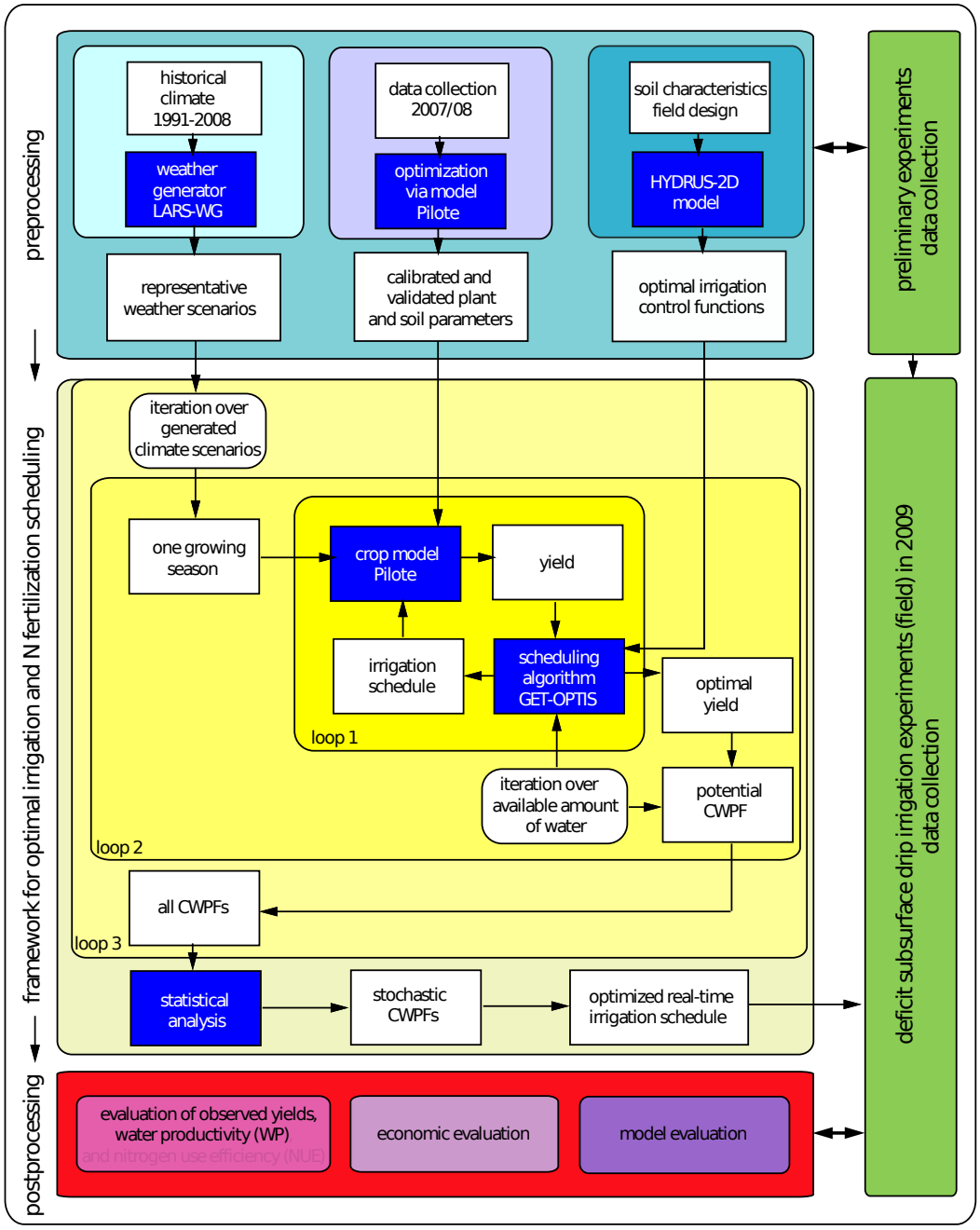

Figure 11.1.: The new approach of simulation based optimal experimental design consisting of (i) the preprocessing, (ii) the determination and experimental application of the optimized deficit irrigation schedules and (iii) the postprocessing for case study II. Not implemented steps of the approach are transparent

11.2. Experimental site and field design

In an annual field experiment in 2009, a high yielding corn variety (*Zea mays L.*, hybrid PR35Y65) was cultivated at the Cemagref Institute of Montpellier, France (43°38'48" N, 3°52'21" E, 30 m altitude). The experimental site, located in the Mediterranean climate, shows an average annual precipitation of 767 mm (1991 – 2008). The region has erratic and limited in-season precipitation and a high water deficit during summer of around 350 mm between potential evapotranspiration and precipitation. Daily average (1991 – 2008) maximum and minimum air temperatures are 20.9 and 8.6 °C, respectively. The soil of the experimental site is of loamy sandy to loamy clayey sandy texture (18 % clay, 44 % silt, 38 % sand). It is from both colluvial and alluvial origin being very deep, with a water table which is deeper than 5 m in summer and does not contribute to water supply of the crops. The soil water storage capacity ranges from 120 to 180 mm m^{-1}. The parameters of the van Genuchten/Mualem soil model taken from Wöhling and Mailhol (2007) are given in Table 11.1.

Table 11.1.: Van Genuchten/Mualem parameters (θ_s [$cm^3\,cm^{-3}$], θ_r [$cm^3\,cm^{-3}$], α [m^{-1}] and n [-]) and parameter K_s [$m\,s^{-1}$] of the experimental site at Cemagref, Montpellier taken from Wöhling and Mailhol (2007).

soil layer	θ_r	θ_s	n	α	K_s
0.00 – 0.55 m	0.05	0.35	1.457	1.5	$7.50 \cdot 10^{-6}$
0.55 – 0.95 m	0.05	0.38	1.447	1.3	$1.85 \cdot 10^{-6}$
0.95 – 2.00 m	0.05	0.41	1.310	1.9	$5.17 \cdot 10^{-7}$

Optimal adaptive irrigation scheduling was applied to two plots which were irrigated by a SDI system of Jain Irrigation Systems Ltd. (India) with a drip lateral depths of 0.35 m below the soil surface underneath tilling. Drip line spacings were 120 cm (referred to as SDI120, row spacing: 60 cm, plot size: 0.12 ha) and 160 cm (SDI160, row spacing: 75 cm, plot size: 0.11 ha), respectively. The dripper discharge rate for the SDI system was 2.5 l h^{-1} per meter drip line.

Moreover, two non irrigated (rainfed) treatments with row spacings of 60 (RF60) and 75 cm (RF75, both plot sizes about: 0.02 ha) and a surface drip irrigated full irrigation treatment where no water stress occurred (here called FULL, row spacing: 75 cm, drip line spacing: 150 cm, plot size: 0.095 ha) were established as control treatments. For the full irrigation treatment, a soil water balance approach based on FAO-56 (Allen, 2000) was used to estimate crop evapotranspiration (ET_c) and thus the irrigation water amount (for further explanations refer to Khaledian et al. (2008)).

An automatic meteorological station (CIMEL Enerco 411) located nearby at the experimental site of Cemagref Institute provided hourly data of average temperature, radiation, wind speed, air pressure, relative humidity and precipitation, amongst others.

The corn was grown using conventional production practices. At the beginning of October 2008, disc harrow was used to chop and bury the residues of the precedent crop. At the end of November, soil was plowed up to a soil depth of 25 cm. Corn was sown at a soil depth of 5 cm on 23/04/2009 (SDI160, FULL, RF75, row distances: 0.75 m) and on 07/05 (SDI120, RF60, row distances: 0.60 m), respectively. Sowing density was 100,000 plants per ha. The selected corn variety was indicated as a high yielding, above-average drought tolerant with about 3100 heat units until ripening, and with potential grain yields varying from 15.5 to 21.9 t ha^{-1} within a study of Pioneer Hi-Bred International, Inc. (USA).

Fertilizers were applied to sowing and during the season on the basis of soil analysis in order to fully satisfy plant requirements. At sowing, soil N mineral in the maximum rooting zone of corn varied from 50 to 60 kg N ha^{-1}. Treatment FULL was fertilized with 300 k N ha^{-1}, both SDI treatments with 210 kg N ha^{-1} and the rainfed treatments with 150 kg N ha^{-1}, respectively. Adequate amounts of phosphor (100 kg P ha^{-1}) and potassium (100 kg K ha^{-1}) fertilizers were applied to all treatments.

11.3. Data collection during the experiment

Soil water content was monitored during the cropping season on a crop row, between two crop rows next to a drip line and between two crop rows using aluminum access tubes with a neutron probe CPN 503DR (Campbell Scientific, USA) which were regularly read from 0 to 2 m soil depth at a 0.1 m depth interval. Moreover, mercury tensiometers (SDEC, France) were installed at 0.1, 0.2, 0.3, 0.45, 0.6, 0.9, 1.1, 1.3, and 1.5 m soil depths next to a row and at a distance of 0.4 m of a neutron probe and were monitored every morning. Initial soil water content observed at SDI160 on 07/05 ranged from 0.24 (at 10 cm soil depth) to 0.41 (at 2 m soil depth).

Seven sub-samples per treatment (2.5 m within two rows) were harvested on 17/09, 133 (SDI120, RF60) and 147 (SDI160, FULL, RF75) days after sowing, respectively. Grain yield (expressed at 15 % moisture content) and leaf and stem weight (oven dried until constant weight) of the sub-samples were determined for all treatments, respectively. For all observed plant variables, treatment means and standard deviations were calculated.

11.4. Calibration and setup of the crop growth model Pilote

For simulation based irrigation schedule estimation, crop growth model Pilote was applied. Pilote validation was carried out prior for different crops under different environmental contexts (Mailhol et al., 1997, 2004; Khaledian et al., 2008; Taky et al., 2009). The calibrated plant parameter file can be found in Appendix B. The crop growth model was used to simulate yield, LAI and soil water reserve at the experimental site. For calibration and validation of the model Pilote for corn cultivated under subsurface drip irrigation, data of two preceding years (2007/08) at the same experimental site (five treatments) were used (for further explanation refer to Khaledian et al. (2008)). For example in 2008, the grain yields Pilote predicted for two SDI treatments (simulation results vs. observed grain yields) were 14.7 vs. 15.0 $\mathrm{t\,ha^{-1}}$ and 15.2 vs. 15.1 $\mathrm{t\,ha^{-1}}$, respectively. The results of Khaledian et al. (2008) indicate that Pilote satisfactorily simulated LAI, soil water reserve, grain yield and dry matter yield at that site.

The setup of the Pilote crop model both SDI treatments was based on the field experiment described in Section 11.2. The management description consisted of the sowing dates on 23/04 (SDI160) and 07/05 (SDI120). For all irrigation events, a constant flow rate of 2.5 $\mathrm{l\,h^{-1}}$ per meter drip line was employed. The soil parameters (no initial water deficit, field capacity was set to 320 $\mathrm{mm\,m^{-1}}$) and plant parameters ("Pioneer maize") used in Khaledian et al. (2008) were applied.

Figure 11.2.: The pictures show the corn field of SDI120 and the buried SDI dripline.

11.5. Derivation of optimal irrigation control functions for different drip line spacings

The preprocessing steps contained the derivation of the optimal irrigation control function $q_t\,(\theta_{t=0}$, drip line spacing $\triangle l)$ to estimate the appropriate irrigation time for the specific drip line spacing and discharge rat (see Fig. 11.7, step 1). Determining the appropriate irrigation time for a given drip line spacing and discharge rate involves the consideration of the soil parameters (e.g. soil texture, retention curve) and initial soil moisture. In order to optimize the irrigation control, the widely used water transport model Hydrus 2D (Šimůnek et al., 1999) was applied.

11.5.1. Initial Hydrus 2D/3D simulations

At first, three dimensional Hydrus 3D simulations were conducted to test the assumption of a horizontal symmetric water flow in the 3D domain, thus to test the suitability of the Hydrus 2D model for the field designs. In other words, Hydrus 3D simulations were intended to show the formation of an axially symmetric water bulb along the drip line, in the same manner representable by Hydrus 2D.

Using Hydrus 3D, a soil column (in total 100 cm x 165 cm x 90 cm) with one drip line (5 emitter) was set up. The model boundaries were set to variable flux for irrigation, free drainage at the bottom of the column and no flow for border and the rest of the upper boundary condition. The initial pressure head was -10 m, irrigation duration was 15 h, followed by 85 h for redistribution. The soil hydraulic characteristics of Table 11.1were taken.

Hydrus 3D simulations were carried out with challenging initial conditions – initial pressure head was -10 m and the irrigation amount was low – however a homogeneous distribution was achieved after 48 h. Thus, a higher initial soil moisture as occurred in the experiment in 2009 together with the irrigation enforce a uniform distribution of the applied irrigation water in the considered loamy soil. Hydrus 3D simulations showed that – after an irrigation event of 15 h and a redistribution time of 85 h – the water bulbs of all emitters along the drip lines conjoined to an horizontally symmetric line (see Fig. 11.3). Thus, an application of Hydrus 2D using only one cross section of the field is adequate to represent the transient 3D water flow of the whole domain.

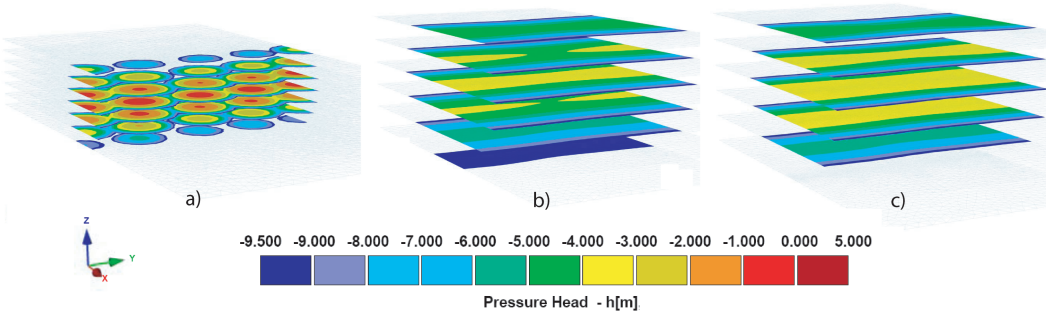

Figure 11.3.: The figures show Hydrus 2D/3D simulation results. Irrigation duration of the event was 15 h, followed by 85 h of redistribution. The pressure head conditions after 4 (a), 50 (b) and 69 h (c) are illustrated. The initial pressure head was −10 m. Emitter distances and drip line depth are 30 cm and −35 cm, respectively. a) shows the soil layers at 15 cm, 20 cm, 25 cm, 30 cm, 35 cm, 40 cm and 45 cm. Figures b) and c) show the soil layers at top soil, 15 cm, 30 cm, 45 cm, 60 cm and 75 cm soil depths.

11.5.2. Determination of the irrigation control functions

Since the arrangement of the crop rows and drip lines is non-uniform (e.g. for SDI160 the row spacing is 75 cm and the drip line spacing is 160 cm), some crop rows are remote to irrigation drip lines. Hydrus 2D was utilized to derive characteristic irrigation control functions for the determination of optimal irrigation times and water amounts. The objective was to provide an almost uniform distribution of the irrigation water supplying irrigation water to all crop rows with a high adequacy. Meanwhile, deep percolation provoked by heavy water application amounts and/or elevated initial soil moisture contents had to be minimized. The main focus of interest were the worst case scenarios where the widest distance to the next drip line for one row occurred (Fig. 11.4).

Using Hydrus 2D, a soil column with four sections (in total 120 cm x 200 cm) was generated for SDI120 and SDI160. The model boundary conditions were set to atmospheric at the soil surface, seepage at the bottom of the column, and no flow (border). The initial value for the soil moisture was set for all 3 layers with a given relative soil moisture $\theta_{t=0} = \theta_s \cdot \theta_{rel}$ with $\theta_s = 0.35$ although the value for the upper soil layer was $\theta_s = 0.38$. $\theta_{t=0}$ ranged from 0.3 to 0.85. Periods of 3 and 6 days were predicted for redistribution, resulting in lower soil moisture values in the upper layer because of percolation. Afterward, transpiration (6 mm per day) and evaporation (0.75 mm per day) from the soil were considered (for a day light of 15 h). The root water distribution function by Vrugt et al. (2001) was applied. A rooting depth of 100 cm at the 50th day after sowing was assumed after simulations with a SVAT model.

Exemplary for SDI160, the center of the roots were located at x=0 cm (left root zone) and x = 75 cm (right root zone), see Fig. 11.4. The duration of the irrigation with a discharge rate of $2.5\,\mathrm{l\,h^{-1}\,m^{-1}}$ was increased in each simulation. After three simulation days for redistribution, the mass balances of sections I and IV were calculated. Percolation V_p [mm] is given by:

$$V_p = \Delta V^{III} + \Delta V^{IV} + Sp \tag{11.1}$$

where V stands for water volume in a given section and Sp stands for seepage, both in mm. The water flowing from section II to section I (Q^{I}) equals the amount of irrigated water the plants of the left root zone I can use, where $\Delta V^I = \Delta V(t) - \Delta V^I(t_0)$, i.e. $\Delta V > 0$ means that the water volume in that section increased between t_0 and t.

The fraction of applied water volume flowing from section I to section II , Q^{I-II}, was calculated for SDI160 (row spacing of 75 cm, drip line spacing of 160 cm) by:

$$Q^{I-II} = \Delta V^I + ET_0^I + \Delta V^{III} + \frac{75}{2}/160 \cdot Sp \tag{11.2}$$

where ET_{c} is crop evapotranspiration. The mass balances of all sections were calculated after various irrigation durations up to 30 h. Calculations were done for SDI120 and SDI160 for various initial relative soil moistures and for three and six simulation days, respectively. Furthermore, Hydrus 2D calculations to estimate the application efficiencies of SDI120 and SDI160 and for hypothetical drip line spacings of 60 cm (referred to as SDI60) and 200 cm (SDI200) were conducted, respectively.

The simulations with Hydrus 2D showed that an increased duration of subsurface drip irrigation and higher initial soil moisture both increased the amount of water reaching the left root zone (see Fig. 11.5). Percolation decreased with lower initial soil moisture content and, at the beginning, with increased duration of irrigation, while the amount of water percolating out of the root zone increased after reaching a threshold, which depended on the initial soil moisture.

In the agricultural practice, drip irrigation water is often applied in high frequencies (e.g. daily) with little irrigation water amounts per application. At that site, this strategy would result in low percolation but highly non uniform water distribution and thus lead to yield reduction at under-supplied rows.

The application of Hydrus 2D confirmed that irrigation amounts of about 20 – 35 mm (depending on initial soil moisture, discharge rate at $2.5\,\mathrm{l\,h^{-1}\,m^{-1}}$) are a good choice for distributing the water uniformly in a satisfactory manner while restricting deep percolation at the same time. These findings were applied within the irrigation scheduling described below.

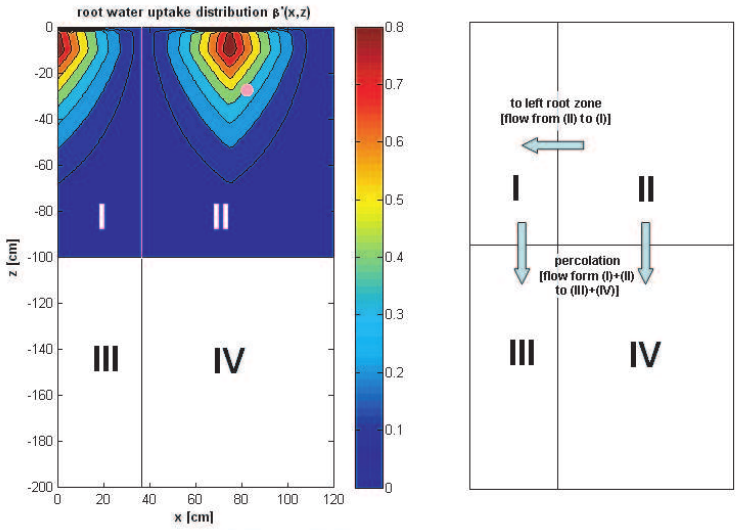

Figure 11.4.: Model setup for calculating the distribution of the irrigation water for SDI160. The distance of the crop rows and the drip lines is 75 cm and 160 cm, respectively. The worst case scenario (widest distance to next drip line) for the left root zone is shown. The emitter (pink dot) is located at a soil depth of 35 cm ($z = -35$ cm) and 5 cm from the root center of the right root zone which is at $x = 75$ cm.

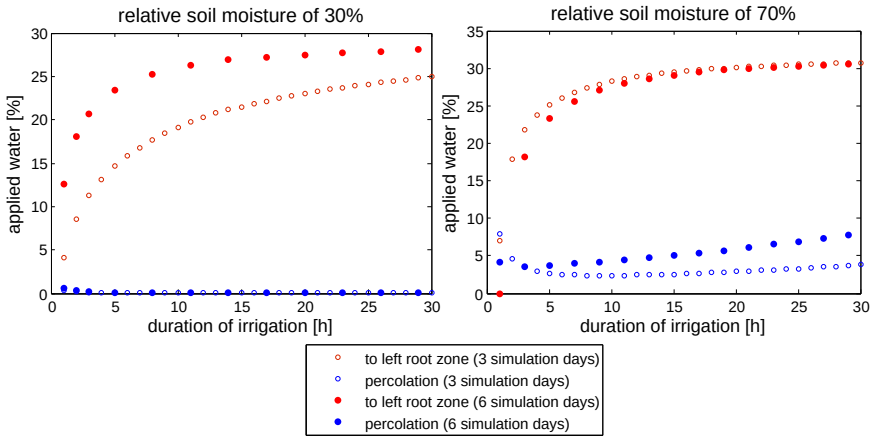

Figure 11.5.: This figure shows the percentage of applied water reaching the left root zone and the percentage of percolated water in section I depending on the duration of irrigation [h]. 29 and 12 simulations were performed for 3 and for 6 simulation days (for redistribution), respectively. The initial relative soil moisture was $\theta_{t=0} = 30\,\%$ (left side) and 70 % (right side).

11.5.3. Verifying measurements

Observed water distribution after a heavy test irrigation event of 33.5 mm applied on SDI160 in 2009 was compared to former measurements in 2007/08 (high frequent irrigation events with low water amounts) aiming to verify the presumptions. In 2009, neutron probes observed water contents before, 20 min past and 2 days after the test irrigation event. The restricted percolation after the heavy irrigation event can bee seen in Figure 11.6.

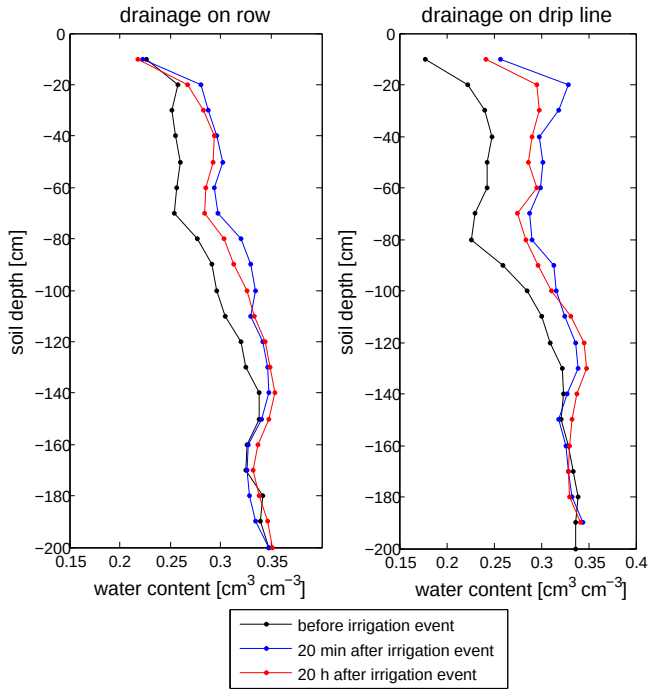

Figure 11.6.: Observed soil water contents before, and 20 min and 48 h after an heavy irrigation event of 33.5 mm at SDI160 in 2009.

Even at the heavy irrigation test event with an irrigation amount of 33.5 mm on a relatively wet soil, only marginal percolation was observed. The lateral extension of the moistened zone was around 45 cm from the drip line for a soil depth of 70 cm (Mailhol et al., 2011).

By contrast, in 2008 were high frequent irrigation events with low water amounts were applied, significant vertical movement of water was found only until the soil depth of 45 cm. Additionally, there was almost no horizontal distribution of water measured, meaning that this drip line did barely contribute to the water supply of the next crop row (Rosique et al., 2009).

11.6. Real-time deficit irrigation scheduling

In the present case study, the new approach of optimal experimental design consisted of (i) preprocessing steps (crop growth model calibration, determination of the optimal irrigation control (both explained above) and synthetic weather scenario generation), (ii) the real-time irrigation scheduling during the growing period, and (iii) postprocessing steps (*WP* and economic evaluations), see Figure 11.7.

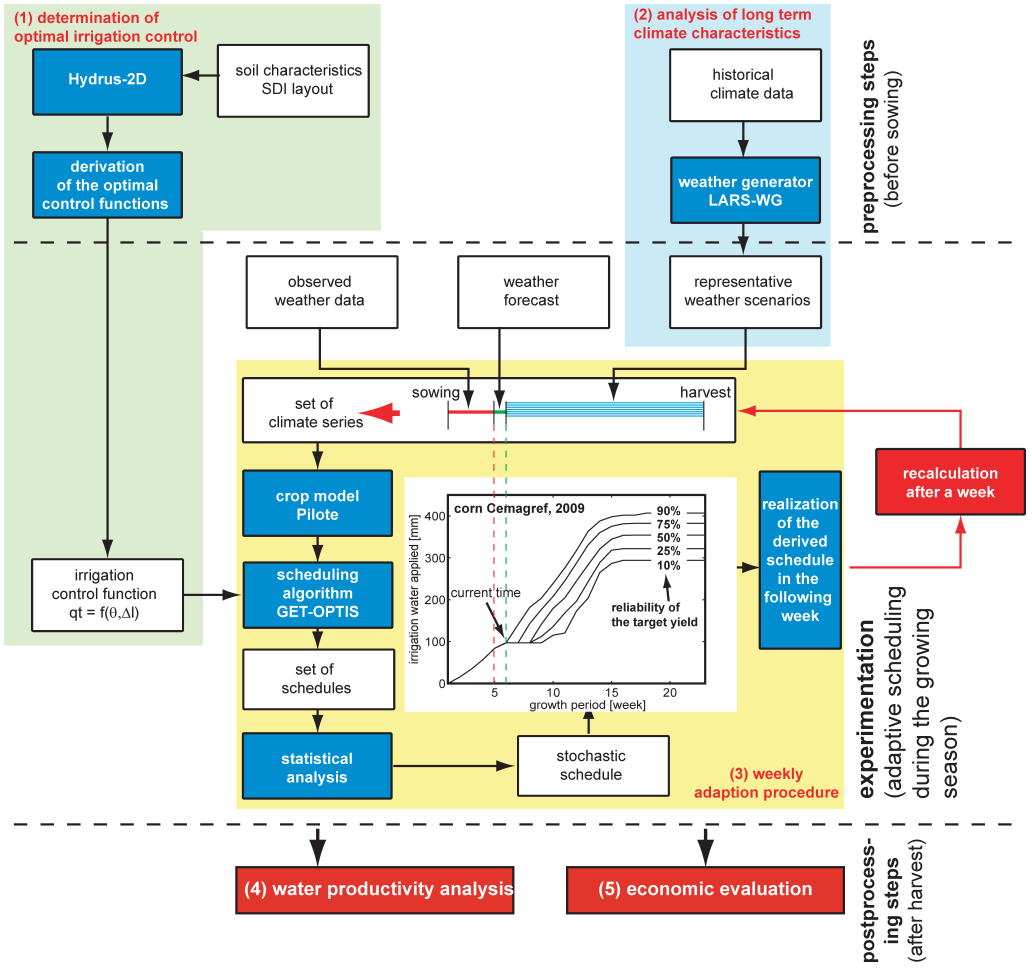

Figure 11.7.: The optimization framework for real-time deficit irrigation scheduling consists of the determination of the optimal control functions (1), the generation of representative weather scenarios (2), real-time scheduling (3), and an evaluation of water productivity (4) and economic aspects (5).

The real-time irrigation scheduling shown in Fig. 11.7 (step 3) was weekly employed until the end of the growing season and was based on a climate series consisting of (i) observed weather data of the current growing season since sowing, (ii) the weather forecast, and (iii) a set of generated weather scenarios for the remaining time until harvest. The weather generator LARS-WG was used to generate representative weather scenarios for the long-term climate characteristics based on historical climate data observed at Cemagref from 1991 – 2008.

The deficit irrigation scheduling is based on a simulation based optimization method including the scheduling algorithm GET-OPTIS and the Pilote crop growth model. Since GET-OPTIS is an open-loop optimization technique that calculates optimal schedules throughout the growing season in advance, it was necessary to adapt this method including a feedback control which responds to external events (i.e. deviations of the predicted climate conditions from the observed climate conditions e.g. in case of precipitation). The procedure developed to solve the feedback problem is based on a stochastic approach which uses a set of climate series consisting of observed weather data, actual weather forecasts and weather scenarios which are representative for the long term climate pattern until the end of the growing season (see Fig. 11.7, step 3). The simulation/optimization package comprising Pilote and GET-OPTIS generates then a set of corresponding schedules which are evaluated by a statistical analysis in order to provide a reliable schedule for the actual date of the growing season.

In this study, a simulation based deficit irrigation schedule that reaches a given grain yield of $14\,\mathrm{t\,ha^{-1}}$ with a reliability of 90 % – which maximizes *WP* – was provided for SDI120 and SDI160 and adapted weekly according to actual weather by the stochastic optimization framework. The weather data of the current growing season since the sowing at the experimental site was used once a week to rerun the optimization algorithm calculations. For example, every Monday the observed weather data of the last week was implemented and the stochastic scheduling algorithm was rerun defining a certain amount of irrigation water to be irrigated in the following week. This irrigation water amount was applied considering possible precipitation using the weather forecast. The 90 % quantiles of cumulative irrigation amount of the generated set of schedules were used as the tool for irrigation decision; by subtracting occurring precipitation from the one week's estimated irrigation depth, precipitation was manually adapted.

Statistics about the minimum amount of water needed for achieving $14\,\mathrm{t\,ha^{-1}}$ grain yield based on GET-OPTIS and Pilote simulation-optimization and weather scenarios composed of the 2009 time series and scenario series from a parametrized LARS-WG show that, for a reliability of about 95 % to reach $14\,\mathrm{t\,ha^{-1}}$, 330 mm have to be irrigated whereas for a reliability of 50 % about 250 mm are needed. The span narrows with the weekly optimizations as variability of the yield decreases with approaching ripening. Most irrigation

events have to take place between the 7th and the 15th week after sowing. The recommendation of the irrigation amount was adapted weekly using the optimization framework (see Fig. 11.7). Figure 11.8 exemplary shows the results of the 5th week (SDI160) of the calculations separated into single irrigation events.

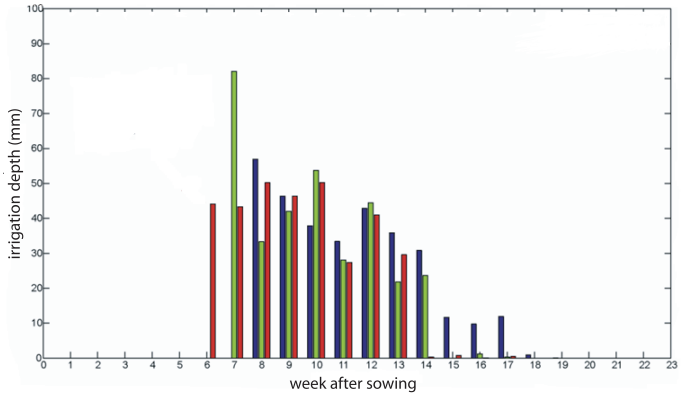

Figure 11.8.: Estimation of the irrigation amount. 50 % quantiles (blue), 95 % quantiles (green) and 99 % quantiles (red) of no-rain scenarios for SDI160.

For instance, using the 95 or 99 % quantiles, about 80 or 90 mm of irrigation water should be applied within the 6th and 7th week after sowing, respectively. In contrast, the schedule assuming a 50 % reliability suggests no irrigation in the next two weeks since the standard reliability was set to 90 % and the actual soil water content was above the average of the 50 % reliability scenario. The other way around, the scheduled applications of the 95 and 99 % scenario are relatively high because the actual soil water content was below the average of these scenarios.

Due to some restrictions (fertilization, management), some of the applied irrigation amounts were smaller than predetermined by the Hydrus 2D simulations. Moreover, some irrigation events were spit into two days. All these modifications lead to an overall reliability which was ultimately below the assumed 90 %. Table A.2 in the Appendix shows the applied irrigation schedules for SDI120 and SDI160 in 2009. The difference of 6.2 mm between both total irrigation sums resulted from the different sowing dates and thus different initial soil moistures and weather data.

Runoff was not monitored but is not likely to occur due to the fields even slope. Moreover, runoff was not noticed by the staff. Due to the deep water table, it is assumed that groundwater recovery is not possible. Using model Pilote, cumulative seasonal actual evapotranspiration was estimated to be 449 mm for SDI120 and 480 mm for SDI160 (Mailhol et al., 2011).

11.7. Evaluation of the experimental results

The postprocessing steps consist of the evaluation of the experimental results, namely observed crop yields and calculations of *WP* (see Fig. 11.7, step 4). Furthermore, prognostic simulations were conducted to evaluate the profitability of differing field designs.

11.7.1. Crop yields

The entire growing season in 2009 can be characterized as dry: precipitation from sowing to harvest was only 96 mm (SDI160, FULL, RF75), and for the later sowing date (SDI120, RF60) even only 63 mm, respectively. In general, yields increased with increasing applied irrigation water. Irrigation, ranging from 0 to 382 mm, enormously affected yield, especially with precipitation being very low. The highest yield of 16.0 t ha^{-1} was obtained by the fully irrigated treatment (FULL). As expected, comparing the controlled deficit irrigated SDI treatments to treatment FULL, total grain yield and grain yield per plant was higher for the control. The difference of 4.2 t ha^{-1} between the FULL and both SDI treatments was due to an intended water deficit which occurred applying the deficit irrigation strategy at both SDI treatments. Compared to SDI160 with almost the same drip line and row distances than the control, FULL showed higher 1000 – seed weight and plant density resulting in higher yields. The harvest index was 59 and 62 % for SDI120 and SDI160, respectively (Table A.3 in Appendix).

For both SDI treatments, grain yield was 11.8 t ha^{-1}, with a higher variability for SDI160 (11.8 ± 1.9) due to the broader drip line and row distances compared to SDI120 (11.8 ± 1.4). However, due to a later sowing date of SDI120, yield could have been higher for a similar growth duration. The growth durations were 133 (SDI120, RF60) and 147 days (SDI160, FULL, RF75). The higher 1000 – seed weight / *TSW*) of SDI160 compensated for the lower plant density and led to higher grain yield per plant compared to SDI120 (167 vs. 130 g per plant). The two rainfed treatments resulted in very low grain yields due to high drought stress were RF75 yielded higher than RF60 (3.3 vs. 2.5 t ha^{-1}) with a lower plant density but higher *TSW*. Plant data and applied water amounts for all treatments are shown in Table 11.2.

The visual condition of the corn plants from 2007 to 2009 suggested that different drip line spacings resulted in different patterns of crop biomass distribution on the field (e.g. plant height, biomass), with biomass generally decreasing with increasing distance from the emitter. The higher variability in grain yields and dry matter for SDI160 compared to SDI120 and FULL confirm these field observations. Conducted root profiles verified assumptions of maximum root depth of 1.2 m of corn at harvest. For further details about the experiment and the root profiles, refer to Mailhol et al. (2011).

Table 11.2.: Water received and plant data (value ± standard deviation): Amount of irrigated water applied I [mm], precipitation P [mm], total applied water TAW (sum of applied irrigation water and precipitation during the growth period [mm]), grain yield with a water content of 15 % Y [t ha^{-1}], total dry matter TDM [t ha^{-1}], 1000 – seed weight TSW [g], plant density PD [plants per ha], and grain yield per plant GYP [g per plant] for corn in Montpellier, 2009.

treatment	I	P	TAW	Y	TDM	TSW	PD	GYP
SDI120	249	63	312	11.8 ± 1.4	19 ± 4.1	278	90,820	130
SDI160	243	96	339	11.8 ± 1.9	20 ± 5.7	323	70,800	167
FULL	382	96	478	16.0 ± 1.2	25 ± 2.2	365	75,090	213
RF60	–	63	63	2.5	7.5	165	84,300	30
RF75	–	96	96	3.3	8.4	221	69,440	47

11.7.2. Water productivity

In order to evaluate the achieved yields and WPs of the annual experiment in 2009, data from irrigation experiments conducted with corn at the same site in 2007 and 2008 were observed. Within two deficit irrigated (referred to as 2007 T4 and 2007 T5) and one full irrigated (2007 FULL) experiment in 2007, a different irrigation schedule was applied: irrigation took place every working day (on Monday and Friday the applied irrigation water amount was doubled). The high frequency led to small applications per irrigation event (Rosique et al., 2009). In 2008, the SDI system was installed and a deficit irrigation schedule (70 % of maximum water requirement) similar to 2007 was applied (Khaledian et al., 2008; Mailhol et al., 2004). Unpublished data were kindly provided by the staff of Cemagref. WPs were calculated if adequate data was available.

With little exceptions, all calculated WPs (WP, WP_{RF}, WP_{SW}) were higher for both optimized SDI treatments compared to the treatments in 2007 and 2008. Due to the higher precipitation in 2007 and 2008, WP_{IRR} was higher for most treatments in these years compared to 2009. In 2009, WPs reached 3.8 ± 0.4 (SDI120), 3.5 ± 0.6 (SDI160), 3.3 ± 0.3 kg m^{-3} (FULL). WP was highest for SDI120, but SDI160 still showed higher WP than FULL. The soil water depletion from the root zone during the growing season (SW) was 130 mm for both optimized treatments SDI120 and SDI160 in 2009. In 2007, the surface irrigated treatments reached WPs of 2.7 kg m^{-3} (2007 FULL), 3.2 kg m^{-3} (2007 T4) and 3.4 kg m^{-3} (2007 T5). In 2008, grain yield barely differed for both SDI treatments which lead to a WP of 3.2 kg m^{-3} for both treatments. Table 11.3 shows that WP was highest for the treatments where the optimization framework was applied.

WP was increased by more than 13 % within the treatments in 2009 and up to 30 % within all irrigation treatments since 2007, respectively. The results show that the application of the optimization framework for optimal irrigation scheduling led to increased *WP*s.

Table 11.3.: Irrigation treatments for corn from 2007 to 2009 at Cemagref, Montpellier. Irrigation water applied I and effective precipitation P [mm], grain yields Y (water content of 15 %) and grain yields of rainfed treatments Y_{RF} [t ha^{-1}], soil water depletion from the root zone during the growing season SW [mm], and several *WP*s [kg m^{-3}] (value ± standard deviation).

treatment	P	I	Y	Y_{RF}	SW	WP	WP_{IRR}	WP_{RF}	WP_{SW}
2007 FULL	205	430	17.4	4.9	170	2.7	4.0	2.0	2.2
2007 T4	205	306	16.4	4.9	–	3.2	5.4	2.3	–
2007 T5	205	260	15.6	4.9	–	3.4	6.0	2.3	–
2008 SDI120	236	235	15.1	–	105	3.2	6.4	–	2.6
2008 SDI160	236	198	15.0	–	130	3.2	6.4	–	2.5
2009 FULL	96	382	16.0 ± 1.2	3.3	–	3.3 ± 0.3	4.2 ± 0.3	2.7 ± 0.3	–
2009 SDI120	63	249	11.8 ± 1.4	2.5	130	3.8 ± 0.4	4.7 ± 0.6	3.0 ± .5	2.7 ± 0.3
2009 SDI160	96	243	11.8 ± 1.9	3.3	130	3.5 ± 0.6	4.9 ± 0.7	2.5 ± 0.7	2.5 ± 0.4

In 2009, an increasing variability of the grain yield with increasing drip line spacings was observed. In 2008, the non-uniformity of the high frequent irrigation water applied was covered by the uniform distribution of high precipitation. However, precipitation was very little in 2009 compared to 2008.

11.7.3. Prognostic simulations

For prognostic planning, two hypothetical field designs with drip line spacings of 60 (SDI60) and 200 cm (SDI200) were evaluated. Model Hydrus 2D was built up for both hypothetical field designs similar to the ones explained above to determine the application efficiencies. In the case of SDI60, row and drip line distances were 75 and 60 cm, respectively, the rows were installed near the drip lines. In the case of SDI200, row and drip line distances were 75 and 200 cm, respectively. One row in the middle was installed above a drip line, two rows (on left and right side) were 75 cm distant to that drip line. The estimated application efficiencies for both layouts were taken for prognostic simulations with crop model Pilote (setup see Section 11.4), and for comparisons with the real cases (SDI120 and SDI160).

The application efficiencies of SDI60 and SDI200 were determined using Hydrus 2D. For SDI200, application efficiencies increased with higher $\theta_{t=0}$ (e.g. 55 – 60 % for $\theta_{t=0} = 85$ % and 45 – 55 % for$\theta_{t=0} = 70$ %, both within an irrigation duration of 30 h), and decreased

with shorter irrigation durations. The application efficiency for SDI200 was set to 35 % (at a initial humidity of 50 % and irrigation duration of 30 h). In the case of SDI60, an irrigation could last up to 20 h under dry conditions ($\theta_{t=0} < 50\,\%$) with only little percolation ($V_P < 3\,\%$). Percolation was lowest ($V_P = 0.6\,\%$) within short irrigation durations of 4 – 5 h for $\theta_{t=0} = 85\,\%$, but still low ($V_P = 0.7\,\%$) within irrigation durations of 7 – 10 h for $\theta_{t=0} = 50\,\%$. The application efficiency of SDI60 was assumed to be 100 %.

Table 11.4.: Grain yield [t ha^{-1}] for different irrigation application efficiencies [%] determined with crop model Pilote (based on the deficit irrigation schedule of SDI160 in 2009).

application efficiency	100	95	90	80	75	65	45	35	25
grain yield	12.7	11.8	11.5	10.7	10.3	9.4	7.8	5.6	4.8

Hence, application efficiencies of 95 % for SDI120 and SDI160, 100 % for SDI60 and 35 % for SDI200 were estimated. The grain yields of SDI60 and SDI200, estimated on the basis of the deficit irrigation schedule of SDI160 using Pilote, were 12.7 and 5.6 t ha^{-1}, respectively (see Table 11.4).

11.7.4. Economic aspects

The following data was used to estimate the profit using Eq. 9.1. According to the General Association of the Corn Producers (AGPB, France)[1], the price for corn was around 130 € t^{-1} in December 2009 (southeast France). Fixed costs included the annual payment for financing the initial investment of SDI materials and installation (5 % interest over 10 years). According to Jain Irrigation Systems Ltd, the costs for the subsurface drip line including installation for a drip line spacing of 160 cm are 2700 € ha^{-1}, for a drip line spacing of 120 cm 3600 € ha^{-1}, respectively. The costs were calculated for plots of 10 ha including a filter and a drip line with a thickness of 375 mm. The appropriate lifetime of the SDI system was assumed to be 10 years.

Hence, annual payment for initial installation and material of the SDI system (including 5 %) was 462 (SDI160) and 616 € ha^{-1} (SDI120) and assumed to be 1231 (SDI60) and 369 € ha^{-1} (SDI200), respectively. Additional fixed costs were those associated with corn production (e.g. seeds, fertilization and selling) and were assumed to be 10 € t^{-1}. Water prices were assumed to be 0.04 € m^{-3} (Bontemps and Couture, 2002). The costs of labor and energy were expected to be 10 € per irrigation event (SDI160: 17, SDI120: 18 irrigation events, respectively).

[1] www.agpb.fr

The estimated annual payment costs were more than 2.7 and 1.3 times higher for SDI60 and SDI120 compared to SDI160, but 20 % lower for SDI200. Considering the total costs and gains for corn production in 2009, profit was highest for SDI160 with 774 € followed by SDI120 (568 €), SDI60 (122 €) and SDI200 (61 €).

Table 11.5.: Total profit estimated for two deficit irrigated subsurface drip irrigated (SDI) treatments and two hypothetical treatments with drip line spacings of 60 and 200 cm for corn at Cemagref in 2009. All costs and profit are in € ha^{-1}.

costs and profit	SDI60	SDI120	SDI160	SDI200
costs for material	2,800	1,400	1,100	880
installation costs	4,400	2,200	1,600	1,280
annual payment	1,231	616	462	369
total additional fixed costs	118	160	118	118
total costs (labor and energy)	170	180	170	170
total costs for water applied	10	10	10	10
total costs for 2009	1,529	966	760	667
total price for yield in 2009	1,651	1,534	1,534	728
profit	122	568	774	61

Mainly due to lower annual payments and additional fixed costs at similar grain yields, profit was 27 % higher for SDI160 compared to SDI120. Both hypothetical treatments with extreme wide and short drip line spacings demonstrate that high installation and material costs (SDI60) and low yields due to low application efficiencies (SDI200) both greatly reduce profit. Figure 11.9 shows that the maximal profit can be found around SDI160.

11.8. Discussion and conclusions

Regarding the optimization of the irrigation control, good results were achieved. In 2009, analysis of soil water content and soil tension measurements showed that high percolation rarely appeared. Even at a heavy irrigation test event on a relative wet soil, only marginal percolation was found. By contrast in 2008, when high frequent irrigation (5 times a week) took place, there was almost no horizontal movement observed. Hence, the belief that high frequency irrigation should be preferred in drip irrigation (Shani et al., 2009) is not always true. The variability of the yield which increased with drip line distance can be reduced with a better following of the guidelines.

The crop model performance was evaluated by comparing the previous predicted target yield and harvested yield. The target grain yield of 14 t ha^{-1} moderately met harvested

grain yields of 11.8 ± 1.4 (SDI120) and $11.8 \pm 1.9\,\mathrm{t\,ha^{-1}}$ (SDI160). The reason may be that the reliability of 90 % was set too low. Additionally, the weather generator LARS-WG underestimates extreme events, such as the very dry growth period in 2009. Moreover, there were minor problems by implementing the optimized irrigation schedule due to technical and management restrictions, leading to a few irrigation events with unrequested low water amounts applied.

Most crop models do not consider the drip line layout, equal if they are water balance based like Pilote, or SVAT 1D water flow based. Therefore, the combination of a 2D water flow model to determine irrigation control functions and a crop model performed well. For example, the soil water balance module of Pilote does not adequately present the non-uniform soil moisture distribution of the experimental site caused by drip line layout. The approach only partially represents the situation on the fields, not taking into account the drip line layout, e.g. ignoring higher percolation for wider drip line spaced plot SDI160.

The new approach of optimal experimental design including the real-time irrigation scheduling performed well, confirmed by the high *WP*s achieved and the economic analysis. The study confirmed that *WP* was increased significantly up to 30 % compared to other treatments at the same site by using the optimization framework. Moreover, high *WP*s were achieved compared to typical *WP*s for drip irrigated corn in literature ranging from 0.3 to $2.4\,\mathrm{kg\,m^{-3}}$ (O'Neill et al., 2008; Rodrigues and Pereira, 2009; Dehghanisanij et al., 2009). Even considering the variability, the *WP*s of 3.8 ± 0.4 (SDI120) and 3.5 ± 0.6 (SDI160) are high. *WP* was higher for SDI120 compared to SDI160 due to higher precipitation in the case of SDI160 caused by the earlier sowing date. Grain yield and irrigation amounts for both SDI treatments were similar. Noteworthy, SDI160 reached higher grain yields per plant (167 compared to SDI120 with 130 g per plant), but the lower plant density lead to similar grain yields per ha compared to SDI120.

However, increased profits by investment and material savings may be more meaningful to farmers compared to increased *WP*s. Considering the annual costs for installation and material of SDI systems, total prices and total costs, profit was about 27 % higher for SDI160 compared to SDI120. Main reasons are the lower installation and material requirements for the wider drip line spacing layout and similar yields for SDI120 and SDI160. Additionally, less frequent irrigation events reduced costs due to labor and energy savings. The impact of water amounts was negligible, since water prices are very low in France.

However, in cases where water is a limiting factor or expensive, a higher *WP* of deficit irrigation may be more important than the high yields reached with full irrigation. In this case study, the most profitable field design was the one with the 160 cm drip line spacing. However, the determined control functions are only valid for loamy soil and have to be determined for different soils and field layouts.

The climate was reflected adequately by LARS-WG, but problems may occur in very extreme years e.g. when extreme events are strongly underestimated.

Even if the computational effort and required skills were high, the implementation of the new approach of optimal experimental design lead to considerable cost and water savings. It can be transferred to diverse conditions and can be applied to different soils, field designs and cultivars. The approach proved to be an adequate tool for planning an optimal field design and irrigation schedules.

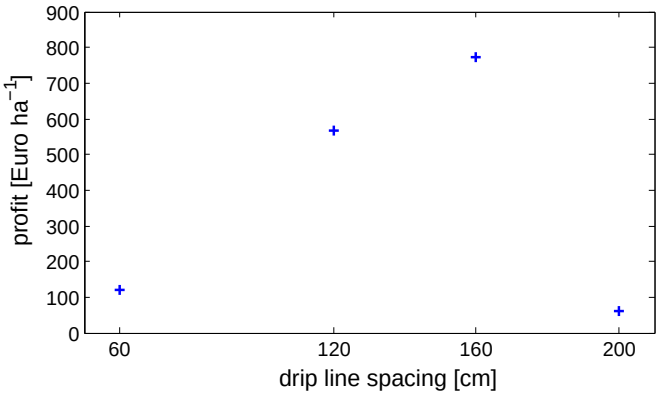

Figure 11.9.: The annual profit [€ ha^{-1} depending on the drip line spacing [cm] for SDI60, SDI120, SDI160 and SDI200.

12. Case study III: Multicriterial optimization of deficit irrigation and N fertilization

12.1. Objectives and summary

In this case study, the new approach was applied in order to evaluate different irrigation and N fertilization strategies for sustainable crop production. In 2010, corn was cultivated in 18 containers in the glass greenhouse of the Dürnast Experiment Station of the Technische Universität München, Germany. The stochastic optimization framework was applied to determine deficit irrigation and N fertilization schedules aiming to maximize *WP* and/or *NUE*. Schedules for four treatments were determined: a deficit irrigated treatment ($T_{def\,irr}$), a deficit N fertilized treatment ($T_{def\,N}$), and a fully irrigated and N fertilized control treatment (T_{full}). Within treatment $T_{def\,irr\,N}$, irrigation and N fertilization both were limited and simultaneously and optimally distributed over the growing period with the objective to maximize both, *WP* and *NUE*.

The results demonstrate that the stochastic optimization framework can be successfully utilized to obtain high *WP*s and *NUE*s. *WP* of the water limited treatment $T_{def\,irr}$ was increased by 22 % compared to the fully irrigated treatment (3.3 vs. 2.7 kg m^{-3}). *NUE* was highest for $T_{def\,N}$ (58 kg grain kg N^{-1}), which means an increase of 76 % compared to $T_{def\,irr}$. It can be concluded that simulation based optimization of irrigation or N fertilization was capable to enhance *WP* and *NUE*. However, a simultaneous optimization of both, irrigation and N fertilization performed only moderate leading to a *WP* of 2.7 kg m^{-3} and a *NUE* of 41 kg grain kg N^{-1} ($T_{def\,irr\,N}$).

After harvesting, postprocessing simulations were accomplished. Daisy 1D satisfactory predicted yields only when radiation was increased by 80 %. It is assumed that the plants received a higher total radiation than the observed one due to the greenhouse conditions (free-standing containers). However, this corrective action is only a compromise which in addition does not lead to accurate predictions of water dynamics. Fig. 12.1 shows the steps of the approach which were considered in that case study. The results were published in Walser et al. (2011b).

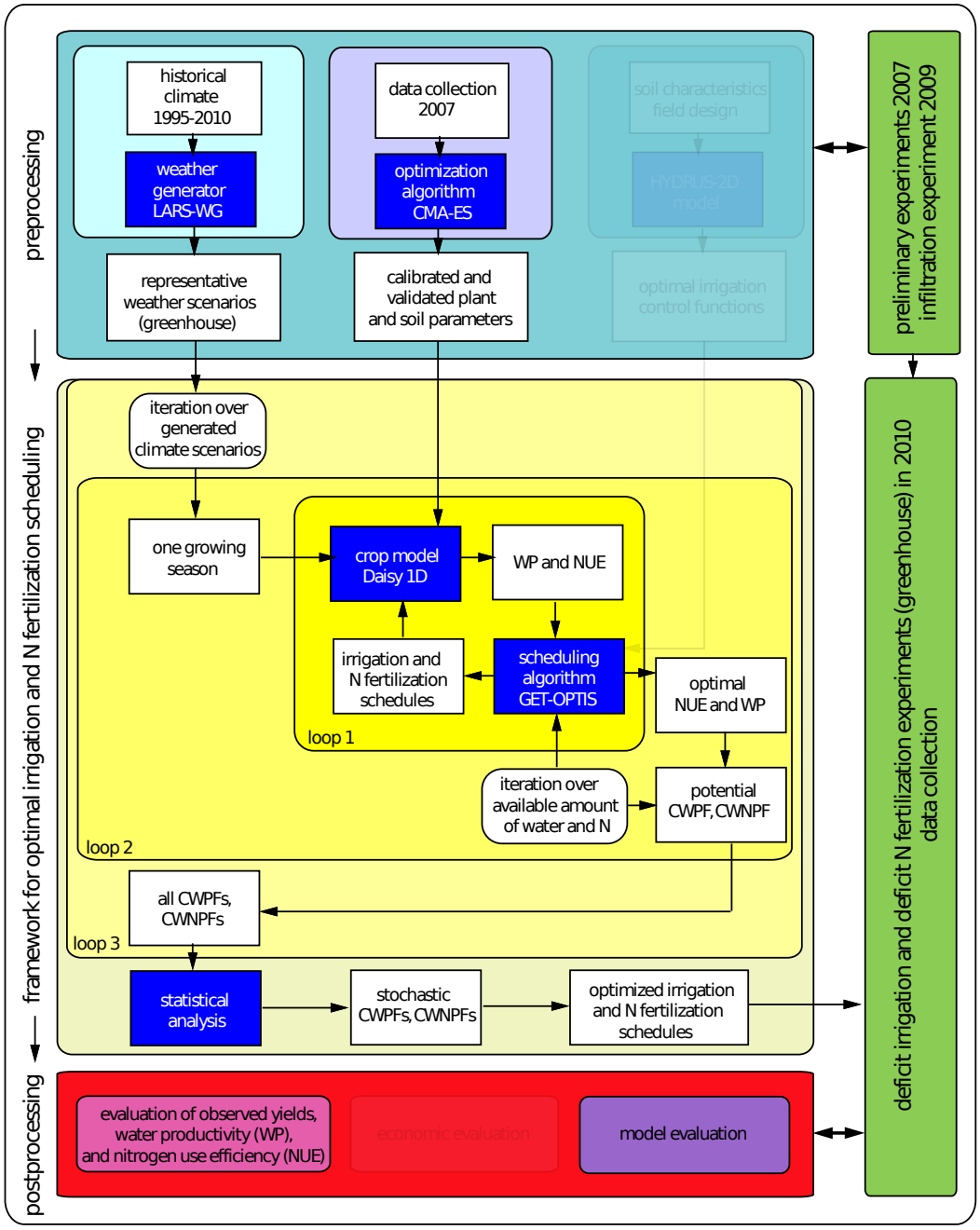

Figure 12.1.: The new approach of simulation based optimal experimental design consisting of (i) the preprocessing, (ii) the determination and experimental application of the optimized deficit irrigation and N fertilization schedules and (iii) the postprocessing for case study III. Not implemented steps of the approach are transparent

12.2. Experimental site and experimental setup

In 2010, experiments with corn (*Zea mays* L., variety PR36K67) were conducted in the greenhouse of the Dürnast Experiment Station of the Technische Universität München, Germany (48°24'11" N, 11°41'23" E, 473 m altitude), similar to case study I. On 14/05/2010, five seeds per container were sown into 18 containers (0.95 m x 0.55 m x 0.73 m, no drainage possible). The three containers of each of the six treatments were placed into three rows, leading to row distances of 75 cm and a seeding density of 6.7 plants per m^2 (Fig. 12.2 and 12.3). The used soil was loamy sand (79.2 % sand, 17.5 % silt, and 3.3 % clay). Adequate amounts of phosphor and potassium fertilizers were applied to sowing. The drip irrigation system NMC-pro (Netafim, Israel) was used. Five emitters per container were installed, one next to each plant, resulting in a discharge rate of 8.5 mm h^{-1}.

Figure 12.2.: Cultivated corn in the greenhouse in 2010. The picture on the left side shows an irrigation event (04/06/2011).The picture on the right side shows the six treatments starting with treatment $T_{def\,N}$ (right) on 10/11/2010.

12.3. Data collection during the experiment

In one of three containers per treatment (middle row), four TDR probes (Campbell Scientific, USA) and four pF-Meters (ecoTech, Germany) were installed at four different heights (20, 30, 40 and 60 cm soil depth) referred to as levels A, B, C and D. One TDR probe and one pF-Meter next to each other are referred to as one sensor pair. The pF-Meters at 30 cm soil depth served for irrigation control within the soil tension controlled treatments T_{full} and $T_{def\,N}$. The sensor pairs at 20 and 40 cm soil depth were installed horizontally deflected at 15 and 10 cm from the middle axis. In each of the other two containers, only

one sensor pair was installed at 30 cm soil depth. Soil tensions and soil water contents were observed by pF-Meters and TDR probes every 10 minutes, respectively. A meteorological station was installed near the experimental setup inside the greenhouse. The roof and side windows of the greenhouse were open whenever the sun was shining.

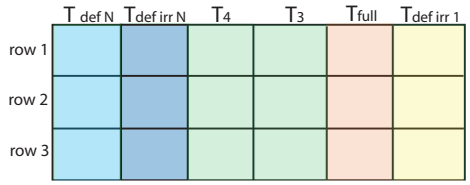

Figure 12.3.: Experimental setup of corn grown in the greenhouse in 2010.

Plant heights and development stages were observed every 10 days. LAI measurement failed probably due to the greenhouses radiation heterogeneity. The chlorophyll which is present in the plant leaves and is closely related to the nutrimental condition of the plant was observed six times during the growth period using a Chlorophyll Meter named SPAD-Meter (Spectrum Technologies Inc., UK). After harvest (28/09/2010), grain yield and total dry matter (both at 0 % humidity) were determined. For further evaluations, WP and NUE were estimated.

12.4. Experimental layout

The positioning of the sensor pairs was based on simulation results of water flow model Hydrus 2D using soil parameters based on laboratory analysis results determined by ROSETTA (Schaap et al., 2001). These Hydrus 2D simulations were used to estimate adequate positions of the sensor pairs and to plan the pre-sowing infiltration event for accurate soil parametrization. The positions of the sensor pairs depend on the horizontal and vertical distribution of the water bulb and, since sensor based irrigation control was conducted, on the root water uptake and rooting depth of the crop. To get information about the horizontal distribution of the water bulb, the sensor pairs at 20 and 40 cm soil depth were installed horizontally deflected at 15 and 10 cm from the middle axis, respectively. Since the highest distribution of corn roots can be found until 40 cm soil depth (Mailhol et al., 2011), the sensors used for sensor based irrigation control were installed at 30 cm soil depth.

12.5. Calibration and validation of the model parameters

The preprocessing steps in case study I included the calibration and validation of the model parameters and the generation of a long time-series of weather data for the greenhouse.

12.5.1. Calibration of the soil parameters

Primarily, soil parameters based on laboratory analysis results were determined by ROSETTA (Schaap et al., 2001). These soil parameters were applied within Hydrus 2D simulations to plan the realization of the pre-sowing infiltration event conducted on 04/06/2010 (treatment T_{full}). For that, Hydrus 2D simulations were accomplished to estimate the amount and timing of that irrigation water application.

Secondly, the inverse soil parametrization was done applying CMA-ES algorithm based on observed soil tension and soil water content data of all levels of that infiltration event (see Equation 6.2). The determined van Genuchten/Mualem parameters and K_s based on infiltration experiment data were used within the simulation-optimization runs (see C1 in Table 12.4).

12.5.2. Calibration and validation of the plant parameters

The plant parameters of corn were determined based on field data of the Cemagref Institute of Montpellier, France where the same variety was cultivated in 2007 and 2009 (see case study II and Table 11.3). After a sensitivity analysis, six plant parameters were found to be very sensitive regarding yield. For calibration of SVAT model Daisy, grain yield and total biomass of both drip irrigated and one rainfed treatment (all with a row distance of 75 m) of 2007 were applied. Within the calibration, the predicted and observed grain yields and total dry matters were 17.4 vs. 17.4 and 26.2 vs. 29.4 t ha^{-1} (2007 FULL), 3.0 vs. 4.9 and 9.8 vs. 12.7 t ha^{-1} (RF) and 15.7 vs. 15.6 and 24.9 vs. 26.1 t ha^{-1} (2007 T5). The following objective function was applied for plant parameter estimation:

$$\begin{aligned} Z_P = \quad & 10 \cdot MSE + \mid \triangle Y_{2007\,FULL} \cdot 2 \mid + \mid \triangle Y_{RF} \cdot 2 \mid + \mid \triangle Y_{2007\,T5} \cdot 2 \mid \\ & + \mid \frac{\triangle TDM_{2007\,FULL}}{2} \mid + \mid \frac{\triangle TDM_{RF}}{2} \mid + \mid \frac{\triangle TDM_{2007\,T5}}{2} \mid \end{aligned} \tag{12.1}$$

where Z_P is the objective function for plant parameter derivation, Y_{RF} and TDM_{RF} represent grain yield and total dry matter of a rainfed treatment in 2007 with a grain yield (Y_{RF}) of 4.9 t ha^{-1} and a total dry matter (TDM_{RF}) of 12.7 t ha^{-1} (Khaledian et al., 2008). $\triangle Y$ and $\triangle TMD$ mean the differences of the predicted and the observed grain yield or total dry matter, respectively.

Model validation took place against data of three treatments of 2009 on the same site and with the same row distance. Observed vs. predicted yields were 11.8 vs. 13.1 t ha^{-1} (2009 SDI160), 16.0 vs. 17.7 t ha^{-1} (2009 FULL) and 3.3 vs. 3.3 t ha^{-1} (rainfed treatment with a row distance of 75 cm), see case study II. Table 12.1 shows the resulting plant parameters for corn.

Table 12.1.: The most sensitive plant parameters of corn (*Zea mays* L., variety 36K67) referred to yield. Default values (dv) of crop „Pioneer maize“ due to Daisy database and calibrated values (cal) using the optimization algorithm CMA-ES.

plant parameter	unit	dv Pioneer maize	cal corn
PARext	–	0.600	0.753
y_{half}	–	–	0.65
Fm	(g $C0_2$)/(m^2 h^{-1})	6.0	6.084
Q_{eff}	(g $C0_2$ m^{-2} h^{-1})/(W m^{-2})	0.040	0.058
DSLAI0.5	–	0.13	0.292
SpLAI	(m^2 m^{-2})/(g DM m$^{-2)}$	0.030	0.017

12.5.3. Setup of SVAT model Daisy

The irrigation and N fertilization schedules were determined once in the first month after sowing. An adaption to precipitation (real-time scheduling) is not required in a greenhouse since all received water comes from irrigation.

For successful germination, full irrigation was applied to all treatments within the first month. Moreover, Daisy simulation results within the first month are not plausible since the root water uptake often is overestimated. The estimated plant and soil parameters were applied.

Due to numeric problems for the lower boundary conditions, a soil layer from 0.65 to 0.70 m with a very low conductivity (K_s = 0.048 cm d^{-1}) was implemented (see setup file horizon B). The lower boundary was set to groundwater deep. Realized irrigation and N fertilization events in the first weeks were indicated according to the applications. Drought and N stresses were allowed. An exemplary setup file of treatment $T_{def\,irr\,N}$ can be found in Appendix B.

12.6. Generation of the climate data

The stochastic weather generator LARS-WG was used to generate long time-series of 200 years which statistically resembled observed weather for the greenhouse. However, only several weeks of observed weather data of the greenhouse were available. Therefore, a regression analysis was conducted to gain the relationships between field and greenhouse for temperature and radiation based on 15 years (1995 – 2009) of observed weather data of the Bayerische Landesanstalt für Landwirtschaft (weather station number 8) and several weeks of observed data in the greenhouse (from 10/04 to 30/07/2009 and from 23/12/2009 to 22/01/2010).

As assumed, radiation was reduced and temperature was increased inside the greenhouse compared to outside. Regression analysis led to three regression functions: i) for temperature outside and inside the greenhouse, ii) for radiation outside and inside the greenhouse when the roof is closed (on rainy days or if radiation is $\leq 80\,\mathrm{W\,m^{-2}}$), and iii) for radiation outside and inside the greenhouse when the roof is open (no rain, radiation $> 80\,\mathrm{W\,m^{-2}}$). Firstly, the long time-series of 200 years based on outside (field) data was estimated. Secondly, the regression functions were applied to generate long-time series of climate data for the greenhouse.

12.7. Optimized irrigation and N fertilization scheduling

The optimization framework consisted of the optimization algorithm GET-OPTIS, SVAT model Daisy 1D and the weather generator LARS-WG. The objective was to achieve maximum *WP* and/or *NUE* for a reliability of 95 %. Since Daisy 1D (version 4.01) runs much faster and robust compared to Daisy 2D (version 4.57) and the experimental setup does not request a two-dimensional consideration, Daisy 1D was chosen for simulation-optimization. For the following four treatments, irrigation and N fertilization schedules were determined (see Table 12.2):

- control treatment T_{full} was fully irrigated and fully fertilized,
- treatment $T_{def\,N}$ was deficit fertilized and fully irrigated,
- treatment $T_{def\,irr}$ was deficit irrigated and fully fertilized,
- treatment $T_{def\,irr\,N}$ was deficit irrigated and deficit fertilized.

For the soil tension controlled fully irrigated treatments T_{full} and $T_{def\,N}$, the soil tension threshold at which irrigation water was applied automatically was estimated using the optimization framework. The aim was to fully irrigate the crops while achieving high *WP*s. The pF-Meters at 30 cm soil depth served for irrigation control. The infiltration event for

soil parametrization conducted at T_{full} before sowing led to higher irrigation amounts compared to $T_{def\,N}$. However, both treatments can be considered as fully irrigated. The optimization variable were the irrigation amounts in the case of $T_{def\,irr}$ and $T_{def\,irr\,N}$, and the soil tension threshold in the case T_{full} and $T_{def\,N}$, respectively. After each irrigation event, a redistribution time of 3 h was forced. In this case study, only four out of six treatments were considered. For further information about the irrigation scheduling and the other two treatments (referred to as T_3 and T_4), refer to Kloss et al. (2011).

The determined irrigation amounts per irrigation event and soil tension thresholds were:

- no water limitation (T_{full} and $T_{def\,N}$): irrigation amounts of 7.2 mm at a soil tension threshold of −130 hPa
- water limitation ($T_{def\,irr}$ and $T_{def\,irr\,N}$): about 60 % of the irrigation water of T_{full} were applied per irrigation event

Regarding the optimized N fertilization schedules, the determined total N amounts were:

- no N limitation ($T_{def\,irr}$ and T_{full}): 234 kg N ha^{-1}
- N limitation ($T_{def\,N}$ and $T_{def\,irr\,N}$): 147 kg N ha^{-1}

The applied irrigation amounts were 398 mm (including the infiltration event) for T_{full}, 351 mm for $T_{def\,N}$, 231 mm for $T_{def\,irr}$ and 225 mm for $T_{def\,irr\,N}$. Concerning the N scheduling, the application in the case of the optimized deficit N fertilization was about 63 % of full N fertilization. The first and second application after 6 and 32 days after sowing (DAS), considered as base fertilization, were not optimized. The first fertilization included an application of potassium and phosphorus. For $T_{def\,irr}$ and T_{full}, N fertilization occurred on DAS 6 (63 kg N ha^{-1}), DAS 32 (63 kg N ha^{-1}), DAS 63 (45 kg N ha^{-1}) and DAS 97 (63 kg N ha^{-1}), leading to a total N fertilization of 234 kg N ha^{-1}. For $T_{def\,N}$ and $T_{def\,irr\,N}$, N fertilization was conducted on DAS 6 (63 kg N ha^{-1}), DAS 63 (21 kg N ha^{-1}), and DAS 97 (63 kg N ha^{-1}), in total 147 kg N ha^{-1}.

Table 12.2.: Treatments and objectives considered in this study.

	full N fertilization	deficit N fertilization
full irrigation	T_{full} no limitations	$T_{def\,N}$ maximization of *NUE*
deficit irrigation	$T_{def\,irr}$ maximization of *WP*	$T_{def\,irr,N}$ maximization of *WP* and *NUE*

Soil sampling at 30 cm soil depth in treatment T_{full} showed that N contents before sowing and after harvest were only about 18 and 1 kg N ha^{-1}, respectively. The resulting yields, *WP*s and irrigation and N fertilization amounts for all treatments are shown in Table 12.3.

12.8. Evaluation of the experimental results

In the following, observed plant variables, weather data and Chlorophyll Meter values will be presented. Moreover, determinations of *WP* and *NUE* and a recalculation of the soil parameters were accomplished.

12.8.1. Observed plant variables and weather data

As expected, grain yield was highest for fully irrigated and N fertilized control treatment T_{full} ($9.0\,\mathrm{t\,ha^{-1}}$), and lowest for the deficit irrigated and N fertilized treatment $T_{def\,irr\,N}$ ($5.1\,\mathrm{t\,ha^{-1}}$), see Table 12.3. Yield of $T_{def\,N}$ ($7.2\,\mathrm{t\,ha^{-1}}$) was reduced due to limitation in N compared to T_{full}. In treatment $T_{def\,irr}$ which was the first row of the experimental setup near the side walls, severe phytosanitary problems occurred (see Fig. 12.4). This fact impeded a proper evaluation of the irrigation schedule and especially of the achieved yield. Nevertheless, the results will be presented for comparison reasons. The harvest index (grain yield over total dry matter) ranged from 58 to 64 % (see Table A.3 in the Appendix).

The grain yields varied between the rows: highest yields of each treatment were achieved in the eastern rows with an average difference of 15% compared to the middle rows. The yields in the middle and the western rows were similar. Flowering, begin of ripening and harvest of corn occurred around DAS 77, DAS 128 and on DAS 137, respectively. The observed plant heights at harvest were 295 (T_{full}), 286 ($\mathrm{T}_{def\,irr}$), 282 ($\mathrm{T}_{def\,N}$) and 278 cm ($\mathrm{T}_{def\,irr\,N}$). During the growth period in 2011, measured global radiation was about 60 % lower in the greenhouse compared to outside. This difference varied at lot depending on the roofs position (open or closed). Average daily reference evapotranspiration calculated with the FAO $\mathrm{ET_0}$ – Calculator[1] was 1.8 ± 1.3 mm inside the greenhouse and 2.6 ± 1.5 mm outside. The lower values inside the greenhouse can be explained by the marginal wind speed measured and a general damping of the weather variables (especially radiation) by the greenhouse.

12.8.2. Water productivities and nitrogen use efficiencies

WP was highest for $T_{def\,irr}$ ($3.3\,\mathrm{kg\,m^{-3}}$), followed by T_{full} and $T_{def\,irr\,N}$ (both $2.7\,\mathrm{kg\,m^{-3}}$), see Table 12.3. Hence, *WP* was increased due to the optimal deficit irrigation scheduling by 22 %. When the maximization of *NUE* was focused ($T_{def\,N}$), *WP* was lowest ($2.4\,\mathrm{kg\,m^{-3}}$). However, when the soil water depletion is considered, WP_{SW} for $T_{def\,irr}$ and T_{full} are identical (for both treatments: $2.5\,\mathrm{kg\,m^{-3}}$) since the soil water depletion was much higher

[1] www.fao.org/nr/water/eto.html

for $T_{def\,irr}$ (83 mm) compared to the fully irrigated treatment (31 mm). $T_{def\,irr\,N}$ still showed the lowest WP_{SW} with 2.0 kg m^{-3}.

The highest NUE of 58 kg grain kg N^{-1} was achieved by fully irrigated treatment $T_{def\,N}$. That means an increase of 29 % compared to T_{full} and even 76 % compared to $T_{def\,irr}$, respectively. However, NUE of $T_{def\,irr\,N}$ (41 kg grain kg N^{-1}) is even lower than NUE of fully fertilized T_{full} (45 kg grain kg N^{-1}).

Table 12.3.: Total irrigation amount I, grain yield (Y, at 0 % and at 15 % humidity in t ha^{-1}), total dry matter (TDM) in t ha^{-1} (value ± standard deviation), water productivities WP and WP_{SW} based on 15 % humidity in grain [kg m^{-3}], total N fertilization (N fert) in kg N ha^{-1}, and nitrogen use efficiency (NUE) in kg grain kg N^{-1} for corn in 2010. Soil water depletion (SW) from the root zone (difference of levels A, B, C and D from sowing to harvest) in mm.

treatment	I	Y(0 %)	Y(15 %)	TDM	WP	SW	WP_{SW}	N fert	NUE
$T_{def\,irr}$	231	6.5 ± 1.4	7.7 ± 1.2	13.2 ± 2.1	3.3 ± 0.5	83	2.5 ± 0.4	234	33
T_{full}	398	9.0 ± 1.3	10.6 ± 1.1	16.5 ± 2.1	2.7 ± 0.3	31	2.5 ± 0.3	234	45
$T_{def\,N}$	351	7.2 ± 0.8	8.5 ± 0.8	13.4 ± 1.1	2.4 ± 0.2	61	2.1 ± 0.2	147	58
$T_{def\,irr\,N}$	225	5.1 ± 0.2	6.0 ± 0.2	10.3 ± 0.7	2.7 ± 0.1	78	2.0 ± 0.1	147	41

12.8.3. Chlorophyll Meter values

Chlorophyll Meters non-destructively determine the chlorophyll which is present in the plant leaves and which is closely related to the nutrimental condition of the plant. As expected, the fully irrigated and fully N fertilized treatment of T_{full} showed the highest chlorophyll contents (see Fig. 12.4).

Due to pests, yield of $T_{def\,irr}$ was reduced. That is confirmed by the SPAD-Meter values of $T_{def\,irr}$, the only ones decreasing sharply after about DAS 80. This decrease indicates the poor condition of the plants reflected by low chlorophyll contents.

Additionally, the limited N condition of $T_{def\,N}$ and $T_{def\,irr\,N}$ are expressed by the high increases of SPAD-Meter values after each N fertilization.

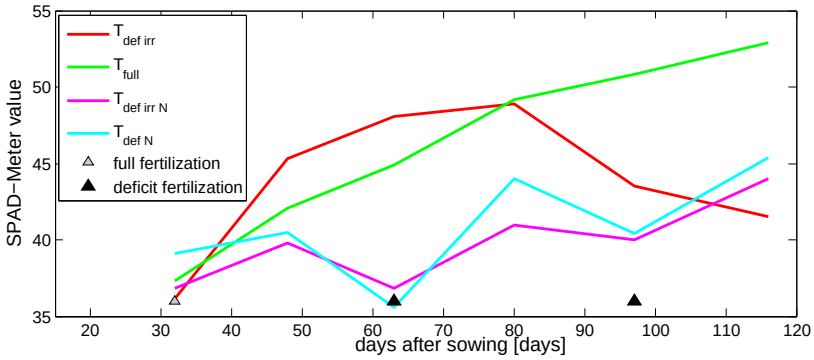

Figure 12.4.: Chlorophyll Meter values (SPAD-Meter) for four treatments. N fertilization events are marked with triangles. The N fertilization on DAS 32 was only applied to the fully N fertilized treatments ($T_{def\,irr}$ and T_{full}), whereas N fertilization conducted on DAS 63 and 97 were applied to all treatments.

12.8.4. Recalculation of soil parameters

After the harvest of corn in 2010, the soil parameters were recalculated based on observed soil water content data of treatment $T_{def\,irr}$. The soil parameters estimated using data before sowing (referred to as C1) were compared with soil parameters determined using data during the whole growth period and after harvest (referred to as C2). Hence, an assumed temporal variability of the soil hydraulic properties due to root growth, irrigation events and further effects was evaluated (Mubarak et al., 2009). Moreover, the soil parametrization is assumed to be more accurate using input data of a longer measuring period and a higher range.

Soil moisture data of the whole growing period including data of a post-harvest infiltration experiment conducted on 11/10/2010 and 12/10/2010 (application of 104 mm) of levels A, C and D were used (data of level B was partly implausible). Treatment $T_{def\,irr}$ was chosen due to the high range of soil water content and soil tension data (dry conditions during the growing season due to the limited water application and wet conditions due to the infiltration event) and mostly plausible data. The vGM parameters θ_s, θ_r, n and α were determined via fitting a retention curve using RET-C (van Genuchten et al., 1991), whereas K_s was estimated applying the optimization algorithm CMA-ES. Figures of the measured soil water contents and soil tensions and the fitted water retention curves for $T_{def\,irr}$ can be found in Appendix A.

Great differences occurred for the vGM parameters θ_r which increased from 0.035 to $0.081\,\mathrm{cm^3\,cm^{-3}}$, and for α and K_s which both decreased about three and four times, respectively. The vGM parameters applied within the simulation-optimization and the

recalculated ones are shown in Table 12.4. The modification of the soil parameters barely lightly influenced the predicted grain yields, see Table 12.6. The simulation of the soil water dynamics improved using soil parameter set C2 (see Fig.12.6 and 12.6).

Table 12.4.: Van Genuchten/Mualem parameters θ_s [$cm^3\,cm^{-3}$], θ_r [$cm^3\,cm^{-3}$], α [cm^{-1}] and n [-] and parameter K_s [$cm\,d^{-1}$] estimated using RET-C and CMA-ES based on soil tension and soil moisture data of the infiltration event on 04/06/2010 (C1), and on soil moisture data of the whole growth period (C2).

	θ_r	θ_s	n	α	K_s
C1	0.035	0.39	1.5725	0.0535	482.4
C2	0.081	0.41	1.6913	0.0159	112.2

12.9. Postprocessing simulations of yield and water and N dynamics

Simulations of yield and water and N dynamics were conducted using Daisy 1D (version 4.01) and Daisy 2D (version 4.57)[2].

12.9.1. Yield predictions using Daisy 1D

Postprocessing simulations with model Daisy 1D were done using the soil parameters applied within the optimization (C1) and the recalculated ones (C2). Furthermore, observed global radiation (R) was increased by 50 %, 60 %, 70 %, 80 %, 90 % and 100 % to compensate the supposed higher total radiation sum received per crop (and not measured by the meteorological station) due to the greenhouse conditions (see explanation in Subsection 10.4.2.3). Drought and N stresses were enabled within all predictions and for all treatments.

Although only four of them were considered within this study, the predicted (radiation increase of 80 %) and observed grain yields of all six treatments are shown in Figure 12.5. Predicted vs. observed grain yields for T_3 and T_4 were 8.9 vs. 8.9 and 8.7 vs. 7.9 $t\,ha^{-1}$, respectively. The simulated yields of T_3, T_4, $T_{def\,N}$ and T_{full} showed good agreement with the observed values if the radiation was increased by 80 %. Observed yield of $T_{def\,irr}$ can hardly considered due to severe phytosanitary problems. The result supports the presumption that an increase of radiation of about 80 % is adequate. The great gap between predicted and observed yield of $T_{def\,irr\,N}$ leads to the assumption that the crop model is not able to reflect crop growth under combined limitation of water and N.

[2]http://code.google.com/p/daisy-model/

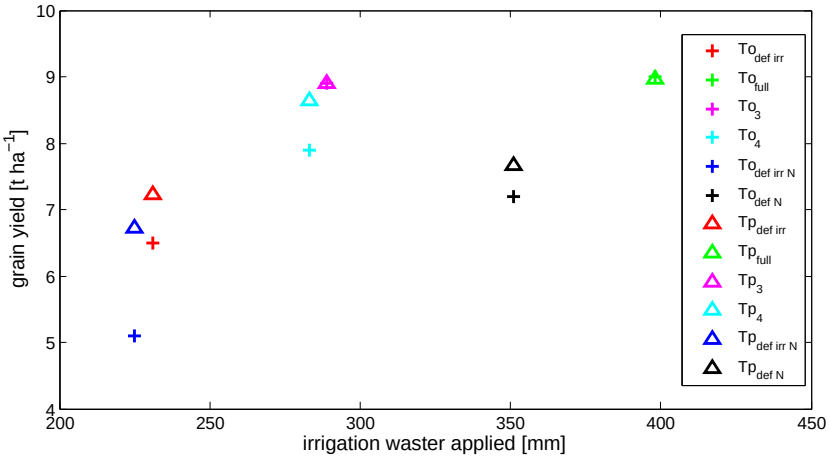

Figure 12.5.: Predicted and observed grain yields using soil parameter set C1 for six treatments (radiation increase of 80 %). To (symbol+) are the observed and Tp (symbol △) the predicted grain yields, respectively.

Table 12.5 shows the predicted and the observed grain yields of the four considered treatments. The model error was high for treatment $T_{def\,irr\,N}$ (model error: $-1.6\,\mathrm{t\,ha^{-1}}$) where water and N both were limited. Moreover, yield prediction was only moderate for $T_{def\,irr}$ ($-0.7\,\mathrm{t\,ha^{-1}}$) were yield reduction occurred due to pests. Observed grain yields were well predicted in the case of T_{full} ($0.0\,\mathrm{t\,ha^{-1}}$), $T_{def\,N}$ ($-0.5\,\mathrm{t\,ha^{-1}}$), T_3 ($0\,\mathrm{t\,ha^{-1}}$) and T_4 ($0.8\,\mathrm{t\,ha^{-1}}$).

The modeling efficiency for all treatments and a radiation increase of 80 % was 0.7. Predicted ripening dates ($DS2$) were 01/10/2010 for R and 03/10/2010 for increased radiation (50 – 100 %), respectively. Hence, ripening was well predicted since harvest of ripe corn took place on 28/09/2010.

The difference between predicted grain yields for both soil parameter sets is marginal, ranging from 0.00 to $0.24\,\mathrm{t\,ha^{-1}}$, see Table 12.6. Due to the fact that treatment $\mathrm{T}_{def\,irr}$ was affected by pests, simulation results for all radiation increases are not shown. Noteworthy, the grain yields of $\mathrm{T}_{def\,irr\,N}$ decrease for a radiation increase of 50 to 100 %.

It can be assumed that radiation is no longer limiting, but water and N limitations impede further yield increases. Predicted ET_{ref} by model Daisy were about 1.2 mm for R and 2.5 mm for 80 % R, respectively.

Table 12.5.: Predicted and observed grain yields in $\mathrm{t\,ha^{-1}}$ (0 % humidity) for corn in 2010. Within the predictions, radiation was increased by 80 % and soil parameter set C1 was applied. The model error in $\mathrm{t\,ha^{-1}}$ was calculated as observed minus predicted grain yield.

treatment	observed	predicted	model error [$\mathrm{t\,ha^{-1}}$]	model error [%]
T_{full}	9.0 ± 1.1	9.0	0.0	0
$T_{def\,irr}$	6.5 ± 1.2	7.2	−0.7	11
$T_{def\,N}$	7.2 ± 0.8	7.7	−0.5	6.9
$T_{def\,irr\,N}$	5.1 ± 0.2	6.7	−1.6	31
T_3	8.9 ± 0.6	8.9	0.0	0
T_4	8.7 ± 0.6	7.9	0.8	9

Table 12.6.: Observed (Y) and predicted grain yields in $\mathrm{t\,ha^{-1}}$ (0 % humidity) of T_{full}, $T_{def\,N}$ and $T_{def\,irr\,N}$ for the soil parameter sets C1 and C2. R, 50 % R, 60 % R, 70 % R, 80 % R, 90 % R and 100 % R are the predicted grain yields with no radiation increase, 50 %, 60 %, 70 %, 80 %, 90 %, and 100 % radiation increase, respectively.

	T_{full}		$T_{def\,N}$		$T_{def\,irr\,N}$	
	C1	C2	C1	C2	C1	C2
Y	9.0 ± 1.3		7.2 ± 0.8		5.1 ± 0.2	
R	4.30	4.29	4.29	4.26	4.23	4.26
50 % R	7.75	7.74	6.94	6.80	6.99	6.79
60 % R	8.16	8.16	7.24	7.08	6.86	6.65
70 % R	8.57	8.56	7.47	7.32	6.79	6.60
80 % R	8.97	8.95	7.67	7.50	6.71	6.51
90 % R	9.35	9.33	7.82	7.65	6.61	6.44
100 % R	9.72	9.71	7.98	7.78	6.51	6.27

12.9.1.1. Simulation of soil water contents and soil tensions

In general, the dynamics of the soil water contents and soil tensions using Daisy 1D and the soil parameter set C2 were moderately predicted. Due to the high root water uptake, the permanent wilting point (PWP, pF = 4.2) was reached often. This led to lower predicted soil water contents and higher predicted soil tensions (especially for the first weeks) compared to the observed ones.

For the most parts, the simulated water dynamics were smoother than the measured ones, for instance in $T_{def\,irr}$ level B. The simulated soil water contents mostly showed better agreement with the observed data for the deficit irrigated treatments than for the fully

irrigated treatments. For T_{full}, simulated soil water contents were much lower than the observed ones due to the high predicted root water uptake. The infiltration event (T_{full}) was not well reflected at level D since observed soil tension reached 0 pF whereas observed soil tension was around 2.5 pF (Fig. A.4 in Appendix). The reason may be that soil water content data of deficit irrigated treatment $T_{def\,irr}$ was used for the recalculation of the soil parameters. Moreover, the plant parameters were calibrated based on experimental data of deficit irrigated treatments.

Figures 12.6 and 12.7 show the observed and predicted soil water contents and soil tensions for $T_{def\,irr}$ applying the soil parameter set C2 for an radiation increase of 80 %. Figures of further treatments can be found in Appendix A.

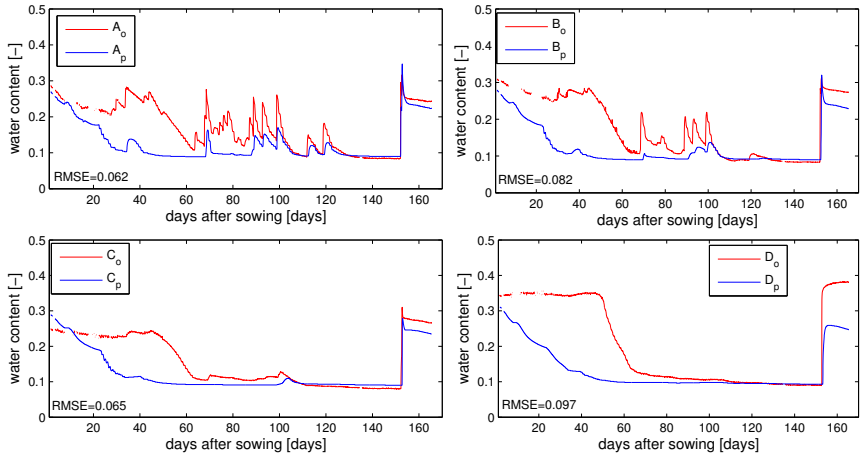

Figure 12.6.: Predicted and observed soil water contents for $T_{def\,irr}$ (radiation increase of 80 % and application of the soil parameter set C2). A stands for the sensor at level A at 20 cm, B stands for the sensor at level B at 30 cm (three sensors), C stands for the sensor at level C at 40 cm and D stands for the sensor at level D at 60 cm soil depth. The red line shows the observed (o), the blue line the predicted values (p). The *RMSE* is given in $cm^3\ cm^{-3}$.

The lowest *RMSE* for observed and predicted soil water content data for all levels (*RMSE* in $cm^3\ cm^{-3}$) was reached by $T_{def\,irr\,N}$ (0.067) followed by $T_{def\,irr}$ (0.077), T_{full} (0.079) and $T_{def\,N}$ (0.084). Fitting was better for lower levels (A: 0.070, B: 0.073, C: 0.080 and D: 0.083). The *RMSE* for observed and predicted soil tension data was lowest for $T_{def\,N}$ (0.666) followed by $T_{def\,irr}$ (0.748), T_{full} (0.763) and $T_{def\,irr\,N}$ (0.802).

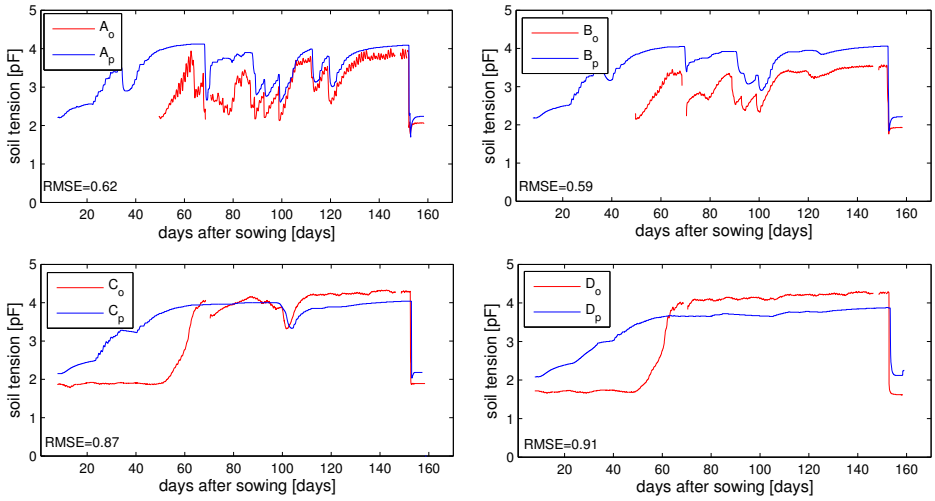

Figure 12.7.: Predicted and observed soil tensions for $T_{def\,irr}$ (radiation increase of 80 % and application of the soil parameter set C2). A stands for the sensor at level A at 20 cm, B stands for the sensor at level B at 30 cm (three sensors), C stands for the sensor at level C at 40 cm and D stands for the sensor at level D at 60 cm soil depth. The red line shows the observed (o), the blue line the predicted values (p). The *RMSE* is given in pF.

Regarding the soil tensions, fitting was best for levels A (0.655) and B (0.670) followed by levels C (0.787) and D (0.866).

Especially during the first weeks after sowing, the predicted root water uptake was overestimated. The higher predicted plant water uptake – which nevertheless led to similar yields to the observed ones – leads to the assumption that the efficiency of the photosynthesis is assumed to be lower within the crop growth model compared to the observed one.

For a radiation increase from R to 80 %, predicted transpiration (T) increased from 175 to 251 mm ($T_{def\,irr}$), from 172 to 332 mm (T_{full}), from 188 to 327 mm ($T_{def\,N}$) and from 163 to 246 mm ($T_{def\,irr\,N}$), respectively. Predicted potential evapotranspiration was about 277 and 590 mm for R and 80 % R, respectively.

12.9.1.2. Prediction of N balance

Regarding the predicted N in soil, higher total soil N contents can be found for both fully N fertilized treatments compared to the deficit N fertilized ones (see Fig. 12.8).

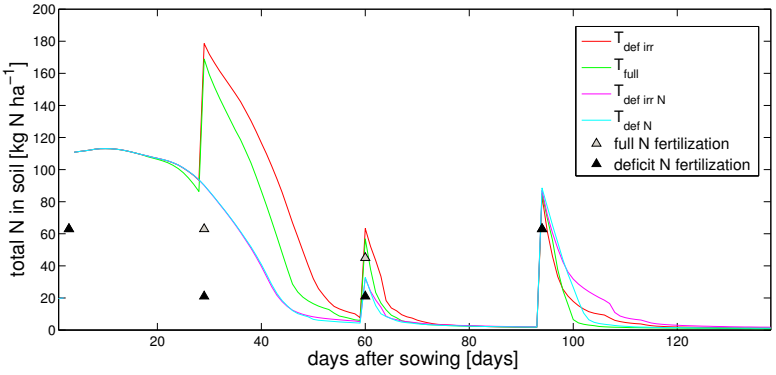

Figure 12.8.: Predicted total soil N [kg N ha^{-1}] for all treatments during the growth period (radiation increase of 80 % and application of the soil parameter set C2).

For the higher yielding T_{full}, lower total soil N contents at harvest were predicted due to higher root N uptake during the crop growth compared to $T_{def\,irr}$. The same is true for both deficit N fertilized treatments where lightly higher yielding $T_{def\,N}$ showed higher N uptake between DAS 100 and 115 compared to $T_{def\,irr\,N}$. Predicted and observed total soil N contents at harvest (DAS 137) both were about zero. However, soil N content was only observed before sowing (about 18 kg N ha^{-1}) and after harvest (about 1 kg N ha^{-1}). Hence, a detailed evaluation of the N dynamics during crop growth was not possible.

12.9.2. Yield predictions using Daisy 2D

For further simulation runs, Daisy 2D (version 4.57) was set up similar to Daisy 1D. To accurately place the 5 drippers per container, subsoil irrigation was applied with the placement of the drippers at 1 cm soil depth in a line the middle of each container (x = 30 cm, z= −1 cm). N fertilization events were indicated according to the applied fertilization management and N stress was allowed. Only for simulation runs where no N limitation was predetermined, luxury N uptake was allowed. An exemplary setup file for $T_{def\,irr\,N}$ is shown in Appendix B.

The simulation results using Daisy 2D were not acceptable (see Table 12.7). Predicted grain yield and total dry matter differed from the ones predicted within the Daisy 1D simulations.

In general, predictions of Daisy 2D were much more differentiating between the different treatments compared to Daisy 1D (e.g. for yields, harvesting dates). In contrast to the 1D simulation results, the predicted yields differed noticeable for both soil parameter sets C1 and C2 (see Table A.4 in Appendix). Predicted yields were lower for soil parameter set C1 compared to C2.

Simulation runs with a radiation increase of 80 %, 90 % and 100 % were accomplished but did not lead to the expected improvements. Similar to the 1D simulation results, root water uptake was overestimated when radiation was increased. At least, the tendency in yield reduction due to water and N stress (highest yield for T_{full}, followed by $T_{def\,N}$ and $T_{def\,irr\,N}$) was reflected.

Furthermore, simulation runs where luxury N uptake was intended were accomplished for soil parameter set C2, referred to as C2 (N not limited) in Table 12.7. All yields increased (for R and for increased radiations) which indicated a limitation in N. However, N limitation was only observed for both N stressed treatments $T_{def\,N}$ and $T_{def\,irr\,N}$ (see Fig. 12.4). The predicted harvesting date ranged from 01/10 to 08/10/2010.

Table 12.7.: Simulation results of Daisy 2D using the soil parameter sets C1 and C2 for full N fertilization (N full) and for N stress allowed (N def). Observed and predicted grain yield Y and total dry matter (TDM, in brackets) in t ha^{-1} for the observed global radiation (R) and radiation increased by 80 % (80 % R), 90 % (90 % R) and 100 % (100 % R).

	T_{full}	$T_{def\,irr}$	$T_{def\,N}$	$T_{def\,irr\,N}$
observed	9.0 ± 1.1	$6.5 \pm .2$	7.2 ± 0.8	5.1 ± 0.2
	(16.5 ± 2.1)	(13.2 ± 2.1)	(13.4 ± 1.1)	(10.3 ± 0.7)
C1 (N def)				
R	4.1 (10.0)	3.6 (7.3)	2.6 (5.7)	2.6 (5.9)
80 % R	3.7 (8.2)	2.2 (5.8)	2.0 (5.5)	1.7 (4.9)
C2 (N def)				
R	6.1 (14.0)	4.1 (10.7)	3.7 (10.9)	2.9 (8.0)
80 % R	6.1 (15.1)	4.9 (11.8)	3.9 (9.3)	2.9 (8.0)
90 % R	6.0 (14.7)	4.9 (12.2)	3.7 (8.9)	3.0 (8.1)
100 % R	6.3 (15.5)	4.9 (12.2)	3.7 (8.9)	3.0 (8.1)
C2 (N full)				
R	4.3 (11.9)	4.3 (11.9)	3.7 (10.9)	4.3 (11.9)
80 % R	8.8 (21.6)	7.3 (17.3)	9.1 (21.1)	6.9 (16.7)
90 % R	9.3 (17.2)	7.3 (17.2)	9.5 (21.5)	7.0 (16.7)
100 % R	9.7 (22.1)	7.2 (17.1)	9.9 (21.9)	7.0 (16.6)

Daisy 2D was not able to reflect the observed crop growth. However, the present study focused on the stable and robust Daisy 1D (version 4.01). The latter was successfully applied within the simulation-optimization. The currently high simulation time of Daisy 2D (about 30 min per treatment vs. about 30 s for Daisy 1D) and the experimental setup which did not require a two-dimensional model (Styczen et al., 2010) additionally encouraged the choice of Daisy 1D.

12.10. Discussion and conclusions

Regarding the experimental design and especially the model parametrization, high effort was undertaken. Simulation based pre-sowing and post-harvest infiltration events and soil water content and soil tension measurements in high resolution supported the accurate determination of the soil parameters. Moreover, long time-series of climate data for the greenhouse were generated via regression analysis for different conditions (roof open or closed).

Optimal deficit irrigation and N fertilization schedules were determined using the stochastic optimization framework before sowing and applied to the treatments. The impact of drought stress and, in case of $T_{def\,N}$ and $T_{def\,irr\,N}$ additionally N stress, was high illustrated by observed grain yields which varied from 5.1 to 9.0 t ha^{-1} for irrigation amounts ranging from 231 to 398 mm and N applications of 147 and 234 kg N ha^{-1}. The observed WPs for corn ranging from 2.4 to 3.3 kg m^{-3} are high compared to literature values ranging from 0.3 to 2.4 kg m^{-3} (O'Neill et al., 2008; Rodrigues and Pereira, 2009; Dehghanisanij et al., 2009). The optimization framework for irrigation scheduling was able to increase WP up to 22 % ($T_{def\,irr}$) compared to the fully irrigated treatment T_{full}. This indicats that optimizing the variable irrigation water amount with the objective to maximize WP led to acceptable high yields while saving water.

NUE achieved in this study varied from 33 to 58 kg grain kg N^{-1}, whereas in literature, it ranged from about 26 to 55 kg grain kg N^{-1} Barbieri et al. (2008); Varga et al. (2008). Regarding the results of the deficit N scheduling at the fully irrigated treatment $T_{def\,N}$, the reached NUE was very high (58 kg grain kg N^{-1}). However, when drought and N stress occurred simultaneously ($T_{def\,irr\,N}$), reached NUE (41 kg grain kg N^{-1}) and WP (2.7 kg m^{-3}) were only moderate. It turns out that simulation based optimization of deficit irrigation or deficit N fertilization were successfully carried out. However, a combined optimization of both, irrigation and N fertilization, performed moderately.

After harvest, postprocessing predictions using model Daisy 1D and 2D were accomplished. Daisy 1D satisfactory predicted grain yields. However, the observed grain yields were only predicted adequately (EF of 0.7) when the input radiation data was increased by

80 %. It is assumed that the plants received a higher total radiation than the observed one due to the greenhouse conditions. Each plant may receive more radiation due to the free-standing containers where the sun can shine through the rows, compared to the shadowing in a field. Hence, the crops receive a higher amount of radiation than the observed one which is compensated by the radiation increase. However, this corrective action is only a compromise which did not lead to acceptable simulation results of soil water dynamics. The predicted soil water dynamics were smoother compared to the observed ones. Moreover, root water uptake was overestimated, especially in the first 60 days after sowing. Daisy 2D application showed poor simulation results regarding yield and soil water dynamic predictions.

The increase of input radiation data for growth predictions under greenhouse conditions can only be a compromise. Crop growth models capable to predict crop growth under greenhouse conditions are required. Differences of morphology and physiology of crops and received global radiation per plant need to be reflected by such a model. A plant parameter calibration using greenhouse data may be helpful to avoid the radiation increase compromise.

Part IV.

General discussion, conclusions and outlook

13. General discussion

The research study presents a *new approach for simulation based optimal experimental design* which integrates crop growth modeling, experiments, and stochastic optimization. The study addresses several challenges which were worked out in the introduction. In the following, the contribution of the study to answer these open research questions and limitations in that are discussed.

Data collection

The reliability of model predictions depends on an appropriate model calibration and validation based on collected field or greenhouse data. According to Wallach (2006), observed data are a major source of uncertainty in crop growth modeling.

To enhance the informative value of experimental data, an optimal experimental design which adjusts crop growth modeling and experiments was developed. For that, a data collection within preliminary experiments for accurate model calibration and validation, and a data collection within the deficit irrigation (and/or deficit N fertilization) experiments for model evaluation are required. In the presented research study, the relevant experimental data to be collected for providing robust simulation based recommendations on irrigation and N fertilization management were identified and listed in detail (see Table 8.1).

However, some limitations occured. Soil N content measurements using soil samples may only be conducted before sowing and after harvesting not to affect crop growth. Continuous non-destructive high-resolution measurements of the soil N content were not found within a comprehensive literature review. Moreover, LAI measurements in greenhouses were not successful. The reason may be the radiative heterogeneity under greenhouse conditions. Moreover, biomass cuts during the growth period can only be accomplished if sufficient plants are available (which may not be the case especially in greenhouse pot experiments with few plants).

Optimal field design

Since field and greenhouse experiments are costly, time-consuming and laborious, an optimal experimental design is crucial. Well performed experiments with the relevant data collected can be used to accurately calibrate and validate models. The number of experiments can then be reduced due to model predictions and generalizations. In this work, the calibrated and validated models were applied for model predictions with different objectives.

In case study I, the potential yield of wheat (field) and the potential *WP*s of barley (field and greenhouse) were determined within a simulation-optimization study. A projected increase of wheat yield by 12 % and of barley (field) *WP* by 41 % compared to observed data shows the high potential of the optimization framework. The results indicate that feasible irrigation water amounts can be saved while achieving higher yields when the proposed optimized irrigation schedules are applied.

In case study II, the potential to save costs via an optimal field design was estimated. Prognostic simulations of two hypothetical field designs (drip line spacings of 60 and 200 cm) using Hydrus 2D and Pilote, and observed data of two field designs (drip line spacings of 120 and 160 cm) were evaluated. Considering the annual costs for installation and material of SDI systems, total prices and total costs, profit was about 27 % higher for SDI160 compared to SDI120. Both hypothetical treatments with extreme wide and short drip line spacings demonstrated that high installation and material costs (SDI60) and low yields due to low application efficiencies (SDI200) both greatly reduce profit (see Fig. 11.9). Maximal profit can be found around a drip line spacing of 160 cm, however, only four different drip line spacings were considered.

In case study III, soil tension controlled irrigation took place, hence, an appropriate and representative position of the instrumentation was of high importance. The positioning of pF-Meters and TDR probes was based on preliminary simulation results of model Hydrus 2D. Hereby, the horizontal and vertical distribution of the water bulb, the root water uptake and the rooting depth of corn were decisive. Furthermore, several optimal irrigation and N fertilization schedules were determined, applied on greenhouse experiments and evaluated.

Model calibration and validation

Accurate calibrated and validated models based on an adequate data base are required for reliable simulation results. A sequential model calibration strategy for soil and plant

parametrization was presented. Hereby, soil and plant parameters were calibrated separately to prevent mutual compensation.

Soil parameters, which are crucial for simulation based irrigation scheduling, should be calibrated using soil water data at the best not influenced by vegetation (e.g. before sowing or after harvesting) prior to plant parameters. For accurate soil parameter determination, it is important that plausible soil water content and/or soil tension data are available for a long period (including precipitation and irrigation events) and for a high range of values. Infiltration events planned using simulation models support the accurate determination of the soil parameters. A high soil heterogeneity may complicate the calibration/validation procedure. In general, soil water dynamics were predicted adequately. However, the predicted soil water dynamics were smoother than the observed ones. Furthermore, predicion results for corn grown under greenhouse conditions were only moderate.

For plant parametrization, experimental data of several plant variables (e.g. yield, total dry matter) are required. Before plant parameter calibration, sensitive parameters regarding yield should be identified via a sensitivity analysis. Calibration of plant parameters using greenhouse data and using data of crops grown under severe drought stress may improve model predicitons under greenhouse and under drought stressed conditions, respectively.

In case study I, model parameters were successfully transferred from field to greenhouse conditions. Barley plant parameters were calibrated using field data and successfully validated against greenhouse data. For that, a differentiation in two inner and to border crop rows and the adaption of two model parameters to greenhouse conditions were necessary.

The CMA-ES optimization algorithm was used for inverse model parametrization and proved to be an appropriate calibration method even for a large number of parameters. Suitable numerical and graphical measures for model assessment were presented.

Determination of optimal irrigation control functions

Optimal irrigation control functions were determined for subsurface drip irrigated corn grown on a loamy sandy soil (case study II). Water flow model Hydrus 2D was used since most crop growth models like model Pilote do not consider the drip line layout. When the proposed guidelines were applied in 2009, analysis of soil water content and soil tension measurements showed that deep percolation rarely occurred. By contrast in 2008, when irrigation took place 5 times a week, there was almost no horizontal movement observed leading to under supplied crop rows and thus yield reductions. Despite the higher drip line spacing of treatment SDI160, similar yields compared to SDI120 were achieved when the proposed guidelines were implemented. Hence, the optimal irrigation control and irrigation

scheduling compensated for the higher drip line spacing. Consequently, high frequency irrigation should not always be preferred in drip irrigation.

In general, the estimation of the control functions is more important under arid than under semiarid climate, as the compensating effect of equally distributed precipitation at the surface is lower. The variability of the yield which increases with drip line distances can be reduced with a better following of the proposed guidelines. Irrigation control functions have to be determined for every specific soil and field layout. However, characteristic irrigation control functions can be estimated for specific soil types.

Stochastic weather generator LARS-WG

The stochastic weather generator LARS-WG was successfully applied in all case studies to generate representative weather scenarios for long term climate characteristics based on historical climate data of the specific sites. For the greenhouse where long term observed weather data was missing, a regression analysis was conducted to gain the relationships between field and greenhouse for radiation (open and closed roof) and temperature resulting in three regression functions. These regression functions were applied to a generated long time-series of climate data based on the observed field data.

Regarding crop growth modeling, limitations using the weather generator may occur. LARS-WG was applied to statistically down scale global climate models. However, statistically down scaling of more precise regional climate models was not intended. Furthermore, there are climate prediction uncertainties. Additionally, LARS-WG may underestimate extreme events, for instance very dry years and convective summer precipitations. Moreover, the weather generator LARS-WG only generates daily solar radiation, minimum and maximum temperature and precipitation. This may cause problems for crop growth models who additionally require relative humidity and wind speed data. A sufficiently long time-series of observed climate data (including extreme events) enhances the quality of the generated climate data.

Stochastic optimization framework

In this work, an integrating approach which combines crop growth modeling, experiments for model calibration and validation, and optimization of irrigation and N fertilization management was presented. For determining the optimal deficit irrigation and/or N fertilization schedules, the optimization technique GET-OPTIS was coupled with a calibrated crop growth model (Daisy 1D or Pilote) and the stochastic weather generator LARS-WG using a Monte Carlo simulation-optimization (Schütze and Schmitz, 2010). The aims were

i) to determine potential yield and *WP*s (case study I), ii) real-time deficit irrigation scheduling (case study II), and iii) to estimate optimal deficit irrigation and deficit *N* fertilization schedules to reach maximal *WP* and *NUE* (case study III).

The optimized schedules were determined before sowing if the experiments were conducted in greenhouses (case study III), or after harvest for subsequent simulation-optimization to estimate the potentials of crop production (case study I). The real-time deficit irrigation schedule was recalculated weekly to respond to external events e.g. in case of precipitation (case study II).

Within all studies, controlled deficit irrigation and/or deficit *N* fertilization strategies were applied to enhance yield, *WP* and/or *NUE*. The experimental results contributed to a better understanding of crop growth under deficit irrigation and/or deficit *N* fertilization. High *WP*s of up to $4.1\,\mathrm{kg\,m^{-3}}$ (barley), $4.3\,\mathrm{kg\,m^{-3}}$ (wheat) and $3.8\,\mathrm{kg\,m^{-3}}$ (corn) were achieved while reaching high grain yields. These *WP*s are very high compared to literature values (Cantero-Martinez et al., 2003; Zwart and Bastiaanssen, 2004). The same is true for *NUE* were achieved values of up to $58\,\mathrm{kg\,grain\,kg\,}N^{-1}$ for corn exceed the ones reported by Barbieri et al. (2008) and Varga et al. (2008). The results of case study III showed, that simultaneous deficit irrigation and deficit *N* fertilization is still a challenge.

Evaluation

The approach was evaluated by observing experimental results (yield, *WP* and *NUE*), economic aspects and by model evaluation. Measures for an adequate evaluation of the experimental results and model assessment were described within this work.

For simulation based optimization, accurate predictions of the crop growth model including crop growth and water and *N* dynamics play a key role. Within this study, primarily the physically based model Daisy 1D was tested regarding crop growth under two specific conditions, namely drought stress and under greenhouse conditions. In the following, the performance of model Daisy and Pilote under drought stress and the performance of model Daisy under greenhouse conditions were evaluated.

Crop growth model performance under drought stress

The models adequacy to predict yield under limited water supply can be illustrated by residue graphs. In Figure 13.1, the residue *R* (or model error, difference between observed and predicted grain yield by model Daisy, see Tables 10.7 and 12.5) is plotted against observed grain yields (upper Figures a, b) and irrigated water amounts (lower Figures c, d).

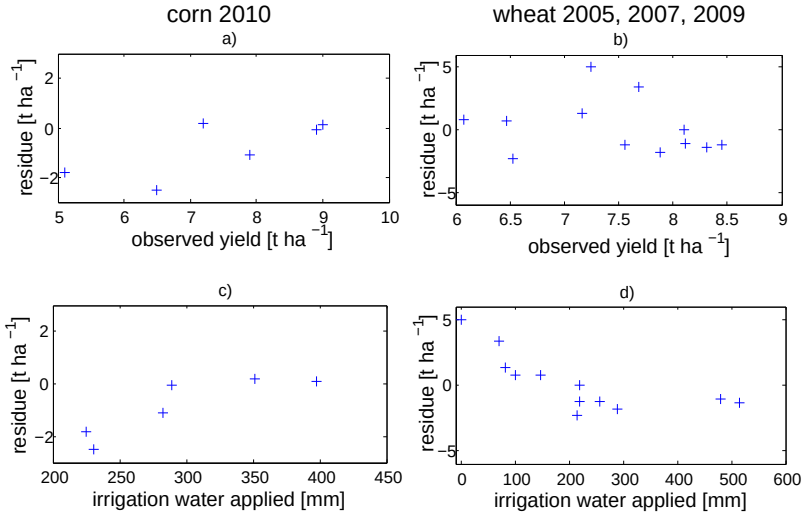

Figure 13.1.: Residue graphs for corn in 2010 (left side) and for winter wheat in 2005, 2007 and 2009 (right side) using model Daisy 1D. The residue is plotted against the observed grain yield [t ha^{-1}] (upper Figures a and b) and the applied irrigated water [mm] (lower Figures c and d). For the simulation of corn, soil parameter set C1 was used and radiation was increased by 80 %.

If the model is correctly specified, there should be no trends in the residues (Wallach et al., 2001). The upper residue graphs show the error against observed yield, however, no clear tendency can be found. The lower residue graphs plotting error against applied irrigation water show that the model error is higher for low irrigation amounts. It has to be kept in mind that, within the corn experiments, the treatment which gained the lowest irrigation amount of 225 mm ($T_{def\,irr\,N}$) was also under N limitation, and that the one irrigated with 231 mm ($T_{def\,irr}$) was affected by pests. Hence, the model error for the other four treatments is more meaningful.

Figures 13.1 c,d lead to the assumption that model Daisy 1D is weak in predicting yield under severe drought stress but still shows adequate results under moderate drought stress. For wheat, the modeling efficiency (EF) increased from -7.6 (all treatments) to -1.6 when considering only the treatments were more than 100 mm of irrigation water was applied. To improve prediction results, the plant parameters need to be calibrated again under drought stressed conditions to accurately predict photosynthesis and yields under these conditions.

The empirical crop growth model Pilote performed moderately for yield predictions under limited water supply. The target grain yield of 14 t ha^{-1} fairly met harvested grain yields of 11.8 ± 1.4 (SDI120) and 11.8 ± 1.9 t ha^{-1} (SDI160). The reason may be that the reliability of

90 % was set too low. Moreover, there were minor problems by implementing the optimized irrigation schedule due to technical and management restrictions, leading to a few irrigation events with unrequested low water amounts applied. Additionally, the weather generator LARS-WG may have underestimated the very dry growth period in 2009. Refering to Section 7.1.4, model Pilote did not meet certain criteria since model parameters showed to be barely transferable and the response of the crop to drought was not presented adequately. Since model Pilote is not able to account for spatial distribution of soil water, Hydrus 2D was applied to determine the optimal irrigation control functions.

Crop growth model performance under greenhouse conditions

The relevance of radiation heterogeneity in greenhouses and its effect on yields often reported in literature (Wang and Boulard, 2000; Jongschaap et al., 2006; Baxevanou et al., 2010) indicate a need of crop growth model adaption to that specific condition. In the present research study, two different adaptions to these conditions were undertaken.

In case study I where barley was grown in four rows in containers, only the inner rows were used for validation of the model parameters which were calibrated on field data. As the harvesting date was underestimated, two parameters depending on the geographic position (which not represented the climate in the greenhouse) were adapted. This adaption led to good predictions of grain yield, total dry matter and harvesting date.

In contrast to that, when corn was grown in one row per container (case study III), the radiation within the post-harvest simulation runs had to be increased by 80 % to adequately predict the observed yields (EF of 0.7). No shading border rows were available, since the setup consisted of three rows of containers, each with one row of corn, respectively. It is assumed that the total radiation sum per crop is much higher compared to shaded corn rows within fields. After the radiation increase, the yields were predicted adequately, however, sofil water dynamics were only moderately predicted by the model.

Consequently, model predictions in a greenhouse showed good agreement with the observed data in the case of barley but only moderate agreement in the case of corn. The reasons are supposed to be the different plant morphology and physiology and the varying experimental layouts. It is assumed that the crop growth model can not represent the changes in morphology and physiology of crops grown under greenhouse conditions. These changes could be ignored in the case of barley since only the inner crop rows were used for validation. However, this adaption was not possible in the case of corn due to the different field design (less plants and rows). The utility of a shading curtains around the experiment to simulate the shading of further rows should be investigated.

14. General conclusions and outlook

Crop growth modeling is a powerful tool to support sustainable crop production management. For reliable predictions, accurate model calibration and validation based on decisive experimental data is required. In this research study, a *new approach for simulation based optimal experimental design* was developed and applied to three case studies. The main objective was to combine crop growth modeling, experiments, and stochastic optimization for sustainable irrigation and N fertilization management.

The presented approach adjusts crop growth modeling and experiments to provide reliable model predictions as well as to assist the improvement of models. The relevant experimental data for appropriate model calibration and validation required for reliable model predictions was identified. Moreover, a sequential calibration strategy and an appropriate calibration method for separate soil and plant parametrization were presented. Furthermore, a model transfer from field to greenhouse conditions was successfully conducted.

Field crop growth under moderate drought stress was adequately predicted in most cases. Model improvements for crop growth prediction under severe drought stress should be addressed in further investigations. Crop growth modeling in greenhouses requires particular adaptations to that condition, the differing experimental layout, and the changes in crop morphology and physiology. Model Daisy was applied successfully for predicting barley crop growth under greenhouse conditions. However, yield predictions of corn greenhouse experiments required an increase of radiation of 80 % and soil water dynamics were only moderately predicted. More research regarding the influence of greenhouse conditions on crop growth and regarding predictions under greenhouse conditions is required.

Within the stochastic optimization framework, several optimal deficit irrigation and/or deficit N fertilization schedules to achieve maximal yield, WP, NUE and/or profits were estimated. Within all case studies, grain yield, WP and/or NUE were enhanced due to the implementation of the approach: grain yield was increased by 12 %, WP by 16 – 41 %, and NUE up to 76 %. However, the simultaneous maximization of both, deficit irrigation and deficit N fertilization, performed only moderately.

The observed and predicted experimental results contributed to a better understanding of crop growth under deficit irrigation and/or deficit N fertilization. Moreover, the approach proved to be an appropriate tool to reduce costs via optimizing the experimental design. Considering crop prices, SDI system and further costs, profit was increased by 27 % due to an optimal field design and the implementation of the proposed irrigation guidelines.

In general, the proposed approach of simulation based optimal experimental design requires considerable computational efforts and broad skills. Moreover, the use of adequate instrumentation for an appropriate experimental data collection is needed. Further non-destructive methods for screening drought tolerance of plants (Winterhalter et al., 2011) and for continuously measuring soil N content could be meaningful.

The presented approach was applied on field and greenhouse experiments in Germany and Southern France under field and greenhouse conditions. However, simulation based optimization of irrigation scheduling, irrigation control and estimation of a profitable field design are important issues in many arid and semi-arid regions. The approach can be adapted to different conditions and applied to different soils, field designs and crop types by calibrating models for the specific soil, field design, crop and climate (Schütze et al., 2011a).

Potential applications of the approach are a model transfer for scaling up from field to regional scales or the evaluation of possible effects on crop growth and crop water demand due to climate change. Furthermore, consulting of farmers can be based on the presented approach for the determination of the optimal field design, irrigation schedules and irrigation control.

Appendix

A. Tables and Figures

Table A.1.: Soil parameters K_s [cm d^{-1}], θ_s [cm^3 cm^{-3}], θ_r [cm^3 cm^{-3}], α [cm^{-1}] and n [-] and macropore parameters for 5 soil layers estimated with ROSETTA (Schaap et al., 2001) based on laboratory analysis results (initial values), and calibrated parameters using the optimization algorithm CMA-ES for both sites (site S1 and site S2) for case study I.

soil layer	soil depth [cm]	initial values	site S1	site S2
			distribution: 38 cm *pressure ini*: −138 cm *pressure end*: −2206 cm	*distribution*: 49 cm *pressure ini*: −138 cm *pressure end*: −2206 cm
1	0 – 35	$K_s = 5.7$ $\theta_s = 0.37$ $\theta_r = 0.066$ $\alpha = 0.0067$ $n = 1.56$	$K_s = 14.28$ $\theta_r = 0.28$ $\theta_r = 0.068$ $\alpha = 0.0028$ $n = 1.71$	$K_s = 6.24$ $\theta_s = 0.35$ $\theta_r = 0.046$ $\alpha = 0.007$ $n = 1.46$
2	35 – 66	$K_s = 5.40$ $\theta_s = 0.41$ $\theta_r = 0.077$ $\alpha = 0.0069$ $n = 1.55$	$K_s = 9.76$ $\theta_r = 0.26$ $\theta_r = 0.12$ $\alpha = 0.001$ $n = 1.61$	$K_s = 12.46$ $\theta_s = 0.29$ $\theta_r = 0.011$ $\alpha = 0.0067$ $n = 1.69$
3	66 – 79	$K_s = 10.43$ $\theta_s = 0.43$ $\theta_r = 0.076$ $\alpha = 0.0061$ $n = 1.60$	$K_s = 3.03$ $\theta_r = 0.49$ $\theta_r = 0.059$ $\alpha = 0.011$ $n = 1.96$	$K_s = 14.16$ $\theta_s = 0.49$ $\theta_r = 0.13$ $\alpha = 0.0094$ n=1.72
4	79 – 92	K_s=6.44 θ_s=0.44 θ_r=0.086 $\alpha = 0.008$ n=1,.50	K_s=14.16 θ_r=0.33 θ_r=0.088 $\alpha = 0.0011$ n=1.57	K_s=10.38 θ_s=0.37 θ_r=0.10 $\alpha = 0.0039$ $n = 1.61$
5	92 – 190	$K_s = 9.27$ $\theta_s = 0.45$ $\theta_r = 0.085$ $\alpha = 0.0067$ $n = 1.53$	K_s=11.41 $\theta_r = 0.34$ $\theta_r = 0.13$ $\alpha = 0.0031$ $n = 1.23$	$K_s = 14.56$ $\theta_s = 0.41$ $\theta_r = 0.10$ $\alpha = 0.0086$ $n = 1.33$

Table A.2.: Irrigation water applied I [mm] at treatments SDI120 and SDI160 in 2009 (case study II). Sowing dates were 07/05/2009 and 23/04/2009 for SDI120 and SDI160, respectively.

SDI120		SDI160	
date	I	date	I
28/05	23.7	12/06	33.5
29/05	10.6	13/06	13.0
10/06	5.7	22/06	6.8
18/06	22.8	30/06	28.1
19/06	20.1	01/07	4.0
25/06	11.6	03/07	8.9
30/06	33.6	07/07	22.0
01/07	6.0	10/07	13.4
03/07	5.0	17/07	17.9
08/07	5.3	22/07	10.6
10/07	12.2	23/07	14.7
17/07	14.8	24/07	8.6
23/07	16.3	30/07	16.8
29/07	9.9	31/07	15.6
06/08	17.4	12/08	12.7
07/08	4.3	18/08	7.4
14/08	14.7	20/08	8.8
20/08	14.9		
sum	249.1	sum	242.9

Table A.3.: Harvest index [%] of corn grown in a field in Southern France (2009) and in the greenhouse at Dürnast in Southern Germany (2010) for case studies II and III, respectively.

treatment	harvest index
France 2009	
SDI160	62
SDI120	59
Germany 2010	
$T_{def\,irr}$	58
T_{full}	64
$T_{def\,N}$	63
$T_{def\,irr\,N}$	58

Table A.4.: Simulation results of Daisy 2D using the soil parameter sets C1 and C2 (case study III). Observed and predicted grain yield Y and total dry matter (TDM, in brackets) in t ha^{-1} for the observed global radiation (R) and radiation increased by 80 % (80 % R).

treatment	observed	C1		C2	
	Y (TDM)	Y (TDM) for R	Y (TDM) for 80 % R	Y (TDM) for R	Y (TDM) for 80 % R
T_{full}	9.0 ± 1.3 (16.5 ± 2.1)	4.1 (10.0)	3.7 (8.2)	6.1 (14.0)	6.1 (15.1)
$T_{def\,irr}$	6.5 ± 1.4 (13.2 ± 2.1)	3.6 (7.3)	2.2 (5.7)	4.1 (10.7)	4.9 (11.8)
$T_{def\,N}$	7.2 ± 0.8 (13.4 ± 1.1)	2.6 (5.7)	2.0 (5.5)	3.7 (10.9)	3.9 (9.3)
$T_{def\,irr\,N}$	5.1 ± 0.2 (10.3 ± 0.7)	2.6 (5.9)	1.7 (4.9)	2.9 (8.0)	2.9 (8.0)

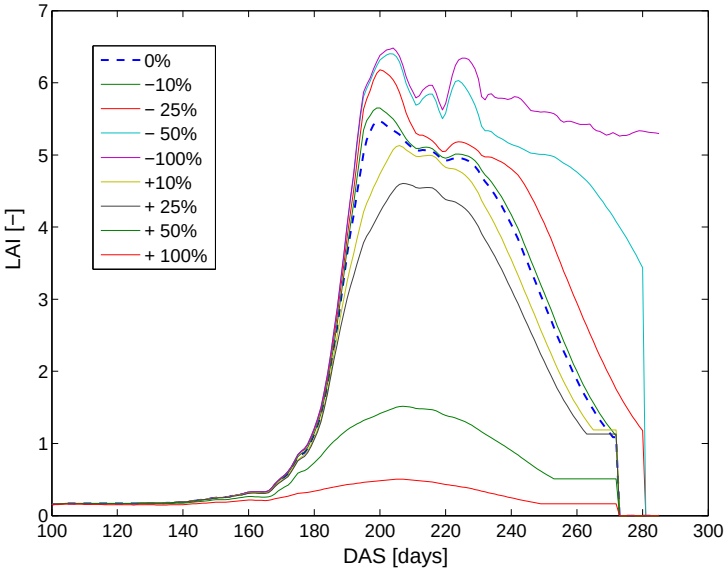

Figure A.1.: LAI development for a variation of the wheat crop parameter $DSRate1$ of crop model Daisy (case study I).

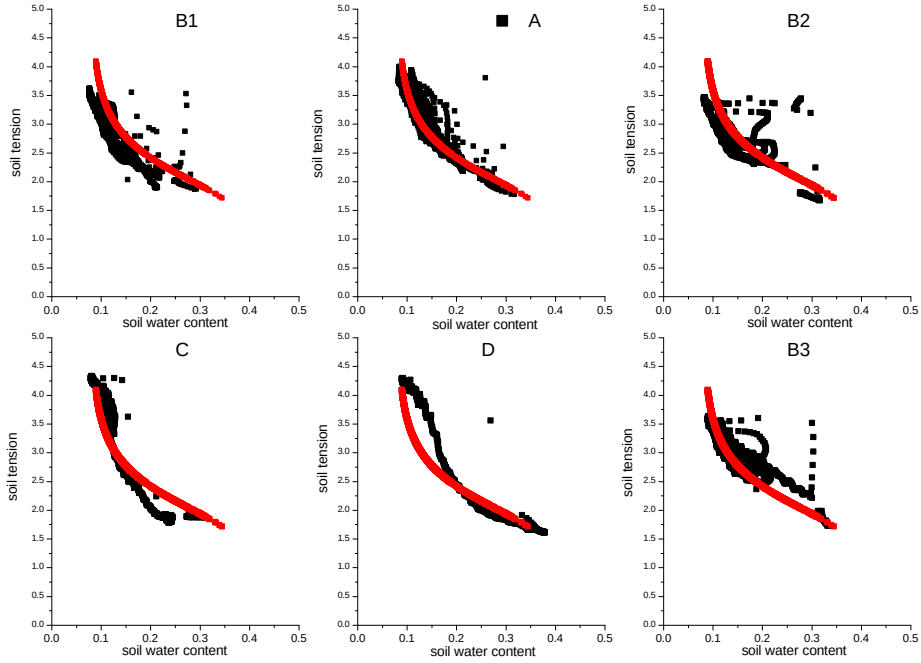

Figure A.2.: Observed (black) and fitted (red) water retention curve of treatment $T_{def\,irr}$ for levels A, B (three curves, one for each container), C and D (case study III).

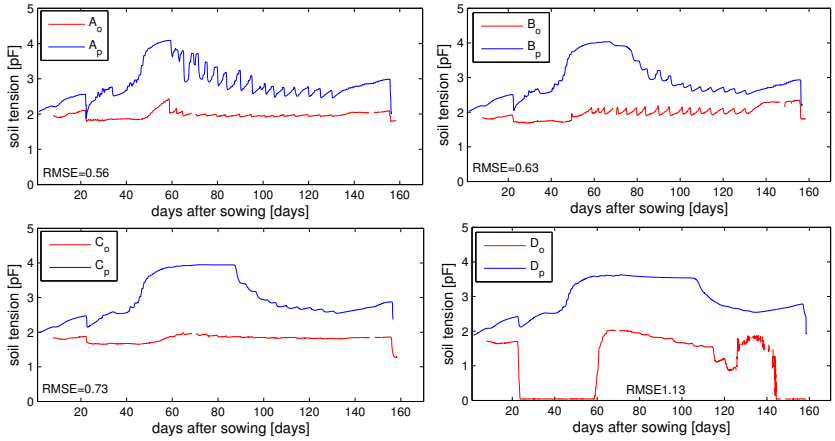

Figure A.4.: Predicted and observed soil tensions for T_{full} (radiation increase of 80 % and application of the soil parameter set C2) of case study III. A stands for the sensor at level A at 20 cm, B stands for the sensor at level B at 30 cm (three sensors), C stands for the sensor at level C at 40 cm and D stands for the sensor at level D at 60 cm soil depth. The red line shows the observed values (o), the blue line the predicted ones (p). The *RMSE* is given in pF.

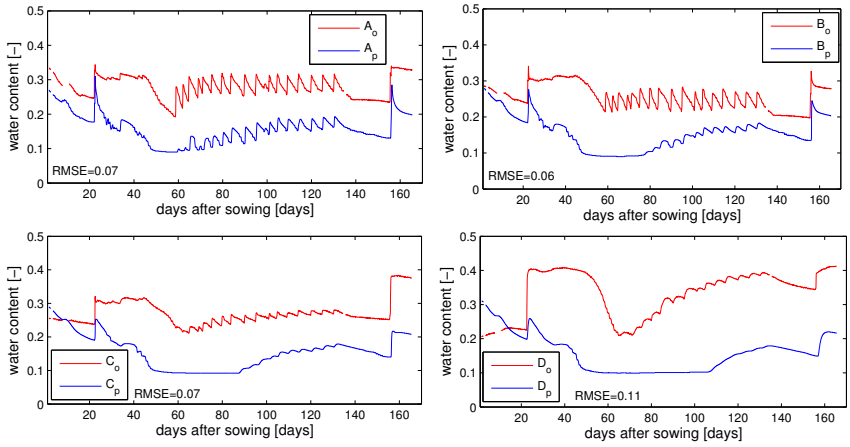

Figure A.3.: Predicted and observed soil water contents for T_{full} (radiation increase of 80 % and application of the soil parameter set C2) of case study III. A stands for the sensor at level A at 20 cm, B stands for the sensor at level B at 30 cm (three sensors), C stands for the sensor at level C at 40 cm and D stands for the sensor at level D at 60 cm soil depth. The red line shows the observed values (o), the blue line the predicted ones (p). The *RMSE* is given in cm^3 cm^{-3}.

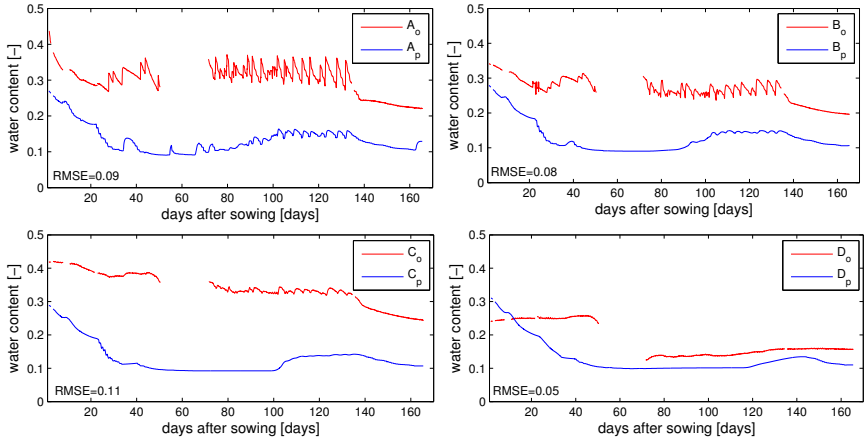

Figure A.5.: Predicted and observed soil water contents for $T_{def\,N}$ (radiation increase of 80 % and application of the soil parameter set C2) of case study III. A stands for the sensor at level A at 20 cm, B stands for the sensor at level B at 30 cm (three sensors), C stands for the sensor at level C at 40 cm and D stands for the sensor at level D at 60 cm soil depth. The red line shows the observed values (o), the blue line the predicted ones (p). The *RMSE* is given in cm^3 cm^{-3}.

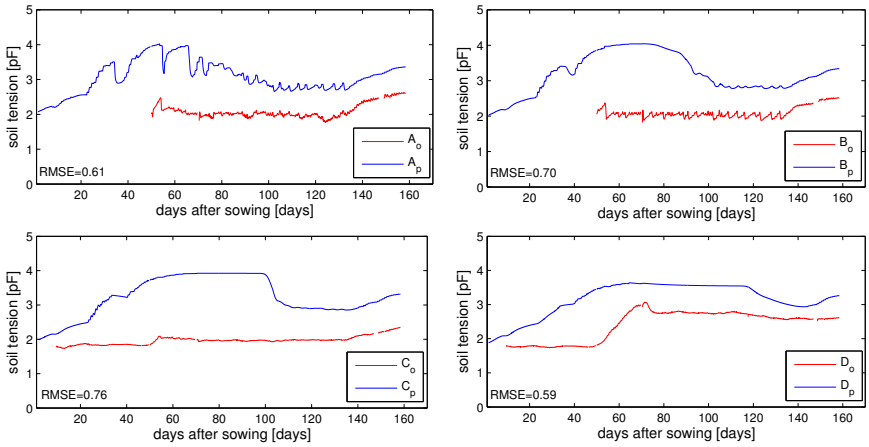

Figure A.6.: Predicted and observed soil tensions for $T_{def\,N}$ (radiation increase of 80 % and application of the soil parameter set C2) of case study III. A stands for the sensor at level A at 20 cm, B stands for the sensor at level B at 30 cm (three sensors), C stands for the sensor at level C at 40 cm and D stands for the sensor at level D at 60 cm soil depth. The red line shows the observed values (o), the blue line the predicted ones (p). The *RMSE* is given in pF.

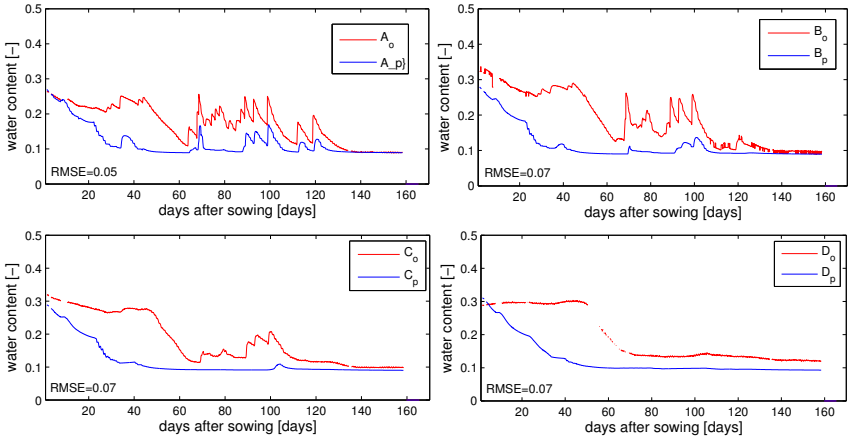

Figure A.7.: Predicted and observed soil water contents for $T_{def\,irr\,N}$ (radiation increase of 80 % and application of the soil parameter set C2) of case study III. A stands for the sensor at level A at 20 cm, B stands for the sensor at level B at 30 cm (three sensors), C stands for the sensor at level C at 40 cm and D stands for the sensor at level D at 60 cm soil depth. The red line shows the observed values (o), the blue line the predicted ones (p). The *RMSE* is given in cm^3 cm^{-3}.

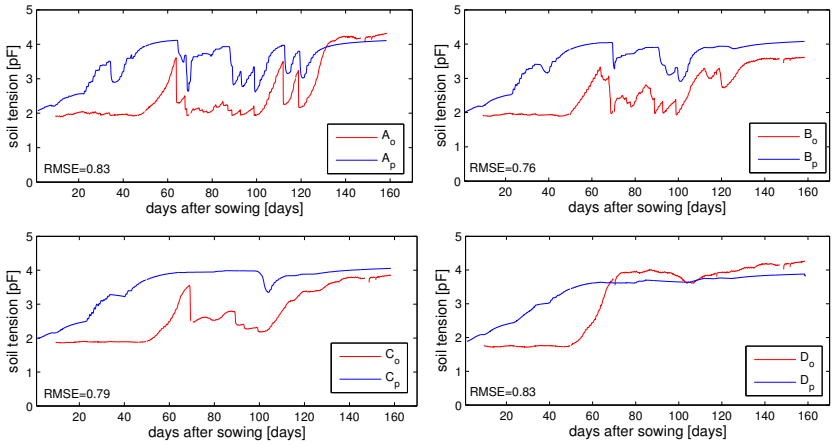

Figure A.8.: Predicted and observed soil tensions for $T_{def\,irr\,N}$ (radiation increase of 80 % and application of the soil parameter set C2) of case study III. A stands for the sensor at level A at 20 cm, B stands for the sensor at level B at 30 cm (three sensors), C stands for the sensor at level C at 40 cm and D stands for the sensor at level D at 60 cm soil depth. The red line shows the observed values (o), the blue line the predicted ones (p). The *RMSE* is given in pF.

B. Model setup and weather files

Lines starting with ;; (Daisy setup files) or # (Daisy weather files) will be commented out.

Daisy example weather file for 2006/2007 (case study I)

```
dwf-0.0 -- Sample _Daisy _Weather _File.
# General information about the station itself.
Station:  Freising.
Wetterstation Nr.8
Elevation:  470 m
Longitude:  11 dgEast
Latitude:  48 dgNorth
TimeZone:  15 dgEast
# Information about the measurement conditions.
Surface:  reference ScreenHeight:  2.0 m
# General information about the available data.
Begin:  2006-01-01 End:  2007-07-24
# Fixed deposit values
Deposition:  64.9 kgN/ha/year
PAverage:  800 mm DepDry:  0.4 fraction DepDryNH4:  0.6 fraction DepWetNH4:  0.5 fraction
# Temperature averages
TAverage:  8.68 dgC TAmplitude:  7.8 dgC MaxTDay:  187 yday Timestep:  24 hours
PrecipCorrect:  1.0 1.0 1.0 1.0 1.0 1.0 1.0 1.0 1.0 1.0 1.0 1.0
Year Month Day GlobRad AirTemp Precip year month mday W/m^2 dgC mm/d
2006 1 1 27.89 1.30 2.20
2006 1 2 14.59 -0.10 0.40
2006 1 3 23.42 -0.20 0.20
and so on
```

Daisy 1D setup file for full irrigated wheat in 2006/07 (site S1) (case study I)

```
(directory "C:/Programme/Daisy 4.57/...")
(path "." "C:/Programme/Daisy 4.57/Lib")
(input file "tillage.dai")
(input file "crop.dai")
(input file "fertilizer.dai")
(input file "log.dai")
(input file "wwheatFreising.dai")
(weather default "Freising_Wetter2006-2007_optimal bewässert für Westfläche.dwf")
(defcrop "Cubus Freising" "Winter Wheat Freising" (enable_N_stress false))
(defhorizon Ap FAO3
"Schicht 0 - 0.35m"
(dry_bulk_density 1.60 [g/cm^3])
(clay 21.7 [%]) (silt 61.6 [%])
(sand 14.6 [%]) (humus 2.1 [%])
(hydraulic M_vG (K_sat 6.244015 [cm/d])
(Theta_res 0.0463412 [])
(Theta_sat 0.35593 [])
(alpha 0.00714838 [cm^-1])
(n 1.4594)))
(defhorizon Bv-Sw FAO3
"Schicht 0.35 - 0.66 m"
and so on
(defcolumn "Rollfeld" default
(SoilWater (initial_Theta (-10 [cm] 33.51 [%]) (-20 [cm] 32.95 [%]) (-40 [cm]
31.59 [%])(-60 [cm] 21.55 [%]) (-80 [cm] 39.56 [%]) (-100 [cm] 41.87 [%])))
(Soil (MaxRootingDepth 150 [cm])
(horizons ( -35 [cm] Ap) ( -66 [cm] Bv-Sw)
( -79 [cm] Bv-Sw1) ( -92 [cm] Bv-Sw2) ( -190 [cm] Cv)))
(Movement vertical (Tertiary old (macro default
(distribution (-49.17758 1) (0 0))
(pressure_initiate -138.385 [cm])
(pressure_end -2205.545 [cm])))
(Geometry (zplus -0.5 -1.75 -3.25 -4.75 -6.5 -7.25 -8.5 -11.5 -14.5 -17.5 -22.5
-27.5 -32.5 -37.5 -42.5 -47.5 -52.5 -57.5 -62.5 -67.5 -72.5 -77.5 -82.5 -87.5
-92.5 -97.5 -102.5 -120 -130 -135 -140 -150 -155 -160 -170 -180 -190 [cm]))
(matrix_water (richards (debug 2) (max_time_step_reductions 8)
```

```
(time_step_reduction 8)(max_iterations 100) max_absolute_difference 0.02[cm])
(max_relative_difference 0.001 []) (K_average geometric))))(Groundwater lysimeter))
(defaction wwheat_management_west activity
(wait (at 2006 03 14 1)) (sow "Spring Rape")
(fertilize (mineral (weight 80 [kg N/ha]) (NH4_fraction 0.7 [])))
(wait (crop_ds_after "Spring Rape" 2.0))
(harvest "Spring Rape" (stub 15 [cm]) (stem 1.0 []))
(wait (at 2006 10 01 1)) (plowing) (wait (at 2006 10 10 1))
(seed_bed_preparation)
(wait (at 2006 10 11 1)) (sow "Cubus Freising" ) (
wait (at 2007 03 07 1)) (fertilize (mineral (weight 70.0 [kg N/ha])
(NH4_fraction 0.7 []))) (wait (at 2007 03 13 1)) (fertilize
(mineral (weight 40.0 [kg N/ha]) (NH4_fraction 0.7 [])))
(wait (at 2007 04 13 1)) (irrigate_overhead 20 [mm/h])
(wait (at 2007 04 14 1)) (irrigate_overhead 20 [mm/h])
and so on
(at 2007 07 19 1))) (harvest "Cubus Freising" (stub 15 [cm]) (stem 1.0 [])))
(column "Rollfeld") (time 2006 01 01 1)
(manager activity wwheat_management_west (wait (at 2007 07 24 1)) stop)
(output Harvest "Root form parameter" "Crop Production"
("Root Zone Water Balance" (to -150 [cm])(when daily) (where "Daily_WB.dlf"))
("Root Zone Water Balance" (to -150 [cm])(when monthly) (where "Monthly_WB.dlf"))
("Soil Water Content" (when daily)) ("Soil Water Potential" (when daily)))
```

Daisy 1D setup file for fully irrigated barley (rain-out shelter) in 2009 (case study I)

```
(directory "C:/...")
(path "." "C:/Program Files/Daisy 4.57/lib")
(input file "tillage.dai")
(input file "srape.dai")
(input file "sbarley.dai")
(input file "RF-Barke.dai")
(input file "fertilizer.dai")
(input file "log.dai")
(weather default "RF-Meteo.dwf")
(defhorizon Ap FAO3 "Ap 0.00-0.35m"
(dry_bulk_density 1.60 [g/cm^3])
```

```
(clay 21.7 [%]) (silt 61.6 [%])
(sand 14.6 [%]) (humus 2.1 [%])
(hydraulic M_vG (K_sat 14.287411 [cm/d]) (Theta_res 0.0688448 [])
(Theta_sat 0.280485 []) (alpha 0.00288258 [cm^-1])(n 1.716044)) )
and so on
(defcolumn "Acker-Braunerde-Pseudogley" default
(SoilWater (initial_Theta
(-10 [cm] 33.51 [%]) (-20 [cm] 32.95 [%])
(-40 [cm] 31.59 [%]) (-60 [cm] 21.55 [%])
(-80 [cm] 39.56 [%]) (-100 [cm] 41.87 [%])))
(Soil (MaxRootingDepth 100 [cm])
(horizons ( -35 [cm] Ap) ( -66 [cm] Bv-Sw) ( -79 [cm] Bv-Sw1)
( -92 [cm] Bv-Sw2) ( -190 [cm] Cv)) )
(Groundwater lysimeter) ("Deep" als freie Perkolation)
(Movement vertical (Tertiary old (macro default (distribution (-38.27525 1) (0 0))
(pressure_initiate -242.46 [cm]) (pressure_end -2890.265 [cm]) ))
(Geometry (zplus -0.5 -1.75 -3.25 -4.75 -6.5 -7.25 -8.5 -11.5 -14.5 -17.5
-22.5 -27.5 -32.5 -37.5 -42.5 -47.5 -52.5 -57.5 -62.5 -67.5 -72.5 -77.5
-82.5 -87.5 -92.5 -97.5 -102.5 -120 -130 -135 -140 -150 -155 -160 -170 -180 -190 [cm]) )
(matrix_water (richards debug 2) (max_time_step_reductions 8) (time_step_reduction 8)
(max_iterations 100) (max_absolute_difference 0.02[cm])(max_relative_difference 0.001 [])
(K_average geometric)) )))
(defcrop "Barke mod" "Barke" (enable_N_stress false) )
(defaction BARKEfull activity
(wait (at 2008 03 14 1))
(progn (sow "Spring Rape")
(fertilize (mineral (weight 80.0 [kg N/ha])
(NH4_fraction 0.7 []))))
(wait (crop_ds_after "Spring Rape" 2.0))(harvest "Spring Rape"(stub 15 [cm])(stem 1.0 []))
(fertilize (mineral (weight 60.0 [kg N/ha]) (NH4_fraction 0.7 [])))
(wait (at 2009 04 01 1)) (plowing)
(wait (at 2009 04 05 1)) (seed_bed_preparation)
(wait (at 2009 04 06 1)) (sow "Barke mod")
(wait (at 2009 04 15 1))(fertilize (mineral (weight 80.0 [kg N/ha])(NH4_fraction 0.7 [])))
(wait (at 2009 04 23 1)) (irrigate_overhead 30.0 [mm/h])
and so on
(wait (or (crop_ds_after "Barke mod" 2.0) (at 2009 07 22 1)))
(harvest "Barke mod" (stub 15 [cm]) (stem 1.0 [])) )
(column "Acker-Braunerde-Pseudogley")(time 2008 01 01 1)
(manager activity BARKEfull (wait (at 2009 07 30 1)) stop)
(activate_output (and (after 2009 4 01 23) (before 2009 8 1 0)))
(output cropprod)
```

Daisy 1D setup file for fully irrigated barley (greenhouse) in 2009 (case study I)

```
(directory "C:/...")
(path "." "C:/Programme/Daisy 4.74/lib" "C:/...")
(input file "tillage.dai")
(input file "sbarley.dai")
(input file "VH-Barke.dai")
(input file "fertilizer.dai")
(input file "log.dai")
(weather default "VH-Meteo.dwf")
(defhorizon H1 FAO3 "H1 0.00-0.725m"
(dry_bulk_density 1.6 [g/cm^3])
(clay 19 [%]) (silt 44 [%])(sand 37 [%]) (humus 0.1 [%])
(hydraulic M_vG (K_sat 16.0 [cm/d]) (Theta_res 0.06 []) (Theta_sat 0.25 [])
(alpha 0.00288258[cm^-1]) (n 1.716044)) )
(defhorizon Stau FAO3 "TON 0.725-0.80m"
(clay 100 [%]) (silt 0 [%]) (sand 0 [%]) (humus 0.01 [%])
(hydraulic M_vG
(K_sat 0.048 [cm/d]) (Theta_res 0.0563 []) (Theta_sat 0.38 [])
(alpha 0.008 [cm^-1]) (n 1.09)) )(defcolumn "Container" default
(Soil (MaxRootingDepth 72.5[cm]) (horizons ( -72.5 [cm] H1) ( -80.0 [cm] Stau)))
(Groundwater lysimeter)
(Movement vertical (Geometry (zplus -0.5 -1.75 -3.25 -4.75 -6.5 -7.25 -8.5 -11.5
-14.5 -17.5 -22.5 -27.5 -32.5 -37.5 -42.5 -47.5 -52.5 -57.5 -62.5 -67.5 -72.5 [cm]))
(matrix_water (richards (debug 2) (max_time_step_reductions 8)
(time_step_reduction 8) (max_iterations 100)
(max_absolute_difference 0.02[cm]) (max_relative_difference 0.001 [])
(K_average geometric)))))
(defcrop BarkeRH "Barke" (enable_N_stress false))
(defaction VH-BARKEfull activity
(wait (at 2009 03 23 1))(fertilize (mineral (weight 60.0 [kg N/ha])(NH4_fraction 0.7 [])))
(wait (at 2009 03 26 1)) (sow "BarkeRH") (irrigate_surface 3.0 [mm/h] (hours 10))
(wait (at 2009 03 30 1)) (irrigate_surface 3.2 [mm/h])
(wait (at 2009 03 31 1)) (irrigate_surface 2.0 [mm/h])
and so on
(wait (or (crop_ds_after "BarkeRH" 2.0) (at 2009 08 07 1)))
(harvest "BarkeRH" (stub 15 [cm]) (stem 1.0 [])))
(column "Container")(time 2009 03 01 1)
```

```
(manager activity VH-BARKEfull (wait (at 2009 08 10 1)) stop)
(output CropLog "Root Zone Water Balance" "Soil Water Potential" "Soil Water Content")
```

Pilote plant parameter file (case study II) -> explanation

```
2009,2009,112,261 -> year, start and end of simulation (DOY)
0.32,0.11,1.2 -> field capacity, wilting point, maximal rooting depth
0.6 -> Rfu/Ru
0.015 -> growth of rooting pattern
113 150-> installation of root system
350 1.2,0.3,0 -> Coef.  cultural max, coef.  max evaporation, unknown
5,1.35,0.5 -> LAI max, conversion efficiency, indice of potential yield
1050,900,1650 -> temperature sum for flowering, start and end of critical phase
2000,1.25 -> temperature sum for ripening, stress coefficient
4,1,2.5 -> LAI alpha, LAI beta, LAI gamma
100,6 -> temperature sum for germination
10,10 -> base temperature, optimal plant density
1,2.75,0.17 -> impact of stress (y/n -> 1/0), threshold LAI for stress, growth coefficient
15 -> grain humidity
147 -> unknown
0 0,0 -> unknown
```

Daisy 1D setup file for treatment $T_{def\,irr\,N}$ (case study III)

```
(directory "C:/...")
(path "C:/...")
(input file "tillage.dai")
(input file "maize.dai")
(input file "maizelavalette2.dai")
(input file "log.dai")
(input file "fertilizer.dai")
(weather default "Klimadaten_FS2010.dwf")
(description "nachträgliche 1D Modellierung FS 2010")
(defcrop "Pioneer Freising" "Pioneer Maize Lavalette 2007 ohne Sprinkler, y_half vaiabel"
(enable_N_stress true))
(defhorizon A FAO3 "Schicht 0 - 0.65m"
(clay 0.033 []) (silt 0.175 [])
(sand 0.791 []) (humus 0.001 []) (dry_bulk_density 1.7 [g/cm^3])
(hydraulic M_vG (Theta_res 3.52 [%]) (Theta_sat 39.05 [%]) (alpha 0.05352 [cm^-1])
(n 1.5725288 []) (K_sat 482.4 [cm/d]))) ;; applied vGM parameters
```

```
;; recalculated vGM parameters:  (hydraulic M_vG (Theta_res 8.1 [%]) (Theta_sat 41 [%])
(alpha 0.0159 [cm^-1]) ;; alpha in cm-1 (n 1.6913 []) (K_sat 112.20 [cm/d])))
(defhorizon B FAO3 "Stauschicht 0.65-0.70 m" (clay 0.999 [])
(silt 0.00 []) (sand 0.00 []) (humus 0.001 [])
(hydraulic M_vG (Theta_res 5.63 [%]) (Theta_sat 38.00 [%])
(alpha 0.008 [cm^-1]) (n 1.09 [])
(K_sat 0.048 [cm/d])))
(defcolumn "Freising2010" default
(SoilNO3 (initial_Ms (-30 [cm] 0.75 [ppm]))) (SoilNH4 (initial_Ms (-30 [cm] 0.75 [ppm])))
(SoilWater (initial_Theta (-30 [cm] 29 [%])(-60 [cm] 20 [%]))
(UZtop (richards (max_absolute_difference 0.02 [cm]) (max_iterations 51)
(max_relative_difference 0.001 [])(max_time_step_reductions 16)(time_step_reduction 4)))
(Soil (MaxRootingDepth 65 [cm]) (horizons ( -65 [cm] "A") (-70 [cm] "B"))
(zplus -0.5 -1 -1.5 -2 -3 -4 -5 -6 -7 -8 -9 -10 -11 -12 -13 -14 -15 -16
-17 -18 -19 -20 -21 -22 -23 -24 -25 -26 -27 -28 -29 -30 -31 -32 -33 -34 -35
-36 -37 -38 -39 -40 -41 -42 -43 -44 -45 -46 -47 -48 -49 -50 -51 -52 -53 -54
-55 -56 -57 -58 -59 -60 -61 -62 -63 -64 -65 -66 -67 -68 -69 -70 [cm]))
(Groundwater deep) (column Freising2010)
(defaction PioneerFS_management activity
(wait (at 2010 05 14 16)) (sow "Pioneer Freising" )
(wait (at 2010 5 20 13))(fertilize
(mineral (weight 90.0 [kg N/ha])(NH4_fraction 0.5 [])))
(wait (at 2010 5 20 15))(irrigate_surface 2.7 [mm/h] (hours 1))
(wait (at 2010 5 21 10))(irrigate_surface 2.7 [mm/h] (hours 1))
and so on
(wait (crop_ds_after "Pioneer Freising" 2.0)) (wait (at 2010 10 19 1)) (stop))
(column "Freising2010")(time 2010 05 14 01) (manager activity PioneerFS_management
(output ("Crop Production")("Root Zone Water Balance" (to -70 [cm])
(when daily)(where "daily_WB.dlf"))
("Soil Water Content" (when hourly)) ("Soil Water Potential" (when hourly))
("N Balance" (when daily)(from 0 [m]) (to -0.7 [m])) )
```

Daisy 2D setup file for treatment $T_{def\,irr\,N}$ (case study III)

```
(directory "C:/Programme/Daisy 4.57/...")
(path "C:/Program Files/Daisy 4.57/lib")
(input file "tillage.dai")
(input file "maize.dai")
(input file "maizelavalette2.dai")
(input file "log.dai")
```

```
(input file "fertilizer.dai")
(weather default "Klimadaten_FS2010_180R.dwf") ;; Strahlungsdaten:  TRg
(description "nachträgliche 2D Modellierung FS 2010 T2")
(defcrop "Pioneer Freising" "Pioneer Maize Lavalette 2007 ohne Sprinkler, y_half vaiabel"
;; (enable_N_stress true))
(enable_N_stress false))
(defhorizon A FAO3 "Schicht 0 - 0.65m" (clay 0.033 []) (silt 0.175 [])
(sand 0.791 []) (humus 0.001 []) (dry_bulk_density 1.7 [g/cm^3])
(Theta_res 8.1 [%]) (Theta_sat 41 [%])
(alpha 0.0159 [cm^-1]) (n 1.6913 []) (K_sat 112.20 [cm/d])))
(defhorizon B FAO3 "Stauschicht 0.65-0.70 m"
(clay 0.999 []) (silt 0.00 []) (sand 0.00 []) (humus 0.001 [])
(hydraulic M_vG (Theta_res 5.63 [%]) (Theta_sat 38.00 [%]) (alpha 0.008 [cm^-1])
(n 1.09 []) (K_sat 0.048 [cm/d])))
(defcolumn "Freising2010" default (Groundwater deep)
(Chemistry multi (combine (N (trace (NO3 (initial_Ms (-30 [cm] 1 [ppm])))) (NH4)))))
;; 2D Version von Daisy einschalten; Bodensäule gleich Container (z=70cm und x=60 cm)
(Movement rectangle (matrix_water (Mollerup (max_time_step_reductions 8)(time_step_reduction 4)
(max_iterations 21)) "v+h" const) (Geometry (zplus -1 -2 -2.5 -5 -7.5 -10 -12.5 -15 -17.5
-20 -22.5 -25 -27.5 -30 -32.5 -35 -37.5 -40 -42.5 -45 -47.5 -50 -52.5 -55 -57.5 -60 -62.5
-65 -67.5 -70 [cm])
(xplus 5 7.5 10 12.5 15 17.5 20 22.5 25 27.5 30 32.5 35 37.5 40 42.5 45 47.5 50 52.5 55
57.5 60 [cm])))  (Soil (MaxRootingDepth 70 [cm]) (horizons ( -65 [cm] "A") ( -70 [cm] "B"))) )
(defvolume drip-volumen box (top finite -1 [cm]) (bottom finite -2 [cm]) (left finite 25 [cm])
(right finite 35 [cm])) (defvolume water_balance box "Wasserbilanz für Wurzelbereich"
(top finite 0 [cm]) (bottom finite -70 [cm]) )
(defaction PioneerFS_management activity (wait (at 2010 05 14 16))
(sow "Pioneer Freising" (row_width 60 [cm]) (row_position 30 [cm]))
(wait (at 2010 5 20 13))(fertilize (mineral (weight 90.0 [kg N/ha])(NH4_fraction 0.5 [])))
(wait (at 2010 5 20 15))(irrigate_subsoil 2.7 [mm/h] (hours 1))
(wait (at 2010 5 21 10))(irrigate_subsoil 2.7 [mm/h] (hours 1))
(wait (at 2010 5 28 15))(irrigate_subsoil 2.2 [mm/h] (hours 1))
and so on
(wait (at 2010 10 25 13))(irrigate_subsoil 13 [mm/h] (hours 1)) ;; Infiltration experiment
(wait (crop_ds_after "Pioneer Freising" 2.0)) (wait (at 2010 10 20 01)) (stop))
(column "Freising2010") (time 2010 05 14 01)
(manager activity PioneerFS_management (wait (after_mm_dd 10 19)) stop )
(output ("Crop Production") ("Root Zone Water Balance" (to -70 [cm])(when daily)
(where "daily_WB.dlf")) ("Soil Water Content" (when hourly)))
```

List of Tables

List of Figures

References

P. Abrahamsen. *Daisy Program Reference Manual, Royal Veterinary and Agricultural University, Copenhagen*, 2006. URL `www.dina.kvl.dk/?daisy/ftp/daisy-ref.pdf(10/24/2009)`.

R. G. Allen. Using the FAO-56 dual crop coefficient method over an irrigated region as part of an evapotranspiration intercomparison study. *Journal of Hydrology*, 229(1–2): 27–41, 2000.

J. E. Ayars, C. J. Phene, R. B. Hutmacher, K. R. Davis, R. A. Schoneman, S. S. Vail, and R. M. Mead. Subsurface drip irrigation of row crops: a review of 15 years of research at the Water Management Research Laboratory. *Agricultural Water Management*, 42(1): 1–27, 1999.

P. A. Barbieri, H. E. Echeverria, H. R. S. Rozas, and F. H. Andrade. Nitrogen use efficiency in maize as affected by nitrogen availability and row spacing. *Agronomy Journal*, 100 (4):1094–1100, 2008.

R. Barker, D. Dawe, and A. Inocenio. *Economics of water productivity in managing water for agriculture*. CABI, 2003.

C. Baxevanou, D. Fidaros, T. Bartzanas, and C. Kittas. Numerical simulation of solar radiation, air flow and temperature distribution in a naturally ventilated tunnel greenhouse. *Agricultural Engineering International: CIGR Journal*, 12(3):1380–1386, 2010.

R. Bongiovanni and J. Lowenberg-Deboer. Precision agriculture and sustainability. *Precision Agriculture*, 5(4):359–387, 2004. ISSN 1385-2256.

C. Bontemps and S. Couture. Irrigation Water Demand for the Decision Maker. *Environment and Development Economics*, 7:643–657, 2002.

C. Brouwer, K. Prins, M. Kay, and M. Heibloem. *Irrigation Water Management: Irrigation Methods*. FAO Land and Water Development Division, 1988.

C. Burt. *Selection of Irrigation Methods for Agriculture*. On-Fam Irrigation Committee, 2000.

C. R. Camp. Subsurface drip irrigation: A review. *Transactions of the ASAE*, 41(5): 1353–1367, 1998.

C. R. Camp, P. J. Bauer, P. G. Hunt, W. J. Busscher, and E. J. Sadler. Subsurface drip irrigation for agronomic crops. In *Irrigation–Association Technical Conference Intl. Irrig. Expo. and Conf.*, San Diego, Ca, 1998.

C. R. Camp, F. R. Lamm, R. G. Evans, and C. J. Phene. *Subsurface drip irrigation – Past, present, and future.* Phoenix, Az, 2000.

C. Cantero-Martinez, P. Angas, and J. Lampurlane. Growth, yield and water productivity of barley (Hordeum vulgare L.) affected by tillage and N fertilization in Mediterranean semiarid, rainfed conditions of Spain. *Field Crops Research*, 84(3):341–357, 2003.

R. Casa, A. Cavalieri, and B. Lo Cascio. Nitrogen fertilisation management in precision agriculture: a preliminary application example on maize. *Italian Journal of Agronomy*, 6(5):23–27, 2011.

K. G. Cassman, A. Dobermann, and D. T. Walters. Agroecosystems, nitrogen-use efficiency, and nitrogen management. *Ambio*, 31(2):132–140, 2002.

M. Clop, L. Cots, M. Esteban, and J. Barragan. Economic profitability in the Urgell Canals (Lleida, Spain) irrigation area. *Informacion Tecnica Economica Agraria (ITEA)*, 105(1): 36–48, 2009.

A. H. K. Darusman, L. R. Stone, and F. R. Lamm. Water flux below the root zone vs. drip-line spacing in drip-irrigated corn. *Soil Science Society of America Journal*, 61(6): 1755–1760, 1997.

H. Dehghanisanij, M. M. Nakhjavani, A. Z. Tahir, and H. Anyoji. Assessment of wheat and maize water productivities and production function for cropping system decisions in arid and semiarid regions. *Irrigation and Drainage*, 58:105–115, 2009.

J. Drouet and J. Kiniry. Does spatial arrangement of 3D plants affect light transmission and extinction coefficient within maize crops? *Field Crops Research*, 107(1):62–69, 2008.

S. Elmaloglou and E. Diamantopoulos. Simulation of soil water dynamics under subsurface drip irrigation from line sources. *Agricultural Water Management*, 96(11):1587–1595, 2009.

M. English. Deficit irrigation. I: Analytical framework. *Journal of Irrigation and Drainage Engineering*, 116:399–412, 1990.

M. English and S. Raja. Perspectives on deficit irrigation. *Agricultural Water Management*, 32(1):1–14, 1996.

S. R. Evett, T. A. Howell, A. D. Schneider, D. R. Upchurch, D. F. Wanjura, and A. Asae. Automatic drip irrigation of corn and soybean. In *4th National Irrigation Symposium*, pages 401–408, Phoenix, Az, 2000.

N. K. Fageria and V. C. Baligar. Enhancing nitrogen use efficiency in crop plants. *Advances In Agronomy*, 88:97–185, 2005.

FAO. *World Agriculture: Towards 2015/2030. Summary Report.* Economic and Social Development Department, 2002.

A. Garcia y Garcia, L. Guerra, and G. Hoogenboom. Water use and water use efficiency of sweet corn under different weather conditions and soil moisture regimes. *Agricultural Water Management*, 96(6):912–916, 2009.

S. Gayler, E. Wang, E. Priesack, T. Schaaf, and F. X. Maidl. Modeling biomass growth, N-uptake and phenological development of potato crop. *Geoderma*, 105(3–4):367–383, 2002. ISSN 0016-7061.

H. Gijzen, E. Heuvelink, H. Challa, L. Marcelis, E. Dayan, S. Cohen, and M. Fuchs. HORTISIM: A model for greenhouse crops and greenhouse climate. *Acta Hort. (ISHS)*, 456:441–450, 1998.

N. Hansen. *The CMA evolution strategy: a tutorial*, 2008. URL `www.bionik.tu-berlin.de/user/niko/cmatutorial.pdf(05/24/2010)`.

S. Hansen. *Daisy, a flexible soil-plant-atmosphere system model*, 2002. URL `www.dina.kvl.dk/~daisy/ftp/DaisyDescription.doc(01/14/2010)`.

J. Hatfield, T. Sauer, and J. Prueger. Managing Soils to Achieve Greater Water Use Efficiency: A Review. *Agronomy Journal*, 93(2):271–280, 2001.

J. L. Hatfield and J. H. Prueger. Increasing nitrogen use efficiency of corn in Midwestern cropping systems. *The Scientific World Journal*, 1(2):682–690, 2001.

T. Heidmann, C. Tofteng, P. Abrahamsen, F. Plauborg, S. Hansen, A. Battilani, J. Coutinho, F. Dolezal, W. Mazurczyk, J. Ruiz, J. Takac, and J. Vacek. Calibration procedure for a potato crop growth model using information from across Europe. *Ecological Modelling*, 211(1–2):209–223, 2008.

G. V. Johnson and W. R. Raun. Nitrogen response index as a guide to fertilizer management. *Journal Of Plant Nutrition*, 26(2):249–262, 2003.

R. Jongschaap, T. Dueck, N. Marissen, S. Hemming, and L. Marcelis. Simulating seasonal patterns of increased greenhouse crop production by conversion of direct radiation into diffuse radiation. *ISHS Acta Horticulturae*, 718:315–322, 2006.

M. R. Khaledian, J. Mailhol, P. Ruelle, and P. Rosique. Adapting PILOTE model for water and yield management under direct seeding system (DSM). The case of corn and durum wheat in mediterranean climate. *Agricultural Water Management*, 96(5):757–770, 2008.

J. Kijne. *Note on agronomic practices for increasing crop water productivity.* CABI, 2003.

J. Kijne, R. Barker, and D. Molden. *Improving water productivity in agriculture: Editors overview.* CABI, 2003.

C. Kirda, S. Topcu, H. Kaman, A. Ulger, A. Yazici, M. Cetin, and M. Derici. Grain yield response and N-fertiliser recovery of maize under deficit irrigation. *Field Crops Research*, 93(2-3):132–141, 2005.

S. Kloss, R. Pushpalatha, K. & Kamoyo, and N. Schütze. Evaluation of crop models for simulating and optimizing deficit irrigation systems in arid and semi-arid countries under climate variability. 2011. in print.

K. Kumar, K. Madan, K. Tiwari, and A. Singh. Modeling and evaluation of greenhouse for floriculture in subtropics. *Energy and Buildings*, 42(7):1075–1083, 2010.

F. R. Lamm and T. P. Trooien. Subsurface drip irrigation for corn production: a review of 10 years of research in Kansas. *Irrigation Science*, 22(3–4):195–200, 2003.

C. Lawless and M. A. Semenov. Assessing lead-time for predicting wheat growth using a crop simulation model. *Agricultural and Forest Meteorology*, 135(1–4):302–313, 2005.

Y. Lu, E. Sadler, and C. Camp. Optimal levels of irrigation in corn production in the southeast coastal plain. *Journal of Sustainable Agriculture*, 24(1):95–106, 2004.

Y. Lu, E. Sadler, and C. Camp. Economic feasibility study of variable irrigation of corn production in southeast coastal plain. *Journal of Sustainable Agriculture*, 26(3):69–81, 2005.

P. P. S. Lubana and N. K. Narda. Modelling soil water dynamics under trickle emitters – a review. *Journal of Agricultural Engineering Research*, 78(3):217–232, 2001.

J. Mailhol, A. A. Ayorinde, and P. Ruelle. Sorghum and sunflower evapotranspiration and yield from simulated leaf area index. *Agricultural Water Management*, 35(1–2):167–182, 1997.

J. Mailhol, A. Zaïri, A. Slatni, B. Nouma, and H. El Amani. Analysis of irrigation systems and irrigation strategies for durum wheat in Tunisia. *Agricultural Water Management*, 70(1):19–37, 2004.

J. C. Mailhol, P. Ruelle, S. Walser, N. Schütze, and C. Dejean. Analysis of AET and yield predictions under surface and buried drip irrigation systems using the Crop Model PILOTE and Hydrus-2D. *Agricultural Water Management*, 98(6):1033–1044, 2011.

K. Mmolawa and D. Or. Root zone solute dynamics under drip irrigation: A review. *Plant and Soil*, 222(1–2):163–190, 2000.

D. Molden, H. Murry-Rust, R. Sakthivadivel, and I. Makin. *A water-productivity framework for understanding and action.* CABI, 2003.

I. Mubarak, J. Mailhol, R. Angulo-Jaramillo, P. Ruelle, P. Boivin, and M. Khaledian. Temporal variability in soil hydraulic properties under drip irrigation. *Geoderma*, 150(2): 158–165, 2009.

V. Nalliah, R. S. Ranjan, and F. C. Kahimba. Evaluation of a plant-controlled subsurface drip irrigation system. *Biosystems Engineering*, 102(3):313–320, 2009.

C. J. O'Neill, E. Humphreys, J. Louis, and A. Katupitiya. Maize productivity in southern New South Wales under furrow and pressurised irrigation. *Australian Journal of Experimental Agriculture.*, 48(3):285–295, 2008.

T. Oweist and A. Hachum. Water harvesting and supplemental irrigation for improved water productivity of dry farming systems in West Asia and North Africa. In *Proceedings of the 4th International Crop Science Congress, 26 Sep–1 Oct, Brisbane, Australia.*, 2004.

J. O. Payero, D. D. Tarkalson, S. Irmak, D. Davison, and J. L. Petersen. Effect of timing of a deficit-irrigation allocation on corn evapotranspiration, yield, water use efficiency and dry mass. *Agricultural Water Management*, 96(10):1387–1397, 2009.

B. Pommel, Y. Sohbi, and B. Andrieu. Use of virtual 3D maize canopies to assess the effect of plot heterogeneity on radiation interception. *Agricultural and Forest Meteorology*, 110(1):55–67, 2001.

G. Provenzano. Using HYDRUS-2D simulation model to evaluate wetted soil volume in subsurface drip irrigation systems. *Journal of Irrigation and Drainage Engineering*, 133 (4):342–349, 2007.

L. Quanqia, C. Yuhaib, L. Mengyua, L. Xunbob, Y. Songlieb, and D. Baodia. Effects of irrigation and planting patterns on radiation use efficiency and yield of winter wheat in North China. *Agricultural Water Management*, 95(4):469–476, 2008.

P. Racsko, L. Szeidl, and M. A. Semenov. A serial approach to local stochastic weather models. *Ecological Modelling*, 57(1–2):27–41, 1991.

R. Ragab. *SALTMED Model as an integrated management tool for water, crop, soil and fertilizers*. Manejo da salinidade na agricultura: Estudos basicos e aplicado. Fortaleza, Brazil, Instituto Nacional de Ciencia e Technologia em Salinidade, 2010.

V. Ravikumar, G. Vijayakumar, J. Šimůnek, S. Chellamuthu, R. Santhi, and K. Appavu. Evaluation of fertigation scheduling for sugarcane using a vadose zone flow and transport model. *Agricultural Water and Management*, 98(9):1431–1440, 2011.

M. Reynolds, J. Foulkes, G. Slafer, P. Berry, M. Parry, J. Snape, and W. Angus. Raising yield potential in wheat. *Journal of Experimental Botany*, 60(7):1899–1918, 2009.

G. C. Rodrigues and L. S. Pereira. Assessing economic impacts of deficit irrigation as related to water productivity and water costs. *Biosystems Engineering*, 103(4):536–551, 2009.

P. Rosique, P. Ruelle, and M. R. Khaledian. Subsurface drip irrigation using Chapin tapes - Case study for a corn crop under a Mediterranean climate - 1st experimental campaign. Technical report, 2009.

M. Schaap, F. Leij, and M. van Genuchten. Rosetta: a computer program for estimating soil hydralic parameters with hierarchical pedotransfer functions. *Journal of Hydrology*, 241:163–176, 2001.

U. Schmidhalter. Sensing soil and plant properties by non-destructive measurements. In *Proceedings of the International Conference on Maize Adaption to Marginal Environments*, pages 81–90, 2005a.

U. Schmidhalter. Site-specific crop production and Precision Phenotyping for water lmited areas. In *The 2nd international conference on integrated approaches to sustain and improve plant production under drought stress*, page 286, 2005b.

G. Schmitz, T. Wöhling, and M. de Paly. GAIN-P: A new strategy to increase furrow irrigation efficiency. *Arabian Journal for Science and Engineering*, 32(12):103–114, 2007.

N. Schütze and G. H. Schmitz. OCCASION: A new Planning Tool for Optimal Climate Change Adaption Strategies in Irrigation. *Journal of Irrigation and Drainage Engineering*, 136(12):836–846, 2010.

N. Schütze, J. Grundmann, and G. Schmitz. Prospects for Integrated Water Resources Management (IWRM) through the application of simulation-based optimization methods illustrated by the example of agricultural coastal arid regions in Oman. *Hydrologie und Wasserbewirtschaftung*, 55(2):52–63, 2011a.

N. Schütze, S. Kloss, F. Lennartz, A. Al Bakri, and G. Schmitz. Optimal planning and operation of irrigation systems under water resource constraints in Oman considering climatic uncertainty. *Journal of Environmental Earth Sciences*, 2011b.

N. Schütze, M. de Paly, and U. Shamir. Novel simulation-based algorithms for optimal open-loop and closed-loop scheduling of deficit irrigation systems. *Journal of Hydroinformatics*, 14(1):136–151, 2012.

M. Semenov and E. Barrow. *LARS-WG – A stochastic weather generator for use in climate impact studies - User manual*, 2002. URL `www.rothamsted.bbsrc.ac.uk/mas-models/download/LARS-WG-Manual.pdf(15/11/2010)`.

M. A. Semenov. Development of high-resolution UKCIP02-based climate change scenarios in the UK. *Agricultural and Forest Meteorology*, 144(1-2):127–138, 2007.

M. A. Semenov. Impacts of climate change on wheat in England and Wales. *Journal of the Royal Society Interface*, 6(33):343–350, 2009.

M. A. Semenov and E. M. Barrow. Use of a stochastic weather generator in the development of climate change scenarios. *Earth and Environmental Science*, 35(4):397–414, 1977.

A. Sepaskhah, A. Azizian, and A. Tavakoli. Optimal applied water and nitrogen for winter wheat under variable seasonal rainfall and planning scenarios for consequent crops in a semi-arid region. *Agricultural Water Management*, 84(1–2):113–122, 2006.

U. Shani, Y. Tsur, A. Zemel, and D. Zilberman. Irrigation production functions with water-capital substitution. *Agricultural Economics*, 40(1):55–66, 2009.

D. K. Singh, T. B. S. Rajput, H. S. Sikarwar, R. N. Sahoo, and T. Ahmad. Simulation of soil wetting pattern with subsurface drip irrigation from line source. *Agricultural Water Management*, 83(1–2):130–134, 2006.

M. Smith. *CROPWAT – A computer program for irrigation planning and management, irrigation and drainage Pap. 46.* Food and Agric. Org. of the U.N., Rome, 1992.

K. C. Stone, P. J. Bauer, W. J. Busscher, and J. A. Millen. Narrow row corn production with subsurface drip irrigation. *Applied Engineering in Agriculture*, 24(4):455–464, 2008.

L. R. Stone, A. J. Schlegel, A. H. Khan, N. L. Klocke, and R. M. Aiken. Water supply: Yield relationships developed for study of water management. *Journal of Natural Resources and Life Sciences Education*, 36:161–173, 2006.

M. Styczen, R. Poulsen, A. Falk, and G. Jorgensen. Management model for decision support when applying low quality water in irrigation. *Agricultural Water Management*, 98(3): 472–481, 2010.

A. Taky, S. Bouarfa, J. Mailhol, A. Hamani, P. Ruelle, and A. Bouaziz. The furrow irrigation system: a technique to improve water productivity in the Gharb valley (Morocco). *Irrigation and Drainage*, 58(3):S297–S306, 2009.

D. Thoren and U. Schmidhalter. Nitrogen status and biomass determination of oilseed rape by laser-induced chlorophyll fluorescence. *European Journal of Agronomy*, 30(3): 238–242, 2009.

D. Tilman, K. G. Cassman, P. A. Matson, R. Naylor, and S. Polasky. Agricultural sustainability and intensive production practices. *Nature*, 418(6898):671–677, 2002.

B. J. Van Alphen and J. J. Stoorvogel. A methodology for precision nitrogen fertilization in high-input farming systems. *Precision Agriculture*, 2(4):319–332, 2000. ISSN 1385-2256.

M. T. van Genuchten, F. J. Leij, and S. R. Yates. *The RETC Code for Quantifying the Hydraulic Functions of Unsaturated Soils*. U.S. Salinity Laboratory, U.S. Department of Agriculture, Agricultural Research Service, Riverside, California 9250(1), 1991.

B. Varga, D. Grbesa, K. Kljak, and T. Horvat. Nitrogen uptake and utilization efficiency of maize hybrids under high and limited nutrient supply. *Cereal Research Communications*, 36(S):463–466, 2008.

M. Vazifedousta, J. C. van Dam, R. A. Feddes, and M. Feizi. Increasing water productivity of irrigated crops under limited water supply at field scale. *Agricultural Water Management*, 95(2):89–102, 2008.

J. Vrugt and J. Dane. *Inverse modeling of soil hydraulic properties*, volume 77. Anderson, M. John Wiley & Sons Ltd, West Sussex., 2005.

J. A. Vrugt, J. W. Hopmans, and J. Simunek. Calibration of a two-dimensional root water uptake model. *Soil Science Society of America Journal*, 65(4):1027–1037, 2001.

J. Šimůnek, M. Šejna, and M. van Genuchten. The HYDRUS-2D software package for simulating two-dimensional movement of water, heat, and multiple solutes in variable saturated media. Version 2.0. *International Ground Water Modeling Center, Colorado School of Mines.*, IGWMC-TPS 53, 1999.

D. Wallach. *Working with dynamic crop models - Evaluation, Analysis, Parameterization and Applications*. Elsevier B.V., 2006.

D. Wallach, B. Goffinet, J.-E. Bergez, P. Debaeke, D. Leenhardt, and J.-N. Aubertot. Parameter estimation for crop models: a new approach and application to a corn model. *Agronomy Journal*, 93(4):757–766, 2001.

S. Walser and N. Schütze. Simulation based optimization of irrigation and N-fertilization and monitoring of nitrate and ammonium transport using ion-selective electrodes. In *6th Asian Regional Conference of ICID. 10-10 October 2010, Yogyakarta, Indonesia.*, 2010.

S. Walser, N. Schütze, J. Mailhol, P. Ruelle, and G. Schmitz. Towards higher crop water productivity using a simulation based controlled deficit irrigation strategy. In *6th Asian Regional Conference of ICID. 10-10 October 2010, Yogyakarta, Indonesia.*, 2010.

S. Walser, N. Schütze, M. Guderle, S. Liske, and U. Schmidhalter. Evaluation of the transferability of a SVAT model – results from field and greenhouse applications. 60, 2011a. in print.

S. Walser, N. Schütze, S. Kloss, J. Grundmann, and U. Schmidhalter. Evaluation of simulation based deficit irrigation and fertilization strategies to maximize water productivity and nitrogen efficiency. In *21st International Congress on Irrigation and Drainage. October 15-23, 2011, Tehran, Iran.*, 2011b.

S. Wang and T. Boulard. Measurement and prediction of solar radiation distribution in full-scale greenhouse tunnels. *Agronomie*, 20(1):41–50, 2000.

L. Winterhalter, B. Mistele, S. Jampatong, and U. Schmidhalter. High throughput phenotyping of canopy water mass and canopy temperature in well-watered and drought stressed tropical maize hybrids in the vegetative stage. *European Journal of Agronomy*, 35(1):22–32, 2011.

T. Wöhling and J. C. Mailhol. Physically based coupled model for simulating 1D surface-2D subsurface flow and plant water uptake in irrigation furrows. II: Model test and evaluation. *Journal of Irrigation and Drainage Engineering – ASCE*, 133(6):548–558, 2007. ISSN 0733-9437.

H. Zhang. *Improving water productivity through deficit irrigation: Examples from Syria, the North China Plain and Oregon, USA*. CABI, 2003.

S. Zwart and Bastiaanssen. Review of measured crop water productivity values for irrigated wheat, rice, cotton and maize. *Agricultural Water Management*, 69(2):115–133, 2004.

Dresdner Schriften zur Hydrologie • Heft 12

ISBN: 978-3-86780-282-6